INVESTIGATING THE ROLE OF HEATSHOCK ON DIABETIC WOUND HEALING

Thesis submitted in accordance with the requirements

of the University of Chester

for the degree of Doctor of Philosophy by

Taha Contractor

May 2017

University of Chester

Declaration

The work submitted in this thesis is original and has not been submitted previously in support of any qualification or course.

Signed:

Date:

Acknowledgements

Firstly I would like to thank the late spiritual leader His Holiness Dr Sayedna Mohmmad Burhanuddin Saheb, our 52nd Dā'ī l-Mutlaq (Unrestricted Missionary) for starting me on this path to obtain a doctorate. Your constant encouragement to pursue lifelong education even in old age has been inspirational.

This journey would not have been possible if it weren't for my supervisors John and Elyse who showed confidence in my abilities even in times when I doubted mine. John thank you very much for giving me the opportunity to do my Doctorate here. Elyse your help and advice throughout this endeavour has been invaluable especially in planning my experiments and compiling this thesis. The two of you have been treasure trove of knowledge and have helped me immeasurably. I would like to thank my colleagues Michelle Cordingley for her help for western blots, the proof reading of this thesis and with formatting and constant words of encouragement. Chelle Chelle you are star. I would like to thank Jasmine-Stanley Ahmed for being a confidant and for her wise counsel when I thought things would not be possible.

I would like to thank my parents for supporting throughout this period and for their constant encouragement. Mom and Dad thank you for having faith in me. I know it took a long time but the end is near. I would like to thank my wife Ajab who has been my pillar of strength and support at home. You have enriched my life and always been there since the day I met you. I do not have words to thank you for the balance you brought in my life and managing all things that I could not or found difficult to. Lastly I would like to thank my little princess, Khadijah for making me smile every time I am with her.

Abstract

The increasing occurrence of diabetes in the general population as a result of over nutrition and increasingly inactive lifestyle has led to an obesity epidemic which is set to grow over time. With an ever increasing obese population type 2 diabetes and cardiovascular complications are set to become the major causes of human mortality. Chronic non healing wounds are a major cause of mortality and morbidity in patients with type 2 diabetes. They are predominantly caused by macrophage dysfunction and a lack of migration of fibroblasts into the wound.

This study aimed to investigate diabetic wound healing through development of an artificial scratch assay. An in vitro scratch assay developed in WS1 cells. The effect of heat shock treatments from 39°C to 45° was tested to determine if cell migration increased; however, no significant difference was seen. Mitomycin C was used to determine if wound closure occurred as a result of cell proliferation and migration or migration alone. 10µg/ml of mitomycin C inhibited cell division by 79.9% without exhibiting cytotoxicity over a 12h period. The effect of hyperglycaemia and heat shock was also tested and showed no significant difference when compared to control conditions, suggesting that fibroblast migration in vivo is hindered through other factors such as debridement or macrophage dysfunction in the wound.

GLUT4 is present in insulin sensitive organs (liver, adipose and muscle) and is the major glucose transporter responsible for the clearance of glucose from the blood after a meal, thus playing a central role in glucose homeostasis. Monocytes are precursors to macrophages and can easily be isolated from whole blood. They have also been shown to express GLUT4 in response to insulin and could be used as model to assess inflammation in diabetes. A glucose uptake assay was developed in U937 cells using a fluorescent glucose analogue, 2NBDG. 2NBDG fluorescence was shown to be competitively inhibited by increasing concentrations of glucose suggesting that 2NBDG enters the cell through glucose transporters. 2NBDG uptake was also assessed at different pH and in presence of membrane fluidizers (DMSO, benzyl alcohol and phenethyl alcohol). Extremes of pH significantly reduced cell viability and only at pH 4 was 2NBDG fluorescence significantly reduced. Treatment with DMSO showed that at high concentrations (≤ 1.56%) cell viability was reduced with a concurrent reduction in 2NBDG fluorescence. The effect of benzyl alcohol and phenethyl alcohol was found

to be insignificant at the concentrations and time points tested. The presence of GLUT4 was also determined by flow cytometry and Western blotting and found to be situated in the cytoplasmic region of the cell. This study indicates that monocytes and macrophages could be a potential therapeutic target to improve diabetic wound healing as they are a source of growth factors and cytokines that can bring about resolution of inflammation and it is their dysfunction in diabetic wounds that causes poor clinical outcomes.

Table of Contents

List of figures

List of abbreviations

GIP	Glucose dependent insulinotropic peptide
GLP	Glucagon like peptide
ASP	Acyl stimulating protein
MFS	Major facilitator super family
IR	Insulin receptor
PI3K	Phosphotidyl inositol 3 kinase
IRS	Insulin receptor substrate
IKKβ	Inhibitor of κB kinase
PKC	Protein kinase C
JNK	c-Jun N terminal kinase
HSP	Heat shock proteins
TNF-α	Tumour necrosis factor-α
IL-6	Interleukin-6
MCP-1	Macrophage chemoattractant protein-1
FFA	Non-esterified free fatty acids
TLR	Toll-like receptor
AGE	Advanced glycated endproducts
IKK-NFκB	Inhibitor of κB-Nuclear factor κB
DAG	Diacyl glycerol
C13	Radioactive carbon 13
P31	Radioactive phosphorous 31
JIP1	JNK interacting protein 1
IκB	Inhibitor of κB
LPS	Lipopolysaccharide

Fet A	Fetuin A
CML	N^{ε}-[carboxymethyl]-lysine
RAGE	Receptor for AGE
UPR	Unfolded protein response
ER	Endoplasmic reticulum
ECM	Extracellular matrix
VEGF	Vascular endothelial growth factor
NO	Nitrous oxide
NOS	NO synthetase
iNOS	Inducible NOS
VCAM1	Vascular cell adhesion molecule
TIMP	Tissue inhibitor of matrix metalloproteinase
HIF1-α	Hypoxia inducible factor1-α
ATM	Adipose tissue macrophage
PAPRα	Peroxisome proliferator-activated receptor α
PAPRγ	Peroxisome proliferator-activated receptor γ
TGF-β	Transforming growth factor-β
IGF-1	Insulin like growth factor-1
FBS	Foetal bovine serum
NEAA	Non-essential aminoacids
DMSO	Dimethyl sulphoxide
2NBDG	2-deoxy-2-[(7-nitro-2,1,3-benzoxadiazol-4-yl)amino-D-glucose
BrdU	5 Bromo 2 deoxyuridine
PES	Phenazine ethosulphate
MTS	3-(4,5-dimethylthiazol-2yl)-5-(3-carboxymethoxyphenyl)-2-(4-sulfophenyl)-2H-tetrazolium

Chapter 1 General Introduction

1.0 Introduction

The condition of diabetes has been known recorded as early as 1500 BC by the Egyptians (Kirchhof, Popat, & Malowany, 2009). Diabetes is a metabolic syndrome characterised by the breakdown of insulin signal transduction leading to impaired glucose homeostasis. It can be caused when the patient does not produce insulin (type 1) or when the patient develops resistance to insulin (type 2). As of 2013, 382 million people have been diagnosed with diabetes (International diabetes federation, 2014). In the UK the number people suffering from diabetes has nearly doubled over the last two decades; from 1.8 million in 1996 to 3.4 million in 2014 (Diabetes UK, 2014).

Faults in the immune system have a role to play in both type 1 and type 2 diabetes. Type 1 diabetes is an autoimmune disease where the insulin producing cells of the islets of Langerhans are targeted by the host immune system and as a result insulin production is lost (Van Belle, Coppieters, & Von Herrath, 2011). In type 2 diabetes cells lose sensitivity to insulin and therefore fail to transport glucose into the cell (McGarry, 2002). Type 2 diabetes is closely linked to a chronic inflammation induced by excessive nutrient intake coupled with unhealthy lifestyle choices. This thesis focused principally on type 2 diabetes and the role of fibroblast and monocytes in diabetic wound healing.

- Impaired wound healing: Patients with diabetes have poor wound healing which could be attributed to a lack of growth factors and viable fibroblasts in the wound (Lerman, Galiano, Armour, Levine, & Gurtner, 2003).
- Monocyte responses: In diabetic wounds monocyte and macrophage recruitment has been shown to be delayed, moreover they have been shown to secrete high levels of inflammatory cytokines and very little growth factors (Brem & Tomic-Canic, 2007).

1.1 Glucose Homeostasis

Glucose is main source of carbohydrate in the body and in some organs it is the only source of metabolic energy (e.g. brain) (Thorens, 2014). This makes glucose homeostasis a very important regulatory mechanism for overall energy homeostasis in

the body. Consumption of carbohydrates is the main source of glucose in the body and organs such as liver and muscles store glucose in the form of glycogen. Adipose tissue converts glucose into lipids and stores fat, a long term fuel source. Additionally the liver can breakdown proteins and generate glucose through gluconeogenesis. The liver and muscle can also breakdown their glycogen stores to generate glucose for the brain. These systems are regulated by hormones and ensure a constant supply of glucose within the body at all times. Normal glucose levels are maintained at approximately 5mM/L within the blood. After a meal glucose levels within the blood are raised to about 7.9mM/L and is brought down within 2 to three hours back to 5mM/L (Ceriello, Colagiuri, Gerich, & Tuomilehto, 2008). Blood glucose is maintained at all times through co-ordination of hormones secreted by pancreas, adipose tissue and small intestine and the subsequent binding of these hormones to their receptors.

1.1.1 Hormones

Blood glucose levels are generally maintained and regulated by the action of hormones secreted by the pancreas, adipose tissue and gut. The major hormones are:

Insulin: Insulin is secreted by pancreatic β cells in the islets of Langerhans of the pancreas promotes glucose uptake, inhibits gluconeogenesis, promotes glycogen synthesis, promotes lipogenesis and inhibits lipolysis in insulin target tissues by binding to the insulin receptor and translocating the insulin sensitive glucose transporter GLUT 4 (Kotas & Medzhitov, 2015). Insulin secretion is also increased in response to amino acids and glucose-independent insulinotropic polypeptide (GIP) and glucagon like peptide-1 (GLP-1) (Drucker, 2001; Drucker, 2007). Insulin receptors are present on muscle, liver, adipose and immune cells.

Glucagon: Glucagon is secreted by pancreatic α cells and has opposing action to insulin and promotes lipolysis, glycogenosis and promotes gluconeogenesis. It maintains plasma glucose levels during fasting periods through its action on the liver (Aronoff, Berkowitz, Shreiner, & Want, 2004).

Amylin: Amylin is secreted by the β cells of the pancreas when post-prandial glucose is high. One of its main functions is to inhibit arginine-induced glucagon secretion by α cells of the pancreas in a paracrine manner after a meal (Aronoff et al., 2004). It is responsible for delaying gastric emptying in a dose dependent manner (Schmitz, Brock,

& Rungby, 2004). This gastric emptying has been shown to inhibited by hypoglycaemia in rats (Gedulin & Young, 1998). It primarily acts through the nervous system were receptors for amylin are present in the postrema, a region that can induce vomiting (Aronoff et al., 2004)

GLP-1: Glucagon like peptide-1 (GLP-1) is secreted by intestinal epithelial L cells located in colon and distal ileum and is an incretin which promotes insulin secretion of β cells and enhances β cell survival by promoting cell proliferation. It is stimulated by glucose and monounsaturated fatty acids. It promotes satiety, weight loss and improves cardiac output (Drucker, 2007; Lim et al., 2009).

GIP: Glucose-dependent insulinotropic polypeptide or gastric inhibitory polypeptide (GIP) is another incretin produced in the stomach and proximal small intestine. It promotes insulin secretion fat deposition and bone formation. It is rapidly induce by the ingestion of proteins. (Seino, Fukushima, & Yabe, 2010).

Leptin: leptin is secreted by adipose tissue and was discovered in (ob/ob) mice that had abnormally high feeding rates where it was found to inhibit nutrient intake and reduce weight gain in the long term (Guerre-Millo, 2002) . Leptin acts on the hypothalamus and reports the energy status of the body. Leptins levels have been shown to increase with increasing body mass index (BMI) (Ouchi et al., 2011)

Ghrelin: Ghrelin is secreted in the stomach and levels seem to rise before meal and drop immediately after the meal. Increased ghrelin levels have been shown to correlate with hunger. Like leptin it acts on the hypothalamus but stimulates nutrient intake (Klok, Jakobsdottir, & Drent, 2007).

ASP: Acyl stimulating protein (ASP) is a hormone that is produced within the adipose tissue and inhibits lipolysis, promotes lipogenesis and promotes glucose uptake in adipocytes (Yang et al., 2006). ASP has also been shown to stimulate insulin secretion in in vitro studies. Increasing levels of adiposity correlate with increased production of the hormone (Havel, 2014).

Adiponectin: Adiponectin is a hormone that has been implicated in preventing insulin resistance and promoting insulin sensitivity in animals. Adiponectin levels are reduced with increasing adiposity (Ouchi et al., 2011). Administration of adiponectin has been shown to promote glucose clearance without stimulating insulin secretion, however

the mechanism remains unknown (Havel, 2014). Table 1.1 summarises all the hormones involved in glucose homeostasis.

Table 1.1 Hormones involved in glucose homeostasis

Organ	Cells	Hormone	Function	Reference
Pancreas: Islets of Langerhans	β-cells	Insulin	Promotes glucose uptake by cells Promotes protein and fat synthesis Promotes use of glucose as an energy source Suppresses postprandial glucagon secretion	Kotas and Medzhitov, 2015
		Amylin, or islet amyloid polypeptide (IAPP)	Supresses postprandial glucagon secretion	Schmitz, Brock, & Rungby, 2004 and
			Slows gastric emptying	Gedulin and Young, 1998
	α-cells	Glucagon	Stimulates the breakdown of stored liver glycogen Promotes hepatic gluconeogenesis Promotes hepatic ketogenesis	Aronoff, Berkowitz, Shreiner, & Want, 2004
Intestine	L-cells	GLP-1	Enhances glucose-dependent insulin secretion Suppresses postprandial glucagon secretion Slows gastric emptying Reduces food intake and body weight Promotes cell health	Drucker, 2007; Lim et al., 2009

Organ	Cells	Hormone	Function	Reference
	K-cells	GIP-1	Enhances glucose-dependent insulin secretion Promotes bone formation Promotes fat deposition	Seino, Fukushima, & Yabe, 2010
Stomach	Ghrelin cells	Ghrelin	Promotes hunger	Klok, Jakobsdottir, & Drent, 2007
Adipose Tissue		Leptin	Decrease nutrient intake Increase energy expenditure Regulates weight gain	Guerre-Millo, 2002 and Ouchi et al., 2011
		Acyl simulation protein	Increased glucose uptake by adipocytes Increased lipogenesis Decreased lipolysis	Yang et al., 2006 and Havel, 2014
		Adiponectin	Insulin sensitizing hormone	Ouchi et al., 2011 and Havel, 2014

1.1.2 Glucose Transporters

Hormones described earlier act on cells and tissues to bring about the expression and activity of glucose transporters. Glucose transport in the body is carried out 2 types of glucose transporters (Table 1.2), facultative glucose transporters (GLUT) and sodium dependent glucose transporters (SGLT) (Wood & Trayhurn, 2003).

The GLUT family of proteins are encoded by SLC2 genes and belong to the major facilitator superfamily (MFS) of evolutionary related proteins and have 12 transmembrane helices and carry out glucose transport through facilitated diffusion (Wood & Trayhurn, 2003). 14 GLUT isoforms have been identified and are divided into 3 classes based on sequence homology. SGLT are encoded for SLC5 genes, have 14 transmembrane helices and carryout glucose transport against an electrochemical gradient (Harada & Inagaki, 2012; Thorens & Mueckler, 2014; Wood & Trayhurn, 2003).

SGLTs are usually found in luminal walls of the small intestine and in proximal tubules of the kidney where they bring about glucose transport from the gastrointestinal (GI) tract into tissues (Harada & Inagaki, 2012; Wood & Trayhurn, 2003). SGLT1 is also thought to promote incretin secretion. SGLT1 also works in conjunction with GLUT2 in enterocytes of the small intestine to remove glucose from the GI tract (Gorboulev et al., 2012). SGLT2 is expressed in kidneys where it is thought to be responsible for the majority of glucose clearance in S1 and S2 cells (Harada & Inagaki, 2012). SGLT3 has been thought to act as a glucose sensor (Bianchi & Dez-Sampedro, 2010). Other SGLTs have been identified but their role remains yet to be identified.

The major GLUT proteins that have been studied belong to class 1:

GLUT1: GLUT1 is predominantly expressed in brain and erythrocytes but is present on most cells in conjunction with other GLUT proteins. It has a very high affinity of glucose but can also transport galactose, glucosamine and mannose (Thorens, 2014; Young et al., 2011).

GLUT2: GLUT2 has low affinity for glucose and is expressed in hepatocytes, pancreatic β where it is thought to play a role in glucose sensing and insulin secretion, intestinal enterocytes and in kidneys (Thorens, 2014; Thorens & Mueckler, 2014).

GLUT3: GLUT3 is expressed in many brains cell and is thought to be a neuronal transporter but is also found in heart, sperm, pre-implantation embryo (Simpson et al., 2008)

GLUT4: GLUT4 is the major glucose transporter in insulin target tissue and is responsible for the majority of glucose clearance after a meal. It is expressed in muscle, adipose and liver; however it has recently been shown to be expressed on the membrane of monocytes (Dimitriadis et al., 2005). GLUT4 expression has also been shown to increase in muscle of athletes while its expression has been shown to be reduced in obese individuals (Timothy Garvey et al., 1991).

GLUT5: GLUT5 is a transporter of fructose and is found in kidney, testis, muscle, adipose tissue and brain. With an increasing rise in fructose consumption GLUT5 has now been implicated to induce breast cancer (Douard & Ferraris, 2008).

GLUT8: GLUT8 is a glucose transporter found in testis, brain and in differentiating spermatocytes (Roth et al., 2002). It has a high affinity for glucose and has been shown in blastocysts to play an important role in survival suggesting its importance in development (Pinto, Carayannopoulos, Hoehn, Dowd, & Moley, 2002; Thorens & Mueckler, 2014).

GLUT9: GLUT9 is expressed in liver and kidney and thought to be a urate transporter (Anzai et al., 2008).

GLUT10 to GLUT 14: GLUT10 to GLUT14 have been identified through sequencing of the human genome but their physiological relevance remains to be elucidated (Thorens & Mueckler, 2014).

Table 1.2 summarises all the glucose transporters involved in glucose homeostasis

Table 1.2 Glucose transporters

Protein	Km (mM)	location	Function	Reference
Facultative Glucose transporters (GLUT) SCL2 genes				
GLUT1	3-7	Ubiquitous	Basal glucose uptake	(Young et al., 2011)
GLUT2	17	Liver, islets, kidney, small intestine	High capacity/low affinity	(Thorens, 2014)
GLUT3	1.4	Brain, nerve cells	Neuronal transport	(Simpson et al., 2008)
GLUT4	6.6	Muscle, fat, heart	Insulin-regulated transport	(Garvey et al., 1998; Wood & Trayhurn, 2003)
GLUT5		Testis, brain, kidney, muscle and adipose tissue	Fructose transporter and has been implicated in breast cancer	(Douard & Ferraris, 2008)
GLUT8	~2	testis, brain and differentiating spermatocytes	Role in embryonic developments of the blastocyst	(Pinto et al., 2002)
GLUT9			Urate transporter	(Anzai et al., 2008)
Na^+/glucose cotransporters (SGLT) SLC5 genes				
SGLT1	0.2	Kidney, intestine	Glucose reabsorption	(Gorboulev et al., 2012)
SGLT2	10	Kidney	Low affinity glucose reabsorption	(Harada & Inagaki, 2012)
SGLT3	2	Small intestine, skeletal muscle	Glucose activated Na^+ transport	(Bianchi & Dez-Sampedro, 2010)

As this study investigated diabetes, GLUT4 expression was the main focus as it is the major insulin sensitive glucose transporter.

1.1.3 Insulin Signalling

Insulin secreted by the β cell of the pancreas binds to insulin receptors (IR) on insulin target tissues. Binding of insulin to IR causes auto-phosphorylation of the IR on tyrosine residues (Nystrom & Quon, 1999; Saltiel & Kahn, 2001). IR then activates two major insulin signalling cascades namely Phosphotidyl Inositol 3 Kinase/ Akt (PI3K/Akt) (Akt is also known as protein kinase B (PKB)) and the RAS-mitogen activated protein kinase (RAS/MAPK) cascade (de Luca & Olefsky, 2008; Nystrom & Quon, 1999). PI3k/Akt brings about the translocation of GLUT4 from internal vesicles, supress gluconeogenesis while the RAS/MAPK brings about gene expression (Chang, Chiang, & Alan, 2006). All these process are mediated by the insulin receptor substrate (IRS). Two isoforms of IRS are known; IRS-1 is thought to play a role in glucose metabolism whilst IRS-2 is thought to play a role in lipid metabolism (de Luca & Olefsky, 2008). Activated IR phosphorylates IRS on tyrosine residues and activates IRS and allows phosphotidyl inositol 3 phosphate kinase (PI3K) to bind to IRS via its SH2 domain and then activates Akt/PKB (Björnholm & Zierath, 2005; Nystrom & Quon, 1999). It also translocate to the membrane and binds to RAS to bring about gene expression. Akt phosphorylates GSK-3 and deactivates it which in turn prevents the phosphorylation of glycogen synthase kinase which is un-phosphorylated by protein phosphatase 1 and brings about glycogen synthesis (Fröjdö, Vidal, & Pirola, 2009).

These pathways are activated by tyrosine phosphorylation of IR and IRS and down regulated by serine phosphorylation. Serine phosphorylation is carried out by various signalling serine kinases such as Inhibitor kappa B kinase β (IKKβ), protein kinase C (PKC) and c-Jun N terminal kinase (JNK). Serine phosphorylation of IRS1 inhibits signal transduction while tyrosine phosphorylation promotes insulin signal transduction (Boura-Halfon & Zick, 2009). Heat shock proteins (HSP) inhibit serine phosphorylation of IRS-1 through down regulation of IKKβ and JNK (Simar, Jacques, & Caillaud, 2012). In diabetes there is a lack of HSP and has been thought to prolong inflammation and increase insulin resistance. Several studies have shown induction of

HSP through hyperthermia or through treatment with membrane fluidizer can improve insulin sensitivity (Chung et al., 2008; Hargitai et al., 2003; Karpe & Tikoo, 2014).

1.2 Diabetes

Diabetes is a condition where there is loss of control in glucose homeostasis. This leads to impaired glucose disposal by insulin target tissues. Type 1 diabetes is considered an autoimmune disease where pancreatic β cells are targeted by the host immune system and destroyed; while type 2 diabetes is caused by excessive nutrient intake coupled with unhealthy lifestyle choices. The complications that arise as a result of impaired glucose homeostasis affects both type 1 and type 2 diabetic patients and is caused by low level chronic inflammation in the patient. Impaired glucose homeostasis causes several clinical complications throughout the body such as:

- Nephropathy: Diabetic patients have a higher risk of developing end stage renal failure characterised by protein urea and are the single most reason for kidney transplant in patients (Marshal 2004).
- Retinopathy: Diabetic retinopathy is the leading cause of blindness in patients aged between 20-74 years (Davey et al., 2014).
- Neuropathy: Hyperglycaemic conditions cause the loss and dysfunction of somatic, autonomic and motor neurons which undermine the patient's ability to feel pain or move the limb. This is brought about by local ischemic conditions that have occurred over time due to the systemic loss of peripheral capillaries which cut of blood supply and consequent supply of oxygen and nutrients to peripheral tissues (Yagihashi, Mizukami, & Sugimoto, 2011). Other compounding factors such as chronic inflammation, oxidative damage to endothelial cells and neurones by advanced glycated end products (AGE), presence of inflammatory cytokines in peripheral tissue bring about the loss of neurons and blood vessels in peripheral tissues (Brownlee, 2005). This eventually leads to the formation of non-healing chronic wounds, infection of the limb and its subsequent amputation (Davey et al., 2014).
- Cardiovascular complications: type 2 diabetes patients often suffer from cardiac complications such as cardiovascular disease, stroke, and myocardial infractions (Davey et.al, 2014).

A dramatic rise in cases of diabetes has been brought about by the obesity epidemic. Almost 80%-90% of all cases have been of type 2 diabetes (Van Greevenbroek, Schalkwijk, & Stehouwer, 2013). The onset of insulin resistance is the main cause of type 2 diabetes. Insulin is a peptide hormone that regulates blood glucose and transports glucose into insulin target organs namely liver, muscle and adipose. Insulin is secreted by the β cells present on the islets of Langerhans in the pancreas in response to high circulating blood glucose (Björnholm & Zierath, 2005). In muscle tissue it promotes the translocation of insulin sensitive glucose transporter GLUT 4; in hepatocytes it promotes glycogen synthesis and down regulates gluconeogenesis and in adipose tissue it promotes uptake of free flowing fatty acids, downregulates lipolysis and promotes lipid synthesis (Dimitriadis, Mitrou, Lambadiari, Maratou, & Raptis, 2011).

1.3 Diabetes: a chronic inflammatory disease

The main feature of type 2 diabetes is insulin resistance. Inflammation was first linked to insulin resistance when a study showed that there were high circulating levels of tumour necrosis factor-α (TNF-α) in obese individuals when compared to healthy controls (Hotamisligil, Arner, Caro, Atkinson, & Spiegelman, 1995). Investigators also found high levels TNF-α being expressed in adipose tissue of obese individuals when compared to healthy controls. Furthermore dietary control and resulting weight reduction improved insulin sensitivity and reduced circulating levels of TNF-α in obese patients (Hotamisligil et al., 1995). This discovery lead to a plethora of research that showed that adipose tissue could produce interleukin-6 (IL-6), macrophage chemoattractant protein (MCP-1) and other pro-inflammatory cytokines and other molecules that have collectively been referred to as adipokines (Fried, Bunkin, & Greenberg, 1998; Kamei et al., 2006; Ouchi et al., 2011). These pro-inflammatory cytokines are produced in response to adipocyte stress due to over nutrition and increasing adiposity and appear to create low level inflammation in obese individuals.

Production of pro-inflammatory cytokines by adipose tissue, binding of non-esterified free fatty acids (FFA) to toll-like receptors (TLR) and production of advance glycated end products (AGE), recruits immune cells such as macrophages to the site which then secrete other cytokines and add to the underlying inflammation in adipose tissue. Inflammatory cytokine production activates intracellular signalling cascades in insulin

sensitive tissue namely PKC, IKK-NFκB and JNK (Shoelson, Lee, & Goldfine, 2006). These signalling cascades act either directly or indirectly to promote insulin resistance in insulin sensitive tissue by causing the phosphorylation of insulin receptor substrate (IRS) on serine residues as opposed to tyrosine residues and inhibit the insulin signalling cascade (Aguirre et al., 2002; Griffin et al., 1999). Inhibition of the insulin signalling cascade creates an excess of FFA and sugar in blood which raises fasting glucose concentration. The role of each of these signalling cascades in insulin resistance is discussed below.

1.3.1 The role of PKC in insulin resistance

Protein kinase C are a family of serine kinases that are activated by diacyl glycerol (DAG) and act on several signal transduction pathways that act on cell regulation and tumour development (Blobe, Khan, & Hannun, 1995). Evidence of insulin resistance caused by PKC isoforms comes from studies performed in muscles using euglycaemic-hyperinsulinemic clamps and nuclear magnetic resonance of C13 and P31. Researchers have demonstrated that increasing concentration of free flowing fatty acids (FFA) in blood inhibits the transport of glucose or the phosphorylation of glucose in muscle tissue (Roden et al., 1996). This in turn reduces intermuscular glucose 6 phosphate levels which would account for the low activity of glycogen synthase (Roden et al., 1996). GLUT4 translocation was also shown be retained in dense intracellular vesicles of insulin-resistant and diabetic patient muscle biopsies (Garvey et al., 1998). In rat soleus muscle biopsies phosphorylation of IRS1 on Ser^{307} instead of tyrosine has been shown to cause a decrease in the activity of PI3K in the presence of high intracellular lipid metabolites (linoleoyl CoA). An isozyme of novel protein kinase C (PKCθ), a serine-threonine kinase activated by diacylglycerol, catalysed the phosphorylation of Ser^{307}; however the authors also noted that total concentration of PKCθ reduced after 5 hours of lipid infusion(Yu et al., 2002). They along with Griffin et al., (1999) have also demonstrated that PKCθ translocated to the membrane and cytoplasmic levels of PKCθ were lower than controls (Griffin et al., 1999; Yu et al., 2002). A similar study in humans found that the enzymes PKCβII and were raised in healthy non-diabetics in response to raised lipid concentrations (Itani, Ruderman, Schmieder, & Boden, 2002). The study also confirmed that levels of PKCδ dropped in a time dependent manner as described earlier but the levels of total PKC, PKCβII and PKCδ in both membrane and

cytosolic fractions increased (Itani et al., 2002). In vitro studies using rat hepatic cell line H4IIE, have demonstrated that PKCδ phosphorylates IRS-1 on serine residues (Greene, Morrice, Garofalo, & Roth, 2004).

The role of novel PKC isoforms in insulin resistance has come into question as knockout studies in mice have only shown mild and short term protection to insulin resistance when given a high fat diet. A short term euglycaemic-hyperinsulinemic clamp study in PKCθ knockout mice showed that PKCθ knockout mice were protected from insulin resistance when fed a high fat diet (Kim et al., 2004) while long term studies have shown that PKCθ knockout mice had increased susceptibility of obesity and insulin resistance (Gao et al., 2007). Studies using transgenic mice models expressing a dominant negative form of PKCθ have shown that even before the onset of obesity they show increased insulin resistance and by 6 to 7 months showed increased visceral adiposity when compared to the wild type control (Serra et al., 2003) A problem with clamp studies is that the results only show a correlation to what is being tested and are conducted over a small period of time and so cannot represent long term implications which are more characteristic of diabetes and its related complications. The studies have usually been carried out in muscle tissue where PKC is the dominant kinase (Schmitz-Peiffer & Biden, 2008).

1.3.2 The role of JNK in insulin resistance

The c-Jun NH_2-terminal kinase (JNK) cascade is a sub group of mitogen activated kinases that are specifically activated by environmental stress and inflammation. TNF-α and FFA have been shown to activate the cell stress signalling cascades (Shoelson et al., 2006). Aguirre et al. (2000) first showed that JNK1 phosphorylates IRS-1 at Ser^{307} in CHO cells upon stimulation with anisomycin. This group also showed that substitution of serine to alanine inhibited the phosphorylation of IRS-1 at position 307 (Aguirre et al., 2000). The link between JNK and insulin resistance was confirmed in mouse models where both diet induced and genetic ob/ob mice expressed high levels of JNK in all insulin sensitive tissues. They also showed that gene knockout of JNK1 ($JNK^{-/-}$) in both diet induced and genetic models of obesity decreased adiposity, improved glucose tolerance, lowered body weight and lowered circulating levels of insulin when compared to JNK1 controls (Hirosumi et al., 2002). Interestingly JNK2 knockout had no protective effect on insulin resistance. JNK has also been shown to be activated by

production of reactive oxygen species in the cell and endoplasmic reticulum (ER) stress (Back & Kaufman, 2012).

JNK has also been implicated in in β cell dysfunction and cell death (Kaneto et al., 2005). An in vitro study using the transfected cell line, AN-ins cells which are derived from AN-glu and produce insulin showed higher susceptibility to IL-1β when compared glucagon producing AN-glu (Ammendrup et al., 2000). NO synthesis was found to be similar in both cells, however JNK phosphorylation and activation were significantly increased in AN-ins cells and lead to increased cytotoxicity of these cells to IL-1β (Ammendrup et al., 2000). Inhibition of JNK, with JNK binding protein improved cell survival and confirmed that JNK1 was associated with β cell cytotoxicity (Ammendrup et al., 2000). A novel inhibitory peptide has been developed based on the binding domain of JNK interacting protein-1 (JIP1) (Bonny, Oberson, Negri, Sauser, & Schorderet, 2001; Kaneto et al., 2004). JIP1 also known as islet-brain 1 (IB1) has been shown to competitively inhibit JNK signal transduction and prevent IL-1β induced apoptosis in vitro studies using AN-ins cells when conjugated to HIV-TAT, a 10 amino acid peptide that allows proteins to be imported into cells (Bonny et al., 2001). These results were confirmed in both diet induced and genetic mouse (db/db) models studies where the inhibitory peptide was tagged with a fluorophore (FITC) and delivered to the mice via intraperitoneal injection. Treated mice showed improved glucose homeostasis, reduced IRS-1 serine phosphorylation and reduced JNK1 phosphorylation in insulin target tissue when compared to untreated mice and mice that received a scramble peptide, thus confirming that JNK1 plays an important role in insulin resistance (Kaneto et al., 2004).

1.3.3 The role of IKK in insulin resistance

The IKK-NFκB signalling cascade is normally activated by inflammatory signals in response to free radicals, stress, ultraviolet light, and viral and bacterial antigens (Patel & Santani, 2009). NFκB is ubiquitously expressed in all cells where their action is tightly regulated by the formation of complexes with its inhibitor called inhibitor of κB (IκB). The NFκB.IκB complexes and their activating kinases, inhibitor of κB kinase (IKK) (classical activation) and NIK (alternative activation) translocate freely from cytoplasm and nucleus leading to low level constitutive expression of NFκB transcriptional genes (Birbach et al., 2002). This also enables the signalling cascade to

be modulated rapidly in response to changes in the extracellular environment. High dose of sodium salicylate and aspirin exhibit their anti-inflammatory effect on cells by inhibiting the activity of IKK. Inhibition by the competitive binding of these compounds to IKK and reducing its ATP binding efficiency and has been shown in both purified proteins and cells (Yin, Yamamoto, & Gaynor, 1998). Aspirin and salicylate have been used for years by clinicians to treat type 2 diabetes and the finding that they inhibit IKK-NFκB signalling implicated the role of NFκB in type 2 diabetes (Shoelson, Lee, & Yuan, 2003).

Streptozotocin induced diabetic mice showed poor recovery and increased neuropathy when compared to healthy controls following an ischemic insult (Wang, Schmeichel, Iida, Schmelzer, & Low, 2006). Diabetic mice showed an increased levels of NFκB when compared to controls after seven days of reperfusion suggesting that underlying chronic inflammation brought about by IKK-NFκB lead to poor recovery (Wang et al., 2006). Studies in mouse models overexpressing NFκB have shown that while the mice are resistant to diet induced obesity as NKκB was shown to inhibit lipid accumulation and adipocyte differentiation, there was an increase in inflammatory cytokine production of TNF-α, IL-1, IL-6 and MCP-1 and an increase in adipocyte macrophages (Tang et al., 2010). Global gene knockout of ($Ikbkb^{-/-}$) is lethal in the embryonic stage, thus studies in conditional knock outs have been used to investigate the role of NFκB in insulin resistance. Hepatocyte knockout ($Ikbkb^{\Delta hep}$) and myeloid cell knockout ($Ikbkb^{\Delta mye}$) of IKK in mice have improved insulin sensitivity and glucose tolerance in response to diet induced insulin resistance when compared to controls; however in hepatocyte knockout mice only the hepatocytes retained their insulin resistance whist other tissue such as muscle and adipocyte became insulin resistant (Arkan et al., 2005). Interestingly myeloid cell knockout mice were completely protected from insulin resistance when compared to controls suggesting that myeloid cells such as neutrophils and macrophages were key to maintain insulin sensitivity. Induction of inflammation by lipopolysaccharide (LPS) injection induced hyperglycaemia in both models but hepatocyte knockout mice and myeloid cell knockout mice were more tolerant to hyperglycaemia when compared to controls. Treatment of control mice with IL-1 antagonist prior to LPS injection improved glucose tolerance (Arkan et al., 2005). This study has shown that NFκB signalling plays an important role in insulin resistance and that NFκB signalling in immune cells has a larger impact on glucose homeostasis than

in insulin sensitive tissue linking inflammation to insulin resistance and diabetes (Shoelson, Lee, & Yuan, 2003).

1.4 Factors that cause insulin resistance through inflammation

Inflammation is brought about by various factors in type 2 diabetes. Insulin resistance always manifests in tissue through either one or all 3 signalling cascades described above and can be seen in both insulin sensitive and non-sensitive tissue. The major factors and their roles in the prognosis of type 2 diabetes are discussed below.

1.4.1 Inflammation induced by FFA binding to TLR

One mechanism for insulin resistance is brought about by the binding of fatty acids to toll-like receptor (TLR) on cells which activate pro-inflammatory responses in cells and enable them to secrete cytokines such as TNF-α (Martins et al., 2012). TLR are pattern recognising receptors on cell membranes that activate the innate immune system. TLR binds to LPS from gram negative bacteria which contain saturated fatty acids (Kim & Sears, 2010). Several studies have demonstrated that saturated fatty acids bind to TLR2 and TLR4 and activate the stress kinase cascade JNK and inflammatory cascade IKK-NFκB and bring about insulin resistance. Gene knockout studies in mice have shown that knock out mice have better tolerance to high fat diets and protection from insulin resistance. They also have shown a preference for fat metabolism and lower pro-inflammatory cytokine profile compared to controls (Ehses et al., 2010; Tsukumo et al., 2007). These studies were carried out in germ free conditions, however TLR2 knockout mice when kept under normal conditions have been shown to exhibit diseased phenotypic symptoms of insulin resistance implying that gut microbes and environment may also play a role in insulin sensitivity (Caricilli et al., 2011). They further demonstrated that treatment with antibiotics returned gut microbes population to ones found in the wild type control and returned glucose tolerance to that of wild type controls. They also showed that transplantation of gut microflora from $TLR2^{-/-}$ mice to wild type controls yielded insulin resistance in wild type mice (Caricilli et al., 2011). TLR4 knockout Sprague Dawley rats showed a reduction in calorie intake but were not protected from insulin resistance and development of fatty liver compared to the controls when gavage (force-feeding via a tube) fed a high fat diet (Galbo et al.,

2013). The binding of saturated fatty acids to TLR forms a very plausible mechanism linking insulin resistance to inflammation as high levels of saturated fatty acids are present type 2 diabetes which is thought to be the cause of chronic low level inflammation in insulin target tissues.

Another issue with studies that suggest saturated fatty acids bind to TLR do not account for the LPS contamination present in the experiments that could give them false positive results (Kim & Sears, 2010; Martins et al., 2012). LPS or endotoxin levels can be directly measured but often render the sample unusable moreover, they are designed to measure endotoxin levels in water and not cell culture components. Some studies have measured endotoxin levels indirectly (Kim & Sears, 2010). From these studies it can be concluded that high fat and fructose diets change the gut microflora and increase the levels of LPS in blood causing endotoxemia which in turn is recognised by TLR present on cells and brings about chronic low level inflammation and insulin resistance in type 2 diabetes; thus saturated fatty acids are indirectly responsible for TLR activation and insulin resistance. A second mechanism for FFA binding to TLR 4 has also been identified through a the binding of FFA to fetuin A (Fet A), a glycoprotein secreted by liver that has been shown in vitro to act as a carrier for the incorporation of FFA into cells (Cayatte, Kumbla, & Subbiah, 1990). Raised circulating Fet A levels have been shown in in the serum of obese diabetic humans, in diet induced insulin resistant and genetically modified murine models (Pal et al., 2012). Furthermore they have demonstrated that gene knockdown of either Fet A or TLR 4 in mice, reduced levels of TNF-α IL-6 and phosphorylated NF□B and protected them form insulin resistance induced by a high fat diet (Pal et al., 2012).

1.4.2 Oxidative stress

Oxidative stress is brought about by the presence of high circulating glucose levels and FFA in blood that are not disposed of by insulin target tissue. These form permanent complexes with plasma proteins, lipids and nucleic acids through Maillard reaction and become advanced glycated end products (AGE) (Singh, Barden, Mori, & Beilin, 2001). The formation of AGE is a slow process catalysed by metal ions and thus targets long lived proteins such as connective tissue and collagen in the extracellular matrix, myelin and tubulin (Singh et al., 2001). This random glycoxidation of sugar moieties to

proteins and the subsequent formation of AGE yields a heterogeneous mixture of chemically modified proteins (Boyer et al., 2015).

Production of AGE has been implicated in the development of diabetic retinopathy and nephropathy in a dose dependent manner and the amount of AGE reflected the oxidative stress within the patient (McCance et al., 1993). N^{ε}-[carboxymethyl]-lysine (CML) is one the most well characterised AGE and can be formed from both lipid and glucose oxidation and is thought to be an important biomarker for oxidative stress (Fu et al., 1996). Another feature of AGE is to form cross links with matrix proteins which increase their resistance to proteolytic degradation and decrease flexibility of support proteins. In vitro studies show that treatment of collagen plates with methylglyoxal resulted in decreased adhesion of MG63 and HT1080 in a dose depended manner when compared to untreated control plates (Paul & Bailey, 1999). These findings are confirmed in post-mortem studies of human aortae where arterial stiffness had a direct correlation to increased cross-link formation by NFC-1 (an AGE formed from glucose and lysine) in collagen and was associated with increased denaturation temperature, resistance to enzymatic degradation and decreased solubility in aortae of diabetic individuals when compared to age matched non diabetic controls (Sims, Rasmussen, Oxlund, & Bailey, 1996).

AGE can also bind to its receptor, receptor for advanced glycated end products (RAGE) and bring about inflammatory responses in tissue. Several receptors have been identified and are expressed in monocytes, macrophages, endothelial cells, astrocytes, microglia and pericytes (Singh et al., 2001). Binding of AGE to its receptor (RAGE) has been shown to activate IKK-NFκB signalling cascade and bring about the transduction of inflammatory signals whilst the binding of AGE to AGER-1, another receptor for AGE has been shown to be protective (Boyer et al., 2015; Ott et al., 2014).

1.4.3 ER stress

Before the onset of obesity and insulin resistance pancreatic β cell increase in size and number as compensatory response to over nutrition (Back & Kaufman, 2012). This has been shown in Zucker (fa/fa) rats to occur at 5 weeks and preceded insulin resistance which began between 7 to 10 weeks (Jetton et al., 2005). As insulin resistance increases and results in overt type 2 diabetes pancreatic β cells can no longer compensate for the

increasing demand for insulin in response to hyperglycaemic and hyperlipidaemia and eventually fail and begin to die through apoptosis (Back & Kaufman, 2012).

Insulin is the major protein synthesised and stored in pancreatic β cells and its synthesis occurs in a dose dependent manner in response to glucose (Schuit, In't Veld, & Pipeleers, 1988). This imposes a large metabolic load on its endoplasmic reticulum (ER). The ER is the site of all synthesis within the cell and changes to cell cycle or the response to external stimuli can have significant impact of the ER of a cell. When the homeostasis of the ER is hindered the unfolded protein response (UPR) is activated and cell chaperones assist in the refolding and clearance of protein aggregates from the ER lumen. Failure of the UPR results in the activation of pro-apoptotic signals and leads to cell death (Morimoto, RI, Christen, Shen, & Frydman, 2013).

FFA and inflammatory cytokines have been shown to induce apoptosis in β cells, however their mode of action is different. Cytokines such as IL-1β induce apoptosis through ER stress by the production of iNOS, activation of NFκB genes and increase expression of MCP-1, whilst FFA (palmitate and oleate) induce ER stress but do not activate iNOS or NFκB (Kharroubi et al., 2004). It remains unclear as to the exact mechanisms by which saturated FFA induce apoptosis in β cells, however long chain FFA have been shown to induce a mild ER stress in pancreaticβcells (Back & Kaufman, 2012). Studies in CHO cells that have been induced to produce human coagulation factor 8 (FVIII) but are unable to secrete it have demonstrated that UPR produces ROS and that treatment with antioxidants improves cell survival and promotes FVIII secretion (Malhotra et al., 2008). Pancreatic β cells have been shown to have very little antioxidant enzymes such as glutathione peroxidase and they do not produce catalase, thus they are susceptible to oxidative damage (Back & Kaufman, 2012). Treatment of β cells with lard oil and oleate promoted insulin secretion but delayed proinsulin synthesis in both in vivo and in vitro models, suggesting that prolonged exposure of FFA would not allow β cells to regenerate their insulin stores and would invariably affect cell function in the long run and cause ER stress (Bollheimer, Skelly, Chester, McGarry, & Rhodes, 1998). It is unclear as to exactly how ER stress is induced in β cells, increasing evidence points to both lipotoxicity and glucotoxicity interfere with proinsulin synthesis and induces UPR that eventually leads to ROS generation and β cell death (Back & Kaufman, 2012).

The resulting insulin resistance only progresses the inflammation over time and leads to β cell death the development of type 2 diabetes and their complications. These conditions are fully reversible in early to middle stages by exercise and diet control and reduce complications that arise later stages of the disease.

1.5 Wound healing

Wound healing or repairing damage to maintain cell or tissue integrity is one of the most important facets of survival and can be seen in every living organism studied (Sonnemann & Bement, 2011; Velnar, Bailey, & Smrkolj, 2009). It is also one of the most intensive areas of research as chronic (non-healing) wounds and complicated wounds present a clinical problem and are a major cause for patient mortality and morbidity. They also have a huge impact on healthcare systems; for instance in the UK the cost of caring for chronic wounds for the year 2005-2006 was conservatively estimated to be between £2.3-3.1billon (Posnett & Franks, 2010).

Any disruption in the normal anatomical structure and function of tissue can be defined as a wound. They can be caused by physical injury, disease, age and stress. Wound healing irrespective of the source of the wound is a dynamic physiological response to the wound to restore tissue structure and cell integrity (Velnar et al., 2009). Dermal wound healing process is a dynamic process and most stages overlap each other; but for the ease of understanding can be divided in to 4 phases

- Haemostasis phase: Here the wound closed by the rapid formation of a clot. Haemostasis is initiated immediately post injury (Eming, Martin, & Tomic-Canic, 2014). The clot also provides scaffolding for the recruitment of other cells that would initiate the healing cascade (J. Li, Chen, & Kirsner, 2007).
- Inflammatory phase: Immune cells such as neutrophils and monocytes move in to the site to kill invading microorganisms and clear up cell debris. This phase begins immediately post injury and is also brought in by platelets that secrete cytokines that act as chemo-attractants and recruit leukocytes to the wound. This phase usually lasts for 24h to 48h but in some cases can lasts for up to 2 weeks (Bielefeld, Amini-Nik, & Alman, 2013; J. Li et al., 2007). The appearance of neutrophils can be seen within the first hour of the wound and are peak at 24h whilst macrophages begin to appear at 24h and peak at 48h-

72h and lymphocytes begin to appear after 72h (Harper, Young, & McNaught, 2014)

- Proliferative phase: Growth factors released by macrophages and surrounding cells allow for migration of fibroblasts, endothelial and epithelial cells into the wound and form a temporary extra cellular matrix known as granulation tissue. Fibroblasts are one of the cells that be seen during the proliferative phase which begins at 120h post injury (Harper et al., 2014). They laydown new extra cellular matrix (ECM) and degrade the old and damaged ECM. The cells differentiate at wound edge to form myofibroblasts and initiate wound contraction(Darby, Laverdet, Bonte, & Desmouliere, 2014).
- Remodelling phase. Removal of scar tissue and signs of an injury that occurred. This phase can last for a long time and is thought to be regulated by T lymphocytes (Guo & Dipietro, 2010; Velnar et al., 2009).

Upon coming into contact with collagen and damaged vessels platelets begin to aggregate, adhere and release fibrinogen, fibronectin, vitronectin and several growth factors such as platelet derived growth factor (PDGF), vascular endothelial growth factor(VEDGF), transforming growth factor-α (TGF-α) and transforming growth factor-β (TGF-β) (Sonnemann & Bement, 2011; Velnar et al., 2009). They also ensure the sufficient exsanguination of the wound site which in turn provides a matrix for immune cells, fibroblasts and keratinocytes cells (Velnar et al., 2009). These growth factors allow immune cells to migrate to the wound site through chemotaxis. The platelets themselves allow prothrombin to be converted to thrombin which in turn converts fibrinogen to fibrin and results in clot formation (Olczyk, Mencner, & Komosinska-vassev, 2014). The first immune cells to appear at the wound site are neutrophils which begin to appear and their primary function is phagocytosis of the cell debris and invading microbes (Guo & Dipietro, 2010). They also release several proteases and reactive oxygen species (ROS) such as nitric oxide (NO) which can cause damage to surrounding cells.

Monocytes and macrophages are the next cells that move in to the wound site. Monocytes undergo maturation and become resident tissue macrophages and are an important source of cytokines for the healing wound such as TNF-α and IL-1 (Guo & Dipietro, 2010). They release matrix metalloproteinase such as collagenases and

elastases and perform debridement of the wound through phagocytosis of microbes and neutrophils in the early inflammatory phase (Olczyk et al., 2014). In the late inflammatory phase they become an important sources of growth factors that promote fibroblast migration and proliferation and pave the way for the proliferative phase (Velnar et al., 2009). Studies in guinea pig models have shown that removal of macrophages by hydrocortisone acetate injection and treatment with anti-macrophage serum resulted in delayed wound healing, poor wound debridement and delayed and reduced fibroblast migration after 10 ten days (Leibovich & Ross, 1975).

In the proliferative phase fibroblasts migrate into the wound bed in response to the growth factors secreted by macrophages and begin to divide rapidly and produce collagen and major components of the extracellular matrix (ECM) collectively called granulation tissue. Fibroblasts at the wound edge differentiate into myo-fibroblasts that begin to close the wound and from a scar (Darby et al., 2014). Endothelial cells divide and bring about angiogenesis in response to vascular endothelial growth factor (VEGF) and nitric oxide (NO) to alleviate the temporary hypoxic conditions that were present in haemostasis and inflammatory phases. With the ECM restored epithelial cells migrate in to the wound through cell division and migration and bring about the restoration of function to the wound. The eventual outcome is the formation of scar tissue. Once a scar is formed the remodelling phase begins and can last for a long period. Here the scar tissue is strengthened and replaced with collagen I fibres and the tissue is remodelled to restore it closely to its original form. The remodelling phase id brought about by lymphocytes (Bielefeld et al., 2013). Embryonic wound healing has been shown to heal completely without the development of scar tissue while adult wound healing scar tissue (Sonnemann & Bement, 2011). Some cells such a sebaceous glands and hair follicles are lost and are never replaced in post wound repair (Bielefeld et al., 2013).

The process described here was for an acute wound and depends on several cell types working in conjunction to bring about wound healing. Complications in wound healing arise when one of the cells do not carry out their function in lieu of other compounding factors such as diabetes. In diabetes wound healing is impaired and the wound remains in a quasi-inflammatory phase (Blakytny & Jude, 2006).

1.5.1 Diabetic wound healing

Inflammation in insulin sensitive organs caused by excessive circulating nutrients bring about chronic inflammation and cause insulin resistance in type 2 diabetes. Peripheral neuropathy causes a delay in the healing of both acute and chronic wounds in diabetic patients. Diabetic wounds are characterised by low production of growth factors, lack of macrophages, presence of high matrix metalloproteinase, little to no migration and proliferation of keratinocytes and fibroblasts, poor angiogenesis, prolonged hypoxia and poor debridement of necrotic tissue by immune cells (Brem & Tomic-Canic, 2007). Chronic diabetic wounds such as diabetic foot ulcers present a major problem as they significantly affect patient mortality, morbidity and have a huge cost implication on the health care system. With an increasing ageing population in the west, treatment of chronic diabetic wounds is set to put even more pressure on health care systems, therefore understanding the molecular mechanisms behind poor clinical outcomes and research into new therapies is very important in order to improve patient mortality and morbidity.

Studies form both murine models and human wound biopsies have shown that there is a consistent delay of immune cell recruitment (Blakytny & Jude, 2006). This could be attributed to the presence of a large number of free radicals produced by nitric oxide (NO). NO is produced by endothelial cells, keratinocytes, melanocytes and Langerhans cells in the dermal wound (Bruch-Gerharz, Ruzicka, & Kolb-Bachofen, 1998). It has a very transient role in normal physiological conditions where it acts as a secondary messenger in cells. NO action can cause vasodilation of smooth muscles and increases blood flow into tissues, act as a neurotransmitter between neurons or as an acute toxin released by macrophages during inflammatory responses (Bruch-Gerharz et al., 1998). Nitric oxide is synthesised by two enzymes, nitric oxide synthase (NOS) and arginase using L-arginine as substrate and can be induced during inflammation by inducible NOS (iNOS). In normal wound healing NO is synthesised by NOS in the inflammatory phase and by arginase in the proliferative phase where arginine is converted to ornithine which in turn is converted to proline that is used to create collagen. In patients with diabetes who suffer from chronic venous ulcers; NOS, iNOS activity and arginase activity are upregulated and produce high levels of NO with iNOS being the dominant generator of NO. Excess NO generates free radicals, peroxynitrite and superoxide, that can cause apoptosis of cells. (Abd-El-Aleem et al., 2000; Jude, Boulton, Ferguson, & Appleton, 1999). Treatment with L-arginine to foot ulcers has been shown

to improve wound healing in diabetes (Arana, Paz, González, Méndez, & Méndez, 2004).

In vitro studies have shown excessive iNOS down regulates the expression of vascular cell adhesion molecule-1 (VCAM-1) that allows leukocytes to bind to the endothelial cell wall and migrate towards the wound and could possibly further delay the recruitment of monocytes in diabetic wound healing (Peng, Spiecker, & Liao, 1998). These findings are further corroborated in an in vivo study that showed delayed recruitment of macrophages in db/db mice was a result of a downregulation in mRNA levels for receptors in macrophage inflammatory protein 2 (MIP2) and macrophage chemoattractant protein 1 (MCP1) (Wetzler, Kampfer, Stallmeyer, Pfeilschifter, & Frank, 2000).

Another feature of diabetic wounds is the lack of growth factors such as TGF-β and its isoforms. In healthy wounds TGF-β1 and TGF-β2 expression is increased at the early stages of wound healing whilst TGF-β3 is increased in the later stages of wound healing(Frank, Madlener, & Werner, 1996). Gene knockout of TGF-β1 in mice have shown to have delayed wound healing (Crowe, Doetschman, & Greenhalgh, 2000). Dermal gene knock out studies of TGF-β2 receptor in mouse models have shown that TGF-β is responsible for the recruitment of macrophages and scar formation as both were significantly reduced in the knockout mice. The study also showed that wound closure was mediated by accelerated re-epithelization and reduced granular tissue formation (Martinez-Ferrer et al., 2010). Jude et al. (2002), have shown that TGF-β1 expression was markedly reduced in wound biopsies of diabetic foot ulcers and diabetic skin while TGF-β3 levels were raised in both conditions. TGF-β2 levels were also significantly higher but lower than TGF-β3. They also showed that the receptors for TGF-β remained unchanged in diabetic skin and diabetic ulcers (Jude, Blakytny, Bulmer, Boulton, & Ferguson, 2002). Low levels of TGF-β1 has been implicated in the increased activity of iNOS by macrophages and the overall raised levels of NO in diabetic foot ulcers (Jude et al., 1999).

Another growth factor that is important in wound healing is platelet derived growth factor (PDGF). Almost all cells in the healing wound are sensitive to PDGF (Heldin & Westermark, 1999). PDGF induces fibroblast proliferation (Pierce et al., 1994) and increases production of matrix proteins such as fibronectin (Blatti, Foster, Ranganathan, Moses, & Getz, 1988) and hyaluronic acid (Heldin, Laurent, & Heldin,

1989). Pierce et al. (1995) have shown that PDGF was present in healthy healing wounds while non-healing wounds showed no expression of PDGF. Furthermore treatment with recombinant PDGF-BB (rPDGF-BB) improved wound healing as cells in the granulation tissue expressed high levels of the PDGF-BB receptor (Pierce et al., 1995). Wound fluid analysis of diabetic foot ulcers have shown very little mitogenic activity in diabetic foot ulcers and that samples taken post treatment with rPDGF-BB showed increased mitogenic activity (Castronuovo, Ghobrial, Giusti, Rudolph, & Smiell, 1998). Topical application of rPDGF-BB completed healed diabetic foot ulcers in conjunction with proper wound care (Castronuovo et al., 1998). PDGF levels are thought to be upregulated by TGF-β and this could possibly one of the reasons why PDGF levels remain low in diabetic wounds (Blakytny & Jude, 2006). Today PDGF-BB is the only commercially available growth factor on the market that is used to treat chronic wounds (Castronuovo et al., 1998).

Other compounding factors that prevent diabetic wound closure are poor angiogenesis, hypoxia and the presence of matrix metalloproteinase in high quantities that maintain the wound in its inflammatory phase and do not let it progress any further. Studies have shown that monocytes express the receptor for VEGF, VEGFR1 and high levels of VEGF are present in diabetic wounds; however their response to VEGF stimulation is impaired in diabetes. They do not produce other endothelial growth factors necessary for angiogenesis in response to hypoxia and allow hypoxia to prevail (Kolluru, Bir, & Kevil, 2012; Waltenberger, Lange, & Kranz, 2000). Wound biopsies of diabetic foot have shown increased metalloproteinase activity in patients with diabetes when compared to age-matched healthy controls. There were low levels of tissue inhibitor of matrix metalloproteinase (TIMP) in diabetics in comparison to controls (Lobmann et al., 2002). Matrix metalloproteinase degrade support proteins of the ECM and would prevent new ECM form being produced, thus impairing wound healing.

1.5.2 Macrophage dysfunction

Macrophages are central to the resolution of the inflammatory phase as they carryout wound debridement and are a source of growth factors and cytokines during early and late inflammatory phase (Samaan, 2011). Studies in adipocytes (3T3-L1) cultured in hypoxic medium have shown that adipocytes induce the expression of hypoxia-

inducible factor-1α (HIF-1α), and produce increase expression of pro-inflammatory cytokines TNF-□, IL-6 and MCP-1 and down regulation of anti-inflammatory adipokine, adiponectin (Yu et al., 2011). Media transfer from hypoxic adipocytes to C2C12 myotubes resulted in insulin resistance by elevating serine phosphorylation of IRS-1 through JNK1 (Yu et al., 2011). Antibody neutralization of IL-6 and MCP-1 returned glucose homeostasis to normal as did heat inactivation of cultured media (Yu et al., 2011). Trans well migration assays also showed that hypoxic adipocytes promoted migration of macrophages, suggesting adipose tissue hypoxia and subsequent recruitment of macrophages is a key step in the prognosis of type 2 diabetes in vivo (Yu et al., 2011). Infiltration of macrophages into white adipose tissue and subsequent formation of giant cells has been seen in both wild type and genetic (ob/ob) mouse models (Xu et al., 2003). Treatment with insulin sensitising drugs such as rosiglitazone reduces inflammatory gene expression in white adipose tissue. Inflammation was not observed in liver or muscle and therefore was thought to be adipose tissue specific suggesting that, in obesity inflammation first begins in adipose tissue (Xu et al., 2003).

Macrophages can be sub divided into 2 groups based on how they are activated; M1 macrophages are activated in response to interferon (IFN-□) and lipopolysaccharides (LPS) and secrete pro-inflammatory cytokines such as TNF-□ and produce NO through iNOS activity; usually described as classical activation (Gordon & Martinez, 2010). On the other hand M2 macrophages are activated in response to IL-4 and IL-13 and secrete anti-inflammatory cytokines such as IL-10, upregulate arginase activity and down regulate iNOS activity; usually described as alternative activation (Gordon & Martinez, 2010; Samaan, 2011). It must be noted that there are several intermediator stages of macrophage differentiation as they can be affected by various stimuli that cause them to differentiate to varying degrees of M1/M2 and that M1 and M2 classification is just describing macrophages at the extreme polar opposite. It was always thought that adipose tissue macrophages (ATM) would be of M1 phenotype as they significantly produce pro-inflammatory cytokines, however analysis of ATM by flow cytometry have shown that ATM have an M2 phenotype and that there is direct correlation between ATM presence and BMI (Zeyda et al., 2007). ATM have also been shown to have increased basal expression levels of both pro and anti-inflammatory cytokines when compared to peripheral blood monocytes, classically activated macrophages and alternatively activated macrophages (Zeyda et al., 2007).

IL-4 and STAT6 have been shown to improve insulin sensitivity in mouse hepatocytes by down regulation of peroxisome proliferator-activated receptor α (PAPR), a nuclear receptor that promotes lipid oxidation during fasting conditions (Kersten et al., 1999; Ricardo-Gonzalez et al., 2010). This change in turn activates the nuclear hormone receptor, peroxisome proliferator-activated receptor (PAPR) which promotes lipid uptake and adipogenesis. PAPR expression is increased in presence of IL-4 in macrophages. A deletion of PAPRin macrophages reduced the expression of M2 macrophage markers such as Mrcl, Clec7a and Arg1 and these macrophages resembled M1 macrophages (Odegaard et al., 2007). The PAPR knock out mice also were insulin resistant, implicating the role of PAPR in alternative activation of macrophages. It also showed that alternative macrophage activation had a protective effect on obesity induced complications (Odegaard et al., 2007). More recently macrophages present in diabetic wounds were found to have reduced levels and reduced expression of PAPR and its receptor, CD36 and CPT-1 that are normally expressed in M2 on macrophages showing that wound healing had not progressed (Mirza et al., 2015). Myeloid knock out PAPRsignificantly delayed wound healing with prolonged expression of inflammatory cytokines like IL-1β, TNF-α and delayed expression of TGF-β, VEDGF and IGF-1. Treatment with PAPRagonist improved wound healing and showed promise as a mode of treatment for diabetic wounds (Mirza et al., 2015).

These studies have shown the central role of the macrophage in metabolism and immunity; where altering the metabolic state of the macrophage can change its cytokine profile from pro-inflammatory (M1) to anti-inflammatory (M2) and improve clinical outcomes of type 2 diabetes (Bermudez et al., 2010; Ricardo-Gonzalez et al., 2010). This has provided a new therapeutic target for the treatment of type 2 diabetes and other inflammatory diseases such as pancreatic cancer and arthrosclerosis (Panunti & Fonseca, 2006; Polvani, Tarocchi, Tempesti, Bencini, & Galli, 2016) . A class of drugs known as thiazolidinediones have been shown to be potent agonist for PAPRof which pioglitazone (Actos) and rosiglitazone (Avandia) are currently used to treat type 2 diabetes (Bermudez et al., 2010; Panunti & Fonseca, 2006).

1.6 Heat shock proteins and their role in diabetes

Heat shock response was first observed and described in the 1960s in Drosophila by Ritossa in Naples (De Maio, Gabriella Santoro, Tanguay, & Hightower, 2012). The heat

shock response or cell stress response is a ubiquitous and highly conserved mechanism seen all cell types(Richter, Haslbeck, & Buchner, 2010). When faced with stress such as physical (heat, radiation) or pharmacological (heavy metals, xenobiotics) cells transcribe and produce heat shock proteins (HSP), molecular chaperones that bring help misfolded proteins regain their structure or direct these proteins to the ubiquitin proteasome pathway to be degraded (Whitley, Goldberg, & Jordan, 1999). This prevents the formation protein aggregates within the cell (Verghese, Abrams, Wang, & Morano, 2012). HSP have been shown to inhibit apoptotic pathways and prevent the activation of caspase 3 and bring about cell survival (C Garrido et al., 1999; Carmen Garrido, Gurbuxani, Ravagnan, & Kroemer, 2001). This cyto-protective ability of HSP have also been implicated in tumour drug resistance in cancer where cancer cells have been shown to produce large amounts of HSP (Lianos et al., 2015)

HSP have also been shown to have moonlighting functions when they are present outside the cells and acts as immune modulators that can bring about pro (Calderwood, Mambula, Gray, & Theriault, 2007) or anti-inflammatory responses (Van Noort, Bsibsi, Nacken, Gerritsen, & Amor, 2012). In diabetes the expression of inducible HSP72 was found to lower in patients with type 2 diabetes when compared to controls (Bruce, Carey, Hawley, & Febbraio, 2003; Kurucz et al., 2002). HSP 72 has been shown to have an anti-inflammatory effect by causing PBMC to secrete IL-10 and reduce the production of TNF-α (Detanico et al., 2004) This would suggest that the lack of HSP in type 2 diabetes would hinder the timely resolution of inflammation in a wound. This cyto-protective and anti-inflammatory nature of HSP has been the subject of current research in diabetes and researchers have used heat shock treatments to show that HSP acts on both IKK and JNK signal transduction cascades to bring resolution to the inflammation and improve insulin sensitivity (Chung et al., 2008; Kumar Sharma et al., 2011; W. Li et al., 2007; Morino et al., 2008).

It is currently unclear what effects heat shock treatments would have on a diabetic wound and if heat shock treatments could improve cell migration of fibroblasts into the wound. The effect of heat shock on fibroblast migration was investigated in this study by means of a scratch assay. A scratch assay is an in vitro method that is used to measure cell migration on a 2 dimensional plane (Liang, Park, & Guan, 2007). Adherent cells are grown to confluence and a wound is made using a 200µl pipette tip to create a gap by scraping cells of the monolayer to form a wound. This process of

physically removing cells replicates wound in vivo conditions. Migration of cells into the gap is monitored through microscopy (Jonkman et al., 2014). A scratch assay was developed using WS1 cells used to test the effect of heat shock on fibroblast migration in response to heat shock treatments.

Tissue macrophages have a central role to play in wound healing and inflammation. Recent studies have shown that heat shock treatments cause monocytes to secrete anti-inflammatory cytokines (Simar et al., 2012). The study aimed to investigate if monocytic cell line U937 expressed GLUT4 and the effects of glucose transport on this cell line when treated with insulin, extremes of pH and membrane fluidizers using fluorescent glucose analogue 2NBDG.

1.7 Aims

The aims of this thesis are as follows:

- Development and optimization of a scratch assay
- Test the effect of heat shock on cell migration
- Optimise a glucose uptake assay and to determine the presence of GLUT4.

Chapter 2 Materials and Methods

2.1 Materials

2.1.1 Consumables

Table 1: List of consumables used

Consumable/ equipment	Manufactured by	Catalogue number
0.6ml micro centrifuge tubes	Star lab	E1405-0600
1.5ml micro centrifuge tubes	Star lab	S1615-5500
15ml centrifuge tubes	Star lab	S1415-0200
50ml centrifuge tubes	Star lab	E1450-0200
Adhesive plate seals	Fisher Scientific	11524794
Microplate flat bottom 96 well	Fisher Scientific	11349163
Microplate V bottom 96 well	Fisher Scientific	12697745
Microplate 12 well flat bottom, sterile with lid	Fisher Scientific	10253041
Microplate 24 well flat bottom, sterile with lid	Fisher Scientific	10380932
Microplate 96 well flat bottom, sterile with lid	Fisher Scientific	10687551
Tissue culture flask 25cm^3	Fisher Scientific	10568482
Tissue culture flask 75cm^3	Fisher Scientific	10364131
Coverslips	Fisher Scientific	22-037-169
Filter paper 3 qualitative	Whatman	1003-917
CooBlue max protein gel stain	Interchim	UPR2034A
Interchim Protein quantification kit	Interchim	UP87542A
Nitrocellulose membrane, 0.45µm	Bio-Rad	162-0115
Nalgene Cryoware cryogenic vials 1.8ml	Thermo Fisher Scientific	5000-0020

2.1.2 Sodium Dodecyl Sulphate Poly Acrylamide Del electrophoresis (SDS PAGE) and Western blots

Table 2: List of reagent used for SDS PAGE and Western blot

Reagent	Manufactured by	Catalogue number
Acrylamide	Fisher Scientific	BP170-500
N'N'-methylene bisacrylamide	BDH	443003N
(Hydoxymethyl)-methylamine (Tris-base)	Fisher Scientific	T/3710/60
Glycine	Sigma-Aldrich	G7126-500G
Sodium dodecyl sulphate (SDS)	BDH	442444H
Sucrose	Anal R	102744B
Bromophenol blue	Fisons Scientific	B/5630/44
DL-Dithiotheritol	Sigma-Aldrich	D-0632
Benzamidine	Sigma-Aldrich	B-6506
Ethylene diamine tetra acetic acid (EDTA)	Sigma-Aldrich	E5134-100G
Ammonium persulphate	Sigma-Aldrich	A3678-100G
Triton X-100	Sigma-Aldrich	T9284
ε-Amino-n-caproic acid	Sigma-Aldrich	A7824
Tween-20	Sigma-Aldrich	P1379-500ML
Sodium chloride	Fisher Scientific	S/3160/65
Methanol	Fisher Scientific	M/4056/17
N'N'N'N'Tetramethylethylenediamine (TMED)	Sigma-Aldrich	
Bovine serum albumin (BSA)	Fisher Scientific	BP9700-100
Precision Plus™ Western C™	Bio-Rad	1610376
Precision Protein StrepTactin-Horseradish Peroxidase (HRP) Conjugate	Bio-Rad	1610380
Mem-PER Eukaryotic Membrane Protein Extraction Reagent Kit	Thermo Fisher Scientific	89826
SuperSignal™ West Femto maximum sensitivity substrate	Thermo Fisher Scientific	34094
CooBlue max Protein Gel Stain	Interchim	R2034A
Uptima Cooassay Max IL of Coomassie Max reagent	Interchim	UP87542A

2.1.3 Cell culture

Table 3: List of reagent used for cell culture

Reagent	Manufactured by	Catalogue number
WSI cell line	European Collection of cell Culture	88021104
U937 cell line	European Collection of cell Culture	85011440
MCF-7 cell line	European Collection of cell Culture	86012803
MG-63 cell line	European Collection of cell Culture	86051601
Eagle's Minimal essential Medium (EMEM) with L-glutamine	Lonza	BE12-611F
Roswell Park Memorial Institute (RPMI) 1640 with L-glutamine	Lonza	BE12-702F
Dimethyl Sulfoxide (DMSO) hybrid max	Sigma-Aldrich	D2650-5x5ML
Foetal bovine serum (FBS), E. U Approved, South American origin	Life technologies	10270-106
Mitomycin C from Streptomyces caespitosus	Sigma-Aldrich	M4287-2MG
Trypsin-versene EDTA	Lonza	BE17-161E
Non-Essential Amino Acid Solution (NEAA)	Sigma-Aldrich	M7145
D-glucose solution (45%)	Sigma-Aldrich	G8769
Trypan blue solution (0.4%)	Sigma-Aldrich	T-8154
2-deoxy-2-[(7-nitro-2,1,3-benzoxadiazol-4-yl)amino-D-glucose (2NBDG)	Sigma-Aldrich	72987-1MG
Insulin solution from bovine pancreas	Sigma-Aldrich	I0516-5ML
Culture inserts	Ibidi	80209
Platelet-Derived Growth Factor-BB (PDGF-BB)	Sigma-Aldrich	P3201-10UG

2.1.4 Antibodies

Table 4: List of Antibodies used in this study

Antibody	Manufactured by	Catalogue no:
GLUT4 polyclonal	Santa Cruz Biotechnologies	SC-1608
Mouse anti-goat IgG-FITC	Santa Cruz Biotechnologies	SC-2356
GLUT4 (IF-8)	Santa Cruz Biotechnologies	SC-53566
Anti mouse IgG FITC conjugate	Sigma-Aldrich	F-0257
Anti mouse IgG peroxidase	Sigma-Aldrich	A5278-1ML

2.1.5 Flow cytometry

Table 5: List of reagents used for flow cytometry

Reagent	Manufactured by	Catalogue no:
1Dulbecco's phosphate buffered saline (DPBS) without Ca^{2+} and MG^{2+}	Lonza	BE17-513f
Paraformaldehyde	Sigma-Aldrich	158127
BD Cytofix/Cytoperm™ fixation and permeablization solution	BD Biosciences	51-2090KZ
Phenethyl Alcohol, Kosher	Sigma-Aldrich	W285811-SAMPLE-K
Benzyl Alcohol	Sigma-Aldrich	30,519-7

2.1.6 Cell viability assays

Table 6: list of reagents used for cell viability assays

Reagent	Manufactured by	Catalogue number
Propidium iodide	Sigma-Aldrich	P4170-25MG
Phenazine Ethosulphate (PES)	Santa Cruz Biotechnologies	SC-215699
CellTitre 96®Aqueous 3-(4,5-dimethylthiazol-2yl)-5-(3-carboxymethoxyphenyl)-2-(4-sulfophenyl)-2H-tetrazolium (MTS) Reagent Powder, 1g	Promega	G1111
5 bromo-2' deoxy uridine (BrdU) cell Proliferation (Enzyme-Linked Immunosorbent Assay) ELISA kit	Abcam	Ab126572

2.1.7 Equipment

Table 7: List of equipment used

Equipment	Manufactured by	Catalogue number
Bio-Rad mini protean 3 gel electrophoresis system	Bio-Rad	165-3301
Bio-Rad Chemi doc XRS molecular imaging system	Bio-Rad	170-8070
Power pack	Bio-Rad	Power pack 1000
EVOS auto FL microscope	Thermo Fisher Scientific	AMAFD1000
EVOS auto FL onstage incubator	Thermo Fisher Scientific	AMC1000
EVOS XL core	Thermo Fisher Scientific	AMEX1000
Heraeus Multifuge xl	Thermo Fisher Scientific	75004210
Hermle Z323K refrigerated centrifuge	VWR International	5210221
BD Accuri™ C6 flow cytometer	BD Biosciences	
Bright-Line™ Haemocytometer	Sigma-Aldrich	Z359629
Vortex mixer mini	Thermo Fisher Scientific	GBI-900-010E
E100 Binocular Microscope	Jencons Scientific	450-951
Bio-Tek Synergy™ HT Multi-Detection Microplate Reader	Labtech International Ltd.	SIAFR
Sigma A 1-14 micro centrifuge	Sigma-Aldrich	12084
GXCAM 5	GX Optical	ID1122
TC120 heated circulating water bath	Grant Instruments	TC120-P5
Trans-Blot®Turbo™ blotting system	Bio-Rad	170-4155
MSC-Advantage™ Class II Biological Safety Cabinet	Thermo Fisher Scientific	5102541l

2.2 Buffers and solutions

2.2.1 Cell culture

All solutions used for cell culture we prepared under aseptic conditions.

2.2.1.1 Complete culture medium for U937 cells

To make complete culture medium for U937 cells 50ml of foetal bovine serum (FBS) was added to 1000ml of RPMI 1640 with L-glutamine. The media bottle was labelled and stored at -20°C.

2.2.1.2 Complete culture medium for MG-63, MCF-7 and WSI cells

To make complete culture medium for MG-63, MCF-7 and WSI cells 50ml of FBS and 5ml of non-essential amino acid (NEAA) solution (100x) was added to EMEM with L-glutamine. The media bottle was labelled and stored at -20°C.

2.2.1.3 Heat inactivated media

To make heat inactivated media 50ml of FBS was incubated in a water bath at 60°C for 1h. This heat inactivated FBS was then added to EMEM containing 1% NEAA. The media was stored at -20°C.

2.2.1.4 Freeze media

To make freeze media 5ml of DMSO (hybrid max) was added to 45ml of FBS. The solution was then stored at -20°C.

2.2.1.5 2NBDG stock solution

A stock solution of 2NBDG was made by adding 1ml of DPBS 1mg of 2NBDG and stored at -20°C. A 1:10 dilution of this stock solution freshly prepared at the beginning of every experiment. 10µl of working dilution was used for all experiments.

2.2.1.6 Mitomycin C stock solution

To make mitomycin stock solution 4ml of EMEM supplemented with 10% FBS and 1% NEAA (complete medium) was added to 2mg of Mitomycin C to obtain a final concentration 500µg/ml. the solution was stored at -20°C.

2.2.1.7 PDGF-BB stock solution

To make PDGF-BB stock solution, 5ml of complete EMEM medium was added to 10µg of PDGF-BB to get a final concentration of 2µg/ml.

2.2.2 Cell extraction buffer

Table 8: Cell extraction buffer recipe

Reagent	Quantity (g)
Tris base	0.315
EDTA	0.004
DL- dithiothreitol	0.01
Distilled water	100 ml*
*pH was adjusted to 7.4 and then the remaining reagents were added.	
Phenylmethylsulfonyl fluoride	0.035
Benzamidine	0.016
Amino-n-caproic acid	0.065
Triton X100	100µl

2.2.3 SDS PAGE buffers

Table 9: Acrylamide solution

Reagent	Quantity (g)
Acrylamide	30
N'N'Bismethylene Acrylamide	0.8
Distilled water	100ml

The solution was then filtered and stored in the dark at 4°C

Table 10: 1.5M Tris-HCl pH 8.8 buffer

Reagent	Quantity (g)
Tris-Base	18.50
Distilled water	80ml*

*pH was adjusted to pH 8.8 and topped up to 100ml with distilled water.

Table 11: 0.5M Tris-HCl buffer pH6.8

Reagent	Quantity (g)
Tris-Base	3
Distilled water	25ml*

*pH was adjusted to pH6.8 and topped up to 50ml with distilled water.

Table 12: Electrode buffer pH 8.3

Reagent	Quantity (g)
Tris-Base	3.03
Glycine	14.4
10% SDS solution	10ml
Distilled water	900 ml*

*pH was adjusted to pH 8.3 and topped up to 900ml with distilled water

Table 13: Reducing sample buffer

Reagent	Quantity (g)
Sucrose	2.4
Dithithreitol	0.1
0.05% bromophenol blue solution	0.4 ml
0.5M Tris-HCl pH 6.8	2.0 ml
10% SDS solution	2.0 ml
Distilled water	9.10 ml

Table 14: Resolving gel (10% acrylamide)

Reagent	Quantity (ml)
Distilled water	6.05
1.5M Tris-HCl pH 5.8	3.75
10% SDS	0.15
Acrylamie-bis (30%)	5
Degas gel for 10min using a vaccum pump and then add the following	
*10% Ammonium persulphate	0.05
*TEMED	0.0075

*10% ammonium persulphate and TMED were added after the gel was degassed making sure no bubbles were made. They were mixed into gel by gently swirling the flask.

Table 15: stacking gel (3% acrylamide)

Reagent	Quantity (ml)
Distilled water	3.15
0.5M Tris-HCl pH 6.8	1.25
10% SDS	0.05
Acrylamie-bis (30%)	0.5
Degas gel for 10min using a vaccum pump and then add the following	
10% Ammonium persulphate*	0.05
TEMED*	0.005

*10% ammonium persulphate and TMED were added after the gel was degassed making sure no bubbles were made. They were mixed into gel by gently swirling the flask.

2.2.4 Western blot buffers

Table 16: Tween Tris buffered saline pH 7.5 (TTBS)

Reagent	Quantity (g)
Tris base	4.84
Sodium chloride	58.44
Tween 20	1 ml
Distilled water	1800ml*

*pH was adjusted to pH 7.5 and topped up to 2000ml using distilled water.

Table 17: Blocking Buffer

Reagent	Quantity (g)
BSA	1
TTBS	100ml

2.2.5 Flow cytometry solutions

2.2.5.1 Cell fixative – 4% Paraformaldehyde solution

To make 4% paraformaldehyde solution 4g of paraformaldehyde was added to 80ml of Phosphate buffered saline pre heated and maintained at 60°C. Once all the formaldehyde was in suspension it was solubilized by adding small aliquots of 1M NaOH until solution became clear, pH was adjusted to 7.4 and the solution was made up to 100ml. The solution was stored at 4°C and used within a month.

2.2.6 Cell viability solutions

2.2.6.1 PES stock solution recipe

Phenazine ethosulphate (PES) stock solution was prepared by dissolving 0.0092g of PES in 10ml of DPBS. The solution was wrapped in foil and covered to prevent photo-degradation and stored at -20°C

2.2.6.2 MTS solution recipe

MTS solution was prepared by dissolving 0.042g of MTS powder in 20ml of DPBS and the pH was adjusted to 6.5 by adding 1M HCl or 1M NaOH. The solution was then made to a final volume of 21ml by adding DPBS. MTS working solution was then made by adding 1 ml pf PES solution to 20ml of MTS. MTS solution was then stored as 1ml aliquots in micro-centrifuge tubes wrapped in foil and stored at -20°C.

2.2.6.3 PI stock solution recipe

A 1mg/ml of PI solution was prepared by weighing 10mg of PI and dissolving it in 100ml PBS. The stock solution was aliquoted in 1.6ml centrifuge tubes and wrapped in foil and stored at -20°C.

2.2.6.4 Phosphate buffered saline (PBS) recipe

PBS was prepared by adding NaCl 8g, KCl 0.2g, KH_2PO_4 0.24g and Na_2HPO_4 were added to 900ml of water and dissolved. The solution was made to 1000ml using distilled water.

2.3. Methods

2.3.1 Cell culture

U937 cells were cultured in RPMI 1640 medium supplemented with 10% (v/v) foetal bovine serum (FBS) (complete culture medium). They were maintained by sub-culturing a ratio of 1:10 every 3 to 4 days at and incubated at 37°C, 5% CO_2 in a humidified environment.

WS1 were cultured in EMEM supplemented 10% (v/v) FBS and 1% non-essential amino acids (complete culture medium). They were maintained by sub-culturing at a ratio 1:1 every 3 to 4 days when they had reached a confluence of 75% or higher and incubated at 37°C, 5% CO_2 in a humidified environment. They were a finite cell line and were used in experiments when they between 4 and 8 passages.

MCF-7 cells were cultured in EMEM supplemented with 10% (v/v) FBS and 1% non-essential amino acids (complete culture medium). They were maintained by sub-culturing at a ratio of 1:1every 3 to 4 days when they had reached a confluence of 75% or higher and incubated at 37°C, 5% CO_2 in a humidified environment.

MG-63 cells were cultured in EMEM supplemented with 10% (v/v) FBS and 1% non-essential amino acids (complete culture medium). They were maintained by sub-culturing at a ratio of 1:3 every 3 to 4 days once they had reached a confluence of 75% or higher and incubated at 37°C, 5% CO_2 in a humidified environment.

All adherent cell lines were treated with trypsin EDTA to re-suspend cells in fresh medium for subculture as follows. Cell culture media was discarded and 2ml of trypsin EDTA was added to the flask to wash rinse the cells and remove any residual media. The trypsin was then discarded, a second 2ml aliquot of trypsin was added to the flask and incubated at 37°C for 3-5min. The flasks were observed under the microscope at 1min intervals to assess detachment. Once the cells were in solution the reaction was stopped by adding 8ml of complete culture medium. The cells were aspirated using a pipette to obtain a homogenous solution. Cells were diluted into fresh flasks containing complete culture medium as described earlier.

2.3.2 Counting viable cells using trypan blue exclusion.

For all experiments cell counts of viable cells were carried out by diluting 100µl of cell suspension in trypan blue at a ratio of 1:1. The cell suspension and dye were aspirated using a pipette and 20µl of the cell/trypan blue suspension was used to count viable cells using a haemocytometer. Cells were counted in the central chamber of the haemocytometer. Cells that touched the top and right side of the central grid were ignored. Viable cells would not take up the dye and appear white while dead cells would take in the dye and appear blue. Two cell counts were performed and a mean cell density was obtained. This mean cell density was then multiplied by the dilution factor (x 2) to obtain the actual cell count. Cells were then diluted in complete culture medium to obtain the required cell density for the experiments.

2.3.3 Freezing cells for cryopreservation

U937 cells were cultured until they reached a cell density of 5 x 10^5 viable cells/ml and the cells were centrifuged for 5min at 500g. The culture medium was discarded and the pellet was re-suspended in 1ml freeze media (10%DMSO in FBS). The pellet was gently suspended and aliquoted into labelled cryo-tubes. The cells were then incubated in the vapour phase of liquid N_2 for a minimum of 2h after which they were stored in a designated location in the cryostat.

All adherent cells were sub-cultured and grown until they reached a confluence of 50-60%. The media was then removed and the cells were washed with 2ml of trypsin EDTA. 2ml aliquot of trypsin EDTA was then added to the flask and incubated at 37°C for 3 to 5min. The flask was examined at 1min intervals until the cells layer had dispersed. 8ml of complete culture medium was added to the cells and cell clumps were dispersed by gently aspirating the cells using a pipette. They cells were then centrifuged at 500g for 5min, the media was discarded and the pellet was gently re-suspended in 1ml freeze media. The cell suspension was then aliquoted into labelled cryo-tubes and incubated in the vapour phase of liquid N_2 for a minimum of 2h and then stored in a designated location in the cryostat.

2.3.4 Scratch assays

2.3.4.1 Scratch assay using MCF-7 and MG-63

MCF-7 and MG-63 cells were treated with trypsin EDTA as described earlier in section 2.3.1 to form a homogenised cell suspension. The cells were counted using a haemocytometer and diluted to a cell density of 1 x 10^5 viable cells/ml. 1ml aliquots of the cell suspension was then added to each well of a 12 well plate. The cells were then allowed to adhere for 24h after which they were scratched manually using a 200µl pipette tip. The cells were washed twice in compete EMEM medium and pictures and gap measurements were taken at 24h time intervals, where n=3.

2.3.4.2 General Scratch assay for WS1 cells

A 25cm^3 flask containing WS1 cells was rinsed with 2ml trypsin EDTA. The trypsin was then removed and a second 2ml aliquot of trypsin was added. The flask was incubated at 37°C for 3min and viewed under the microscope at 1min intervals until the cell monolayer had dispersed. After 3min, 8ml of complete EMEM was added to stop the

reaction. The cells were then aspirated using a pipette to obtain a homogenous cell suspension. Cells were counted using a haemocytometer and diluted to a cell density of 5 x 10^4 viable cells/ml. 1ml aliquots of the cells suspension were then used to fill each well of a sterile 12 well culture plate. The plate was incubated at 37°C, 5% CO_2 in a humidified environment for 48h after which they had reached a confluence of 65-85%. After 48h the adherent cell layer was scratched using a 200µl pipette tip with a diameter of <1mm. The cells were washed twice with complete EMEM to remove cell debris and incubated in complete culture medium. Pictures and measurements were taken at hourly intervals at a pre-determined location marked by a marker on the underside of each well of the well plate. The plate was incubated at 37°C, 5% CO_2 in a humidified environment for the duration of the experiment. The number of replicates used in each experiments was 3.

2.3.4.3 The effect of PDGF-BB on WS1 cells

WS1 cells were cultured onto 12 well plates as described in section 2.3.4.2. The cells were scratched and 2 media washes were carried out. After washes were completed control wells received complete EMEM medium while treatment wells received complete EMEM medium supplemented with 15ng/ml of PDGF-BB. Pictures and measurements were then taken at hourly intervals as described previously.

2.3.4.4 The effect of HI media of WS1 cells

WS1 cells were cultured onto 12 well plates as described in section 2.3.4.2. The cells were scratched. Control wells were washed and incubated with complete EMEM medium while treatment wells were washed and incubated with HI media. Pictures and measurements were taken at hourly intervals as described previously.

2.3.4.5 The effect of PDGF-BB prepared in HI media on WS1 cells

WS1 cells were cultured onto 12 well plates as described in section 2.3.4.2. The cells were scratched. Control wells were washed and incubated with complete EMEM medium while treatment wells were washed in HI media and incubated with HI media supplemented with 15ng/ml or 30 ng/ml of PFGF-BB. Pictures and measurements were taken at hourly intervals as described previously.

2.3.4.6 The effect of location on gap closure

WS1 cells were cultured onto a 12 well plate as described in section 2.3.4.2. The cells were then scratched and washes were carried out in complete EMEM medium. Cells

were incubated in complete EMEM medium. Measurements and pictures were taken at 3 locations on each well namely top, middle and bottom at hourly intervals.

2.3.4.7 Testing commercial inserts

Commercially available inserts were purchased; here the inserts adhered to the bottom to the plate and when removed formed a scratch width of 500µm between cells. The insert was placed aseptically using sterile forceps into each well of a sterile 12 well cell culture plate and 70µl of WS1 cells at a concentration of $5x10^4$ viable cells/ml was added to each well of the insert. 300µl of complete EMEM medium was added around the insert (Figure 2.1). The plate was then incubated under optimal culture conditions for 48h. The scratch assay was started by simply removing the inserts. Control wells were washed and incubated with complete EMEM medium while treatment wells were washed and incubated with HI media. Pictures and measurements were taken at 2h intervals.

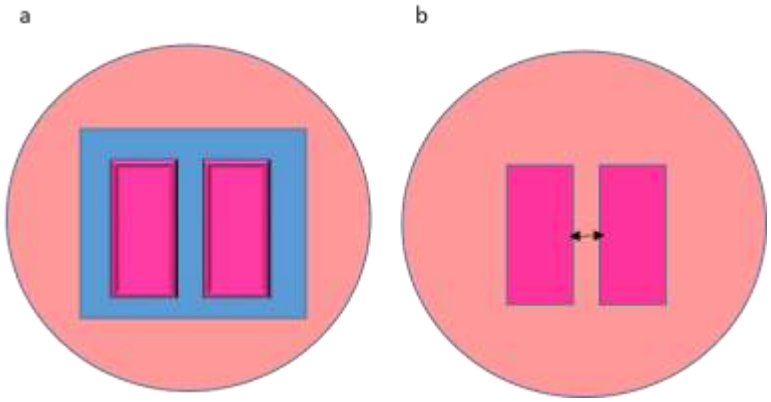

Figure 2.1: A schematic of the culture insert used in the study. Culture inserts were placed aseptically into each well of a 2 well plate. 70µl of WS1 cells were added to each well of the insert and 300µl of culture medium was added around the insert (a). Once the cells had adhered the insert was removed and the cells were washed with media the gap left by the insert was approximately 500µm as shown by the arrow (b).

2.3.4.8 The effect of a recovery period after heat shock on WS1 gap closure

WS1 cell were cultured on two 12 well plates as described in section 2.3.4.2. After 48h one plate of cells was incubated at 40°C, 5% CO_2 in a humidified environment for 1h. The cells in the heat treated plate were then incubated at 37°C, 5% CO_2 in a humidified environment for 2h to recover. The cells were then scratched and washed and

incubated in complete EMEM medium as described in 2.3.4.2. Pictures and measurements were then taken at hourly intervals.

2.3.4.9 The effect of heat shock of WSI cells.

WSI cells were cultured onto two 12 well plates as described in 2.3.4.2. Prior to commencing the scratch assay the heat treatment plate was incubated at either 39°C, 40°C, 41°C, 42°C or 45°C with 5% CO_2 in a humidified environment for 1h. The cells were then scratched, washed twice and incubated with complete EMEM medium. The plates were incubated at optimal culture conditions for the duration of the experiment. Measurements and pictures were taken at 2h intervals.

2.3.4.10 The effect of 45°C incubation on WSI cells

WSI cells were cultured onto two 12 well plates as described in 2.3.4.2. The cells were scratched, washed twice and incubated with complete EMEM medium. The heat treatment plate was incubated at 45°C, 5%CO_2 in a humidified environment for the duration of the experiment whilst the control was incubated under optimal culture conditions. Measurements and pictures were taken at 2h intervals.

2.3.4.11 The effect heat shock and HI media on WSI cells measured using commercial inserts

Inserts were placed aseptically onto the bottom of four 12 well plates as described in section 2.3.4.7. The 2 wells of each insert were inoculated with 70µl of WSI cell suspension with cell density of 5×10^4 viable cells/ml. 300µl of complete EMEM culture medium was added to the surrounding area of the insert. The plates were incubated for 48h. 2 plates were then given a heat shock by incubating them at 39°C, 5% CO_2 in a humidified environment for 1h. The plates were then put through the scratch assay by simply removing the insert. The effect of heat shock and HI media were tested. One of the 2 control plates was washed and incubated in complete EMEM medium whilst the other was washed and incubated in HI medium. The heat treated plates were also treated in the same manner as the controls. Pictures and measurements were taken at 0, 5.5, 8, 12, 24 and 30h.

2.3.4.12 The effect of hyperglycaemia and mitomycin on WSI cells

WSI cells were cultured on a 12 well plate as described in section 2.3.4.2. The cells were scratched and washed in complete EMEM medium. Control wells were incubated in complete EMEM medium whilst test wells received media containing 30mM glucose

or 10µg/ml of mitomycin C. Images were taken using an automated microscope with an onstage incubator where beacons (software generated markers) were placed at the centre of the scratch. 2 time lapse settings were used; for the first 7h images were taken at hourly intervals whilst for the remaining 5h images were taken at 0.5h intervals. The images were analysed using software TScratch.

2.3.4.13 The effect of heat shock and hyperglycaemia on WSI cells

WSI cells were cultured on a 12 well plate as described in section 2.3.4.2. The plate was then subjected to a heat shock treatment by incubating the plate at 40° with, 5%CO_2 in a humidified environment for 1h. The cells were then put through the scratch assay where control wells were washed and incubated with complete EMEM medium whilst treatment wells were washed in complete EMEM medium and incubated in complete EMEM medium supplemented with 30mM glucose. Images were taken using an automated microscope with an onstage incubator where beacons (software generated markers) were placed at the centre of the scratch. 2 time lapse settings were used; for the first 7h images were taken at hourly intervals whilst for the remaining 5h images were taken at 0.5h intervals. The images were analysed using software TScratch.

2.3.4.14 The effect of longer heat shock treatment, mitomycin C and hyperglycaemia on WSI cells

WSI cells were cultured on a 12 well plate as described in section 2.3.4.2. The plate was then subjected to a heat shock treatment by incubating the plate at 42° with, 5%CO_2 in a humidified environment for 3h. The cells were then put through the scratch assay where control wells were washed and incubated with complete EMEM medium whilst treatment wells were washed in complete EMEM medium and incubated in EMEM medium supplemented with 30mM glucose or complete EMEM medium supplemented 10µg/ml mitomycin C. Images were taken using an automated microscope with an onstage incubator where beacons (software generated markers) were placed at the centre of the scratch. 2 time lapse settings were used; for the first 7h images were taken at hourly intervals whilst for the remaining 5h images were taken at 0.5h intervals. The images were analysed using software TScratch.

2.3.5 Measuring Scratch widths using an eyepiece reticule.

The scratches were monitored and measurements were taken at x4 magnification. To measure scratch widths, the eyepiece reticule was calibrated using a stage micrometre

at 4x magnification. When aligned, 37 reticule units = 1mm on the stage micrometre thus the distance between each line on the reticule = 1000µm/37 =27.03µm. All measurements of the scratch were taken at the centre of the scratch (marked using a marker) and recorded as reticule units and converted to µm for analysis. As the scratches were made manually there was high variability between scratches. To minimise variation, scratches of similar size were always selected for analysis. Only images within 4 reticule units were chosen for analysis giving a tolerance of 108.11µm to ensure similar sized scratches were compared and reduced standard error. Pictures were taken at specific time intervals over a course of 12h. All experiments were repeated twice to ensure reproducibility of the assay.

2.3.6 Automated image capture and image analysis

Scratch assays were also carried out using an automated microscope (EVOS Auto FL) with an on stage incubator at x10 magnification. The plates were incubated at 37°C with 5% CO_2. Two time lapse settings were used in each experiment. Pictures were taken using phase contrast settings at 1h intervals for the first 7h and for the remaining 5h pictures were taken at 30min intervals. Each experiment lasted for 12h. Beacons were placed to mark the location of the centre of the scratch in each well. The microscope would automatically take pictures of all the wells at each time point dictated by time lapse setting.

The images were analysed using a free image analysis software called TScratch. The software presents the area of the wound gap as a percentage of the total image. It automatically analyses the image and determines thresholds for the wound gap for each image (Gebäck, Schulz, Koumoutsakos, & Detmar, 2009).

2.3.7 Western blots

2.3.7.1 Heat shock treatment on U937 cells.

U937 cells were cultured in a 75cm^2 flask that was split at a ratio of 1:1 the day before to obtain cells in the log phase of growth. 2 such flasks were pooled and a cell count was determined using a haemocytometer and trypan blue s escribed in section 2.3.2. The cells were then diluted to a cell density of 1 x 10^6 viable cells/ml. 10 ml of cell suspension was centrifuged at 500g for 5min and the culture media was discarded and

re-suspended in 10ml of fresh media. For heat shock treatment, 10ml of this cell suspension was placed in a water bath at 42°C for 1h and then placed in a water bath at 37°C for 2h while the control was incubated in the 37°C water bath for the entire 3h period.

2.3.7.2 Extraction of proteins from cells

Following heat shock treatment, the cells were centrifuged and washed in DPBS twice to remove dead cells. The pellet was re-suspended in 1ml of ice cold cell extraction buffer and incubated at -20°C for 10min. The lysed cell suspension was then centrifuged at 13500g for 20min. The supernatant containing total cell proteins was removed and stored in a fresh micro-centrifuge tube and total protein concentration was determined using the Bradford assay (section 2.3.7.4). All samples were then diluted to the sample containing the lowest protein concentration to ensure equal protein loading during gel electrophoresis and stored at -80°C until required. For gel electrophoresis, a 1:1 dilution of the cell extracts was made with reducing sample buffer and the tube was placed in a water bath set at 85°C for 10 min. The samples were then stored on ice until they were loaded into gels.

2.3.7.3 Membrane protein extraction

Following heat shock treatment membrane protein extraction was carried out using the Mem-PER Eukaryotic Membrane Protein Extraction Reagent Kit. Membrane extractions was carried out on both the control and heat shock treatment. 10ml of cell suspension from each condition were transferred into centrifuge tubes and centrifuged at 850g for 2min. The supernatant was discarded and the pellets were re-suspended 1ml PBS and transferred to micro-centrifuge tubes. The cells were centrifuged again at 850g for 2min and the supernatant was discarded. 150µl of Reagent A was then added to each cell pellet and incubated for 10 min at 18°C and vortexed every 2min. The cell lysate was then placed on ice. 600µl of Reagent C and 300µl of Reagent B were mixed and 450µl aliquot of this mix was added to each tube and placed on ice for 30min and were vortexed every 5min. The tubes were then centrifuged at 10000g for 3min at 4°C and incubated in a water bath at 37°C for 20min. The cells were then centrifuged at 10000g for 2min at room temperature to isolate the hydrophobic fraction. The top hydrophilic layer was then carefully removed into a separate tube and both fractions were stored at -20°C until required. They were then diluted at 1:1 ratio in reducing sample buffer and boiled at 85°C for 10min prior to being used for gel electrophoresis.

2.3.7.4 Braford assay

Concentration of the protein samples for membrane extracts and protein extracts was measured using a colorimetric assay known as Bradford assay. A series of dilutions were made using 2mg/ml BSA as stock and cell extraction buffer as diluent as described in the table below.

Table 18: BSA standard curve dilutions

Concentration of BSA (µg/ml)	Volume of stock BSA solution (µl)	Buffer volume (µl)
2000	100	0
1500	300	100
1000	200	200
750	150	250
500	100	300
250	50	350
125	25	375
25	5	395
0	0	400

10µl of standards and the cells extracts were added to wells of a 96 well plate in triplicate. 300µl aliquots of the CooAssay reagent was added to the wells and the well plate was agitated for 30 seconds. The plate was then incubated in the dark at room temperature for 10min after which the absorbance was measured at 595nm. A standard curve was then plotted for each BSA concentration against its mean absorbance and the concentrations of the cell extracts were interpolated from the curve. The samples were then diluted to the sample with lowest dilution to obtain equal protein concentrations.

2.3.7.5 SDS Polyacrylamide Gel Electrophoresis (SDS-PAGE)

SDS PAGE was carried out using Bio-Rad mini Protean 2 gel assembly kits. The 10% resolving gel was made as described in table 14. A layer of distilled water was overlaid on top of the gel by gently adding distilled water (dH_2O) to the top of the gel to prevent excessive evaporation. The gel was allowed to polymerise for an hour. The layer of dH_2O was then drained and the 3% stacking gel was layered on top as described in table 15.The combs were gently placed at the top of cast to form wells. The gel was allowed to polymerise for 1.5h after which the combs were removed. The fully formed gels were removed from the casting stand and assembled into the electrophoresis tank. Two gels could be run simultaneously so if only one gel was made a dam was used in place of a second gel. Electrode buffer was added to both the inner reservoir and into

to the outer tank. The Precision Protein Plus™ Western C standards (5µl) and samples (20µl) were loaded and the gel was connected to the power supply. Gels were initially run at 75V until the samples reached the resolving gel after which the voltage was increased to 150V and the gels were allowed to run until the dye front reached the bottom of the gel. The gels were removed and one gel was used for total protein stain whilst the second was used to transfer proteins onto nitrocellulose membrane for western blot analysis.

2.3.7.6 Total protein gel stain

The stacking gel was removed and the resolving gel was placed in a container and washed in 20ml of dH_2O for 15min. The water was discarded and 10ml of CooBlue MAX protein gel stain was then added onto the gel and agitated for an hour to stain all the proteins. The gel was the washed in 20ml dH_2O for 1h and water was changed every 15min to remove excess stain. The gel was then photographed.

2.3.7.7 Electro transfer and Immunoblotting

A semi-dry transfer method was employed to transfer samples onto nitrocellulose membrane. The gels were dis-assembled and the stacking gel was removed. The transfer onto nitrocellulose was carried out using trans-blot turbo kits. The resolving gel was placed on top of the membrane and was covered with blotting paper on both sides. The entire sandwich was placed into the transfer cassette and run for 7min at 2.5A up to 25V. Once the transfer was complete the nitrocellulose membrane was placed in 20ml blocking buffer (TTBS with 1% (w/v) BSA). The membrane was agitated for 1h after which the blocking buffer was discarded and the primary antibody diluted in blocking buffer was added. The membrane was agitated for 1h or incubated at 4°C overnight. This blocking buffer was then discarded and the membrane was washed with 10ml of TTBS 3 times with 5min of agitation per wash. The membrane was then probed with the appropriate secondary antibody conjugated to HRP diluted in blocking buffer at a dilution ratio of 1:25000 along with Precision Protein™ StrepTactin-HRP conjugate at a dilution of 1:10000 and incubated for 1h whilst being agitated. The Precision Protein™ StrepTactin-HRP bound to Strep-tagged proteins in the Precision Protein Plus™ Western C standards allow for visualisation of the ladder during chemi-luminiscent imaging to aid determination of the size of the target protein with ease. The secondary antibody and Precision Protein™ StrepTactin were then discarded and the membrane was washed 5 more times in TTBS as described earlier. After the final

wash a 1:1 dilution of reagent A and reagent B of SuperSignal™ West Femto maximum sensitivity substrate was prepared and 400µl was added to the membrane. The membrane was agitated for 5min in the dark and placed in the Bio-Rad Chemi doc XRS molecular imaging system to establish the presence of target protein.

2.3.8 Flow cytometry methods

All experiments were performed on U937 cells that were in log phase of their growth cycle. To obtain cells in the log phase, 10ml of U937 cells growing in 25cm^3 culture flasks were transferred into centrifuge tubes and centrifuged at 500g for 5 min. The supernatant was discarded and the pellets were re-suspended in 20ml complete RPMI medium. 10ml of the culture medium was transferred to two 25cm^3 flasks and cells were incubated under optimal culture conditions overnight.

2NBDG is a green fluorescent glucose analogue that is readily transported into cells by glucose transporters and can easily be detected using flow cytometry in live cells (Zou, Wang, & Shen, 2005). For the glucose uptake assay, 30.8µM of 2NBDG was used throughout this study. A 10µl aliquot of 0.1mg/ml of 2NBDG was added to U937 cells cultured in wells of a 96 well plate and incubated at 37°C for 2h. They were then washed twice in DPBS and analysed by flow cytometry. Fluorescence was detected on FL-1 488nm laser and mean fluorescence of the viable population was recorded

2.3.8.1 Determining the optimal incubation time for 2NBDG

U937 cells growing in 25cm^3 flasks prepared the day before were subjected to a cell count using trypan blue exclusion. The cells were then diluted in fresh culture medium to obtain a cell density of 1 x 10^6 viable cells/ml. Aliquots of 100µl was then added to each well of a 96 well plate. A reverse time course was performed whereby 10µl of working dilution of 2NBDG was added to 3 test wells every hour over a period of 3h. Cells in 0h time point received 2NBDG but were not incubated while cells in the no stain condition received DPBS. At 0h cells were transferred to 96 v-bottomed well plates and centrifuged at 500g for 5min. the supernatant was discarded and cell pellets were re-suspended in Dulbecco's Phosphate buffered saline without Ca^{2+} Mg^{2+} (DPBS). Cells were centrifuged at 500g for 5min and analysed by flow cytometry. Viable cells were gated using cells from the no stain condition and any fluorescence higher than the no stain was recorded (figure 2.2)

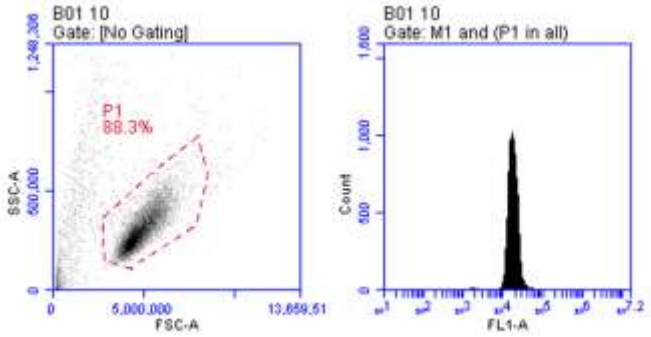

Figure 2.2: Representation of the scatter plot and histogram of U937 cells treated with 2NBDG. Cells were plated out at a seeding density of 1 x 10^6cells/ml and incubated with 2NBDG for 2h. They were washed twice to remove excess 2NBDG and analysed by flow cytometry.

2.3.8.2 Competitive inhibition of 2NBDG by glucose

U937 cells growing in 25cm^3 flasks prepared the day before (as described in 2.3.8) were subjected to a cell count using trypan blue exclusion. The cells were then diluted in fresh culture medium to obtain a cell density of 1 x 10^6 viable cells/ml. Aliquots of 100µl was then added to each well of a 96 well plate. Plate was incubated overnight under optimal culture conditions. The cells were then transferred to a v-bottom plate and centrifuged at 500g for 5min. Cells were then re-suspended in a range of glucose concentrations made in glucose-free culture medium ranging from 5mM to 100mM. 10µl of working dilution of 2NBDG was added to all wells with the exception of cells in the no stain condition that received complete culture medium and 10µl of DPBS. The plate was incubated for 2h under optimal culture conditions. The cells were then centrifuged at 500g for 5min the supernatant was discarded and cell pellets were re-suspended in DPBS. The cells were then washed once more in DPBS and analysed by flow-cytometry.

2.3.8.3 The effect of insulin on 2NBDG uptake

U937 cells growing in 25cm^3 flasks prepared the day before (as described in 2.3.8) were subjected to a cell count using trypan blue exclusion. The cells were then diluted in fresh culture medium to obtain a cell density of 1 x 10^6 viable cells/ml. Aliquots of 100µl was then added to each well of a 96 well plate. Plate was incubated overnight under optimal culture conditions. The cells were then transferred to a v-bottom plate and centrifuged at 500g for 5min. The supernatant was discarded and cells were re-

suspended in 100µl of complete culture medium containing a range of insulin. Control wells and no stain wells received 10µl of DPBS. 10µl of 2NBDG was then added to the cells and the plate was incubated for 2h under optimal culture conditions. The cells were then washed 2 times in DPBS and analysed by flow cytometry.

2.3.8.4 The effect of pH on 2NBDG uptake

U937 cells growing in 25cm^3 flasks prepared the day before (as described in 2.3.8) were subjected to a cell count using trypan blue exclusion. The cells were then diluted in fresh culture medium to obtain a cell density of 1 x 10^6 viable cells/ml. Aliquots of 100µl was then added to each well of a 96 well plate. Plate was incubated overnight under optimal culture conditions. The cells were then transferred to a v-bottom plate and centrifuged at 500g for 5min. The supernatant was discarded and cells were re-suspended in 100µl of complete culture medium whose pH had been adjusted by addition of acid (Hydrochloric acid HCl) or alkali (Sodium hydroxide NaOH). Cells in the control wells and in no stain wells received complete culture medium whose pH was not altered. 10µl of 2NBDG was then added to the cells and the plate was incubated for 2h under optimal culture conditions. The cells were then washed 2 times in DPBS and analysed by flow cytometry.

2.3.8.5 The effect of membrane fluidizers on 2NBDG uptake

U937 cells growing in 25cm^3 flasks prepared the day before (as described in 2.3.8) were subjected to a cell count using trypan blue exclusion. The cells were then diluted in fresh culture medium to obtain a cell density of 1 x 10^6 viable cells/ml. Aliquots of 100µl was then added to each well of a 96 well plate. Plate was incubated overnight under optimal culture conditions. The cells were then transferred to a v-bottom plate and centrifuged at 500g for 5min. The supernatant was discarded and cells were re-suspended in 100µl of complete culture medium supplemented with doubling dilutions of DMSO. The concentrations of the membrane fluidizers used in this study were based on those described by Dempsey, Ireland, Smith, Hoyle, & Williams, (2010). Cells in the control wells and in no stain wells received complete culture medium. 10µl of 2NBDG was then added to the cells and the plate was incubated for 2h under optimal culture conditions. The cells were then washed 2 times in DPBS and analysed by flow cytometry.

2.3.8.6 GLUT4 detection using flow cytometry

U937 cells growing in 25cm^3 flasks prepared the day before (as described in 2.3.8) were subjected to a cell count using trypan blue exclusion. The cells were then diluted in fresh culture medium to obtain a cell density of 1 x 10^6 viable cells/ml. Aliquots of 100µl was then added to each well of a 96 well plate. Plate was incubated overnight under optimal culture conditions. The cells were then transferred to a v-bottom plate and centrifuged at 500g for 5min. The supernatant was discarded and the cells were re-suspended in DPBS. The cells were then re-suspended in 70µl BD Cytofix/Cytoperm™ buffer to fix and permeabilise cells. This would allow for the detection of proteins within the cells. For membrane protein analysis 70µl of 4% paraformaldehyde was used to fix the cells. The plate was then incubated at 4°C for 20min in the dark. 70µl of DPBS was then added to dilute the buffer or paraformaldehyde. The cells were centrifuged at 500g for 5min and re-suspended in 100µl blocking buffer (5% FBS in DPBS). The cells allowed to rest at 18°C for 5min and then the blocking buffer was removed by centrifugation at 500g for 5min. GLUT4 antibody dilutions (1:200 and 1:500) were made in blocking buffer and 50µl of the diluted antibody was used to re-suspend the pellets. The plate was then covered in foil and incubated at 4°C for 45min. 50µl of blocking buffer was added to the wells to dilute the antibody. The plate was then centrifuged at 500g for 5min, the supernatant was discarded. The secondary antibody (1:500 and 1:1000) was then diluted in blocking buffer and 50µl of the antibody was used to re-suspend the pellets. The plate was sealed, covered in foil and incubated at 4°C for 30min. 50µl of blocking buffer was added to the wells to dilute the antibody. The plate was then centrifuged at 500g for 5min, the supernatant discarded and the pellets were re-suspended in 100µl DPBS. The plates were then analysed by flow cytometry.

2.3.9 Cell viability assays

2.3.9.1 MTS assay

The MTS assay measures cellular viability through the reduction of a tetrazolium compound (yellow) to a soluble formazan product which is only converted by viable respiring cells (Riss, Niles, & Minor, 2004). The assay gives an indication of cellular metabolism and changes in cellular metabolism equate to a change in absorbance. MTS is a negatively charged molecule that is impermeable to the cell membrane, thus a cell

permeable electron acceptor phenazine ethosulphate (PES) is added to the MTS solution.

2.3.9.2 Optimizing the concentration of Mitomycin c for WSI cells

The media form a 25cm^3 containing WSI cells was removed. The flask was washed with 2ml of trypsin EDTA followed by 2ml of trypsin being added to the flask. The flask was incubated under optimal culture conditions for 3min. at 1min intervals the flask was examined to see whether the monolayer of WSI cells had dispersed. 8ml of complete EMEM media was then added to flask to stop the reaction. The cells were aspirated using a pipette to obtain a homogeneous cell suspension. The cell were then counted using a haemocytometer and trypan blue exclusion to determine viable cell density. The cells were then diluted to a cell density of 5 x 10^4 viable cells/ml. 100µl aliquots of this cell suspension were used to inoculate each well of a 96 well plate. To make dead cell control 500µl of cell suspension was aliquoted into a sterile micro centrifuge tube. The cells in the tube were then snap frozen by placing the tube in liquid N_2 until all the media was completely frozen. The tube was then thawed using a water bath set at 37°C. This freeze thaw process was repeated a second time, following which the cells were plated out as dead cell control.

The plate was then incubated for 48h under optimal cell culture conditions. The plate was then examined under the microscope to see if cells had adhered to the plate. Media from the wells was removed and complete EMEM culture medium supplemented with different concentrations of mitomycin C were added to wells in triplicate. Control wells received no mitomycin C. the plate was then incubated for a further 48h after which the plate was removed and 20µl of working MTS reagent was added to each well. The plate was then incubated for 2h and absorbance was measured at 490nm using a plate reader.

A mitomycin C time course was also carried out to determine the optimal concentration of mitomycin C for the duration of the scratch assay. Here 4 plates were prepared as described initially and each plate was put through the MTS assay at specific time points. For 0h time point MTS assay was carried out immediately after the addition of mitomycin C.

2.3.9.3 Propidium Iodide (PI) assay

PI is a fluorescent DNA binding dye that is impermeable to the cell membrane, thus heathy cells with an intact membrane do not take up the dye while dying cells or cells whose membrane integrity has been compromised readily take up the dye.

The media form a 25cm^3 containing WSI cells was removed. The flask was washed with 2ml of trypsin EDTA followed by 2ml of trypsin being added to the flask. The flask was incubated under optimal culture conditions for 3min. at 1min intervals the flask was examined to see whether the monolayer of WSI cells had dispersed. 8ml of complete EMEM media was then added to flask to stop the reaction. The cells were aspirated using a pipette to obtain a homogeneous cell suspension. The cell were then counted using a haemocytometer and trypan blue exclusion to determine viable cell density. The cells were then diluted to a cell density of 5 x 10^4 viable cells/ml. 100µl aliquots of this cell suspension were used to inoculate each well of a 96 well plate. To make dead cell control 500µl of cell suspension was aliquoted into a sterile micro centrifuge tube. The cells in the tube were then snap frozen by placing the tube in liquid N_2 until all the media was completely frozen. The tube was then thawed using a water bath set at 37°C. This freeze thaw process was repeated a second time, following which the cells were plated out as dead cell control.

The plate was then incubated for 48h under optimal cell culture conditions. The plate was then examined under the microscope to see if cells had adhered to the plate. Media from the wells was removed and complete EMEM culture medium supplemented with different concentrations of mitomycin C were added to wells in triplicate. Control wells received no mitomycin C. The plate was then incubated for 48h under optimal culture conditions and then taken through the PI assay. A working dilution of propidium iodide was made by making a 1:200 dilution of the 1mg/ml stock solution in phosphate buffered saline (PBS). Equal volume of the working dilution was added to each well on the well plate and incubated at 18°C in the dark for 20min. The fluorescence was then detected using a plate reader

2.3.9.4 Cell proliferation assay

Cell proliferation can be measured by treating cells with a thymine analogue called 5 bromo 2 deoxy uridine (BrdU). Dividing cells would take up the analogue in the place of thymine and incorporate it into their DNA during DNA synthesis in the S phase of growth. BrdU can then be detected using a detecting antibody that binds to it. An

enzyme linked secondary antibody can then be used to quantify the amount BrdU present and assayed to determine if cell division has taken place as growing cells would incorporate large amounts of BrdU thereby generating a signal.

In this study BrdU assay was carried out using a commercially available BrdU assay kit (BrdU cell Proliferation ELISA kit). It was used to determine if mitomycin C inhibited cell proliferation in the scratch assay. The media form a 25cm^3 containing WSI cells was removed. The flask was washed with 2ml of trypsin EDTA followed by 2ml of trypsin being added to the flask. The flask was incubated under optimal culture conditions for 3min. at 1min intervals the flask was examined to see whether the monolayer of WSI cells had dispersed. 8ml of complete EMEM media was then added to flask to stop the reaction. The cells were aspirated using a pipette to obtain a homogeneous cell suspension. The cell were then counted using a haemocytometer and trypan blue exclusion to determine viable cell density. The cells were then diluted to a cell density of 5 x 10^4 viable cells/ml. 100µl aliquots of this cell suspension were used to inoculate each well of a 96 well plate. The cells were incubated under optimal culture conditions for 48h. Following incubation cell culture media was removed and replaced with 50µl of complete culture media containing 2x concentration of 5µg/ml, 10µg/ml and 20µg/ml mitomycin C. A 1:500 dilution BrdU was made in complete culture medium and 20µl was added to positive control and test wells. Concentrations of mitomycin C were brought to test concentrations by adding 30µl of complete culture medium to all wells treated with mitomycin C. Positive control received no mitomycin C but received BrdU and a negative control did not receive and BrdU or mitomycin were used. The plate was then incubated under optimal culture conditions for 12h.

Following the 12h incubation all media from the wells was removed. Each well then received 200µl of fixing solution and was incubated at 18°C for 20mins. The fixing solution was then removed the plate was dried and sealed using a plate sealed and stored at 4°C overnight. A 1:50 dilution of wash buffer was prepared and 200µl was added to each well. The wash buffer was then discarded and the plate was washed 2 more times in wash buffer. 100µl of ready mixed primary antibody was then added to all wells and the plate was incubated at 18°C for 1h. Following the 1h incubation the antibody was removed and the plate was dried onto paper towels. The plate was then washed 3 times in 1x wash buffer as before. A 1:2000 dilution of the secondary anti mouse IgG peroxidase was made in conjugate diluent and 100µl of this solution was

added to all wells. The plate was then incubated at 18°C for 30min. The plate was then washed 3 times in 1x wash buffer as described before. A 1:30 dilution of chemiluminescent substrate was prepared in reaction buffer and 100µl of the buffer was added to all wells. The plate was incubated for 10min at 18°C and luminescence was detected using a plate reader.

2.4 Statistical analysis

All data was analysed using GraphPad Prism™ 7 version 1.0 (GraphPad Software, Inc, San Diego, USA). All data are presented as mean ± Standard error of mean (SEM) and were analysed using either a one way ANOVA or a two way ANOVA with appropriate post hoc test.

Chapter 3 Optimization of the scratch assay

3.1 Introduction

As described in the introductory chapter, fibroblast migration is an important event in wound closure and wound healing. Wound closure maintains the integrity of the surface and prevents further exposure of sensitive tissue to the environment. The wound healing process can easily replicated in vitro through the use of a scratch assay. A scratch assay is an economical and easy method to measure cell migration in vitro (Liang et al., 2007). Cells can easily be cultured to confluence and a wound can be created using a 200µl pipette tip but this leaves a scratch/gap of varying widths. Creation of the scratch is intended to replicate wounds created in vivo and also causes cell stress. Migration of cells in closing the scratch has been shown to mimic their behaviour in in vivo models (Liang et al., 2007). The assay can easily be monitored and cell migration rates can be determined through microscopy (Jonkman et al., 2014). Wound healing in vivo occurs though cell migration and proliferation into the wound therefore an in vitro wound in the context of a scratch assay is composite of cell division and cell movement. This means that gap closure rates obtained would be through cell migration and division and not represent cell migration alone. The aim of this study was to look at the effect of various factors in cell movement, therefore the DNA synthesis inhibitor mitomycin C was used. Mitomycin C is an inhibitor of DNA synthesis (Verweij & Pinedo, 1990) and thus would inhibit cell proliferation.

There are several ways in which an in vitro scratch assay can be modelled depending on the method of cell removal from a monolayer (Ashby & Zijlstra, 2012). These can broadly be divide into 2 categories are briefly described here

3.1.1 Cell removal methods

Here cells are removed through physical, chemical or electrical means. These are simple and easy to use methods and do not require much expertise. Cells are maintained in optimal culture conditions and limited specialist equipment is required. On the other hand they suffer from high variability and the mode of removal can damage the matrix coating used to coat the plate. Wounds can be made using a pipette tip, Teflon wedge or a spinning silicone tip (Kam, Guess, Estrada, Weidow, & Quaranta, 2008). Specialist scratch making assays tools have also been developed to reduce

scratch variability and be used in throughput screening (Yarrow, Perlman, Westwood, & Mitchison, 2004).

Electrical removal via electrical substrate cell impedance sensing (ECIS) methods have the advantage that they reduce errors and cells need not be taken out of the incubator to take measurements and can be monitored in real time; moreover it is a non-invasive technique. Here cells are grown to confluence in an electrode containing substrate and a circular gold chip of 250μm in diameter. Normal culture medium serves as the electrolyte. A current is passed through the culture medium and kills all the cells growing on the chip. As cells migrate into the wound changes in impedance are recorded (Keese, Wegener, Walker, & Giaever, 2004).

Chemical removal is carried out using specialist fluidic devices where cells are grown on microfluidic plates to confluence and subjected to three fluid steams two of which contain culture medium and the middle one contains trypsin which disperses adherent cells and form a wound. The advantage of this system is that there is no damage to the plate coatings, however these systems employ specialist equipment and require specialist personnel to run (van der Meer, Vermeul, Poot, Feijen, & Vermes, 2010).

3.1.2 Cell exclusion methods

Cell exclusion methods compartmentalise cells by growing them in barriers. These barriers when removed create a reproducible cell free space in to which cells can migrate. Several types of barriers are available ranging from solids, semi-solids, liquid and gas. These methods can easily be applied to high throughput screenings, however the additional cost of these barriers can be expensive. Barrier removal can also damage the plate coating and inhibit migration of cells into the wound. Another problem with cell exclusion assays is that they are not representative of physiological conditions that generate a wound (Van Horssen & Ten Hagen, 2011).

3.2 Aims

The aim of this study was to develop and optimise a scratch assay with a view to investigate the effects of heat shock and hyperglycaemia on wound healing. Mitomycin C was optimised as a negative control in order to establish if wound closure occurred through cell proliferation and migration or cell migration alone.

3.3 Methods

3.3.1 Scratch assay

A scratch assay was performed using MCF-7, MG-63 and WSI cells as described in detail the methods chapter 2 section 2.3.4.1 to 2.3.4.7 and 2.3.4.12. Briefly cells were grown to confluence and scratched using a pipette tip. Pictures of the scratches were taken at hourly, 2 hourly or specific time intervals as dictated by the experiment. Widths of the scratch were measured using a microscope reticule calibrated using a stage micrometre at x4 magnification as described in chapter 2 section 2.3.5. In later experiments image capture was automated and time lapse pictures were taken as described 2.3.6. Pictures of one well in each condition are shown over the duration of the time course.

3.3.2 MTS assay

MTS assay was carried out in accordance to the methods described in chapter 2 section 2.3.9.2

3.3.3 PI assay

PI assay was carried out in accordance to the methods described in chapter 2 section 2.3.9.3.

3.3.4 BrdU cell proliferation assay

BrdU assay was carried out using a commercially available kit in accordance to the methods described in chapter 2 section 2.3.9.4.

3.4 Results

3.4.1 Cell selection

In order to confirm findings in the scratch assay 3 cell lines were tested MCF-7, MG63 and WSI (Figure 3.1). For the scratch assay it was required to have cells that have a high migration rate and represent cells in vivo hence WSI cells were chosen as they had a high migration rate and could completely close the wound gap in 12 to 14h. They also have a finite lifespan of 60 population doublings while MCF-7 and MG63 were cancer cell lines and took almost 72h to close with high variability. Moreover this cell line has

also been used by other research groups to study diabetic wound healing (Bizzarro et al., 2012).

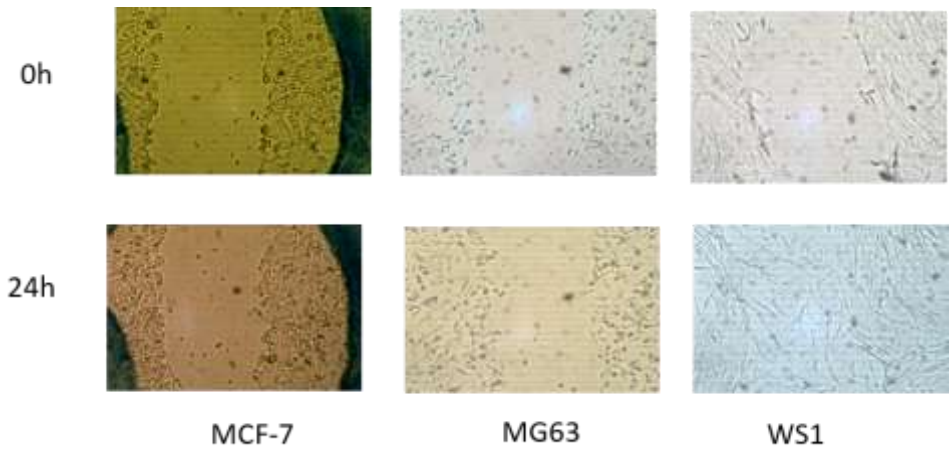

Figure 3.1: Scratches in three different cell lines MCF-7, MG63 and WS1. Cells were plated out onto cell culture plates at a seeding density of 1 x 10^5 viable cell/ml for MCF-7 and MG63 while WS1 were seeded at 5 x 10^4 viable cells/ml. The cells were allowed to adhere and become confluent. They were then subjected to a scratch assay and pictures were taken at two time points 0h and 24h. After 24h only WS1 cells had migrated into the scratch and hence were used further for optimization. Pictures for each cell line are from representative separate experiments and each cell line tested had three replicates.

3.4.2 The effect of PDGF-BB on WS1 cell migration

The effect of PDGF-BB was tested on WS1 wound closure (Figure 3.2). Platelet derived growth factor (PDGF-BB) is potent mitogen for fibroblasts and thus was chosen to provide the scratch assay with a positive control (Heldin & Westermark, 1999). Previous studies by Li et al., (2007) have shown that PDGF-BB at 15ng/ml would induce complete closure of the scratch after 16h, thus 15ng/ml of PDGF-BB was tested on WS1 scratch assays (Figure 3.2 a & b). The cells began to close the wound after 2h and after 6h (Figure 3.2a) wound closure progressed at a constant rate and by 12h they closed the gap by approximately 65% (Figure 3.2b.). Overall no significant difference was seen and PDGF-BB seemed to show no effect on WS1 cell movement into the gap ($p = 0.915$)

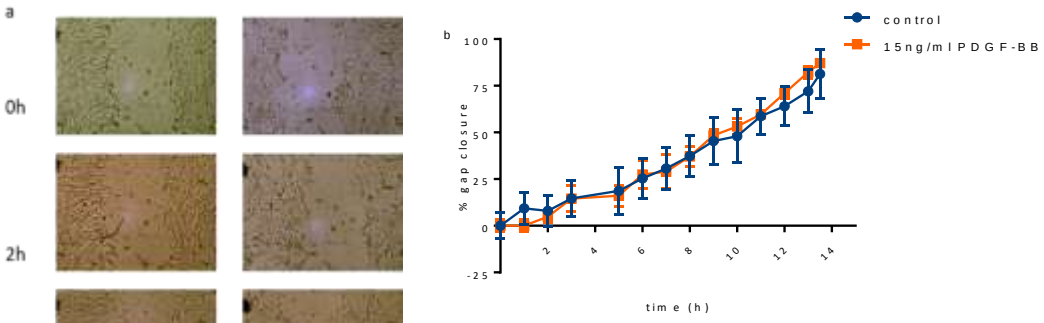

c

Sidak's multiple comparison test	
Time (h)	p values (control vs PDGF-BB)
0	>0.9999
1	0.9997
2	>0.9999
3	>0.9999
5	>0.9999
6	>0.9999
7	>0.9999
8	>0.9999
9	>0.9999
10	>0.9999
11	>0.9999
12	>0.9999
13	0.9992
13.5	>0.9999

Figure 3.2: The effect of PDGF-BB on wound closure of WS1 cells. WS1 cells were cultured at a seeding density of 5 x 10^4 viable cells/ml and allowed to adhere for 48h. The cells were then scratched and control wells received culture medium whilst the rest received media supplemented with 15ng/ml of PDGF-BB. The widths of the scratch were measured and pictures were taken at hourly intervals (a). The data were normalized and presented as means ± SEM, n=3 (b). Mean percentage gap closure between controls and PDGF-BB treatment was analysed by a two way ANOVA with Sidak's multiple comparison as post hoc test. The p values for the comparison between control and treated cells at each time point are shown table (c).

A possibility was that the action of PDGF-BB was masked by growth factors present in the FBS used in culture medium, thus a scratch assay was performed to see if heat inactivated (HI) media had any difference on gap closure rates (Figure 3.3). The cells in HI media followed the same migration pattern as that of the control ($p = 0.988$) thus it was thought that concentration of PDGF-BB used in the experiment was too low.

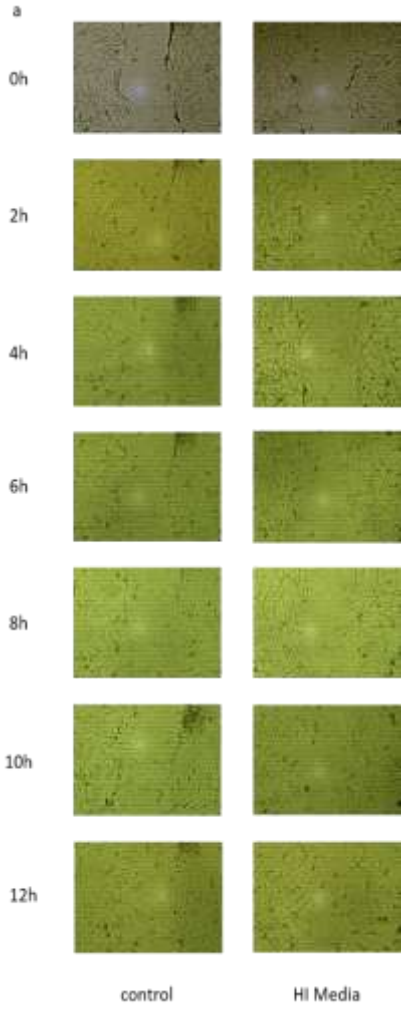

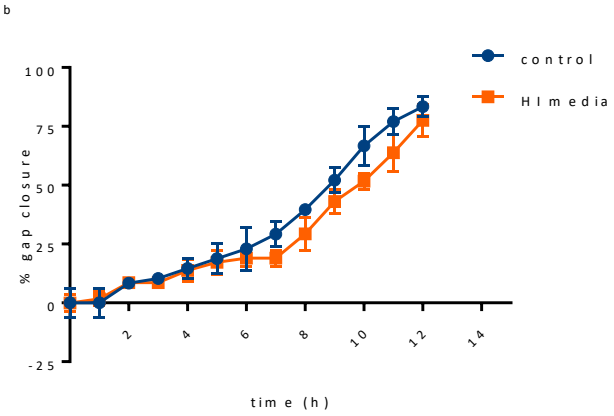

c

Sidak's multiple comparison test	
Time (h)	p values (control vs HI media)
0	>0.9999
1	>0.9999
2	>0.9999
3	>0.9999
4	>0.9999
5	>0.9999
6	>0.9999
7	0.9128
8	0.9087
9	0.9650
10	0.4664
11	0.6439
12	0.9994

Figure 3.3: The effect of HI media on wound closure of WSI cells. WSI cells were seeded at 5 x 10^4 viable cells/ml and allowed to adhere for 48h. The cells were then scratched, control wells were washed and incubated in complete medium while cells in the heat inactivated condition were washed and incubated in complete medium supplemented with heat inactivated serum. Width measurements and pictures were taken at hourly intervals (a). The data were normalized and presented as means ± SEM, n=3 (b). Mean percentage gap closure between controls and HI media treatment was analysed by a two way ANOVA with Sidak's multiple comparison as post hoc test. The p values for the comparison between control and treated cells at each time point are shown table (c).

WSI cells were then treated with 2 different concentrations of PDGF-BB prepared in HI media in the following experiment (Figure 3.4). The data show that there was no significant difference seen in gap closure rates of WSI cells when treated with PDGF-

BB ($p = 0.973$). It was concluded that PDGF-BB had no effect of WSI cells at the concentrations tested.

a

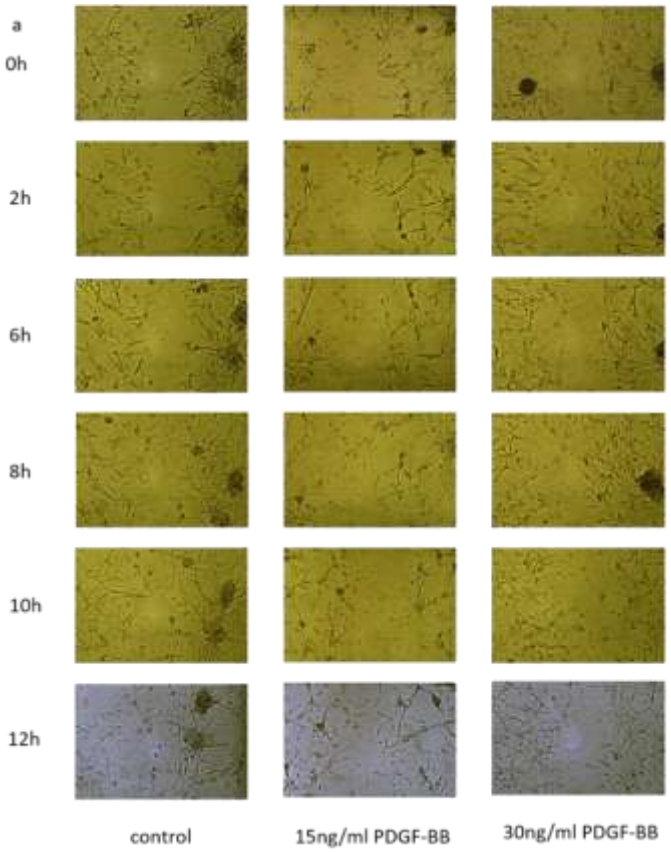

b

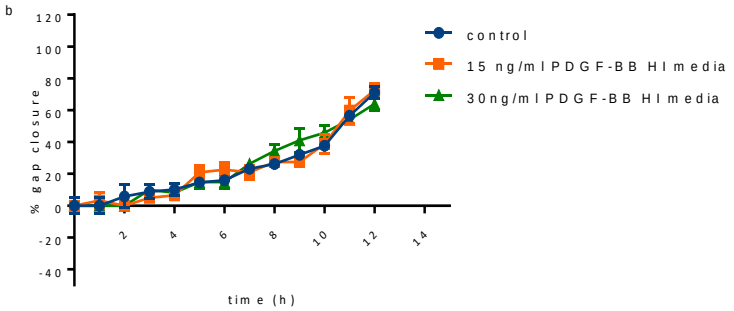

c

Tukey's multiple comparison test	
Conditions	p values
Control vs 15ng/ml PDGF-BB HI media	>0.9999
Control vs 30ng/ml PDGF-BB HI media	>0.9999
15ng/ml PDGF-BB HI media vs 30ng/ml PDGF-BB HI media	>0.9999

Figure 3.4: The effect of PDGF-BB made in HI media on wound closure of WSI cells. WSI cells were cultured in wells at a seeding density of 5 x 10^4 viable cells/ml and were allowed to adhere for 48h. The cells were then scratched, control cells were washed and incubated in complete growth medium while cells while cells treated with PDGF-BB were washed in heat inactivated medium and incubated in heat activated medium supplemented with two different concentrations of PDGF-BB. Width measurements and pictures were taken at hourly intervals (a). The data were normalized and presented as means ± SEM, n=3 (b). Data were analysed by two way ANOVA with Tukey's multiple comparison as post hoc test and the p values for the comparisons are shown in table (c).

3.4.3 The effect of location on gap closure

A second concern that was noted was that during the scratch assay that some parts of the scratches closed at a faster rate in comparison to the reference point. To ensure gap closure was constant throughout the scratch a scratch assay was performed and wound closure over time was measured at three reference points in each well namely top, middle and bottom (Figure 3.5). Form the results it was noted that gap closure remained constant and the closure was more dependent on the size of the gap as no significant difference was found between scratch locations ($p = 0.974$).

a

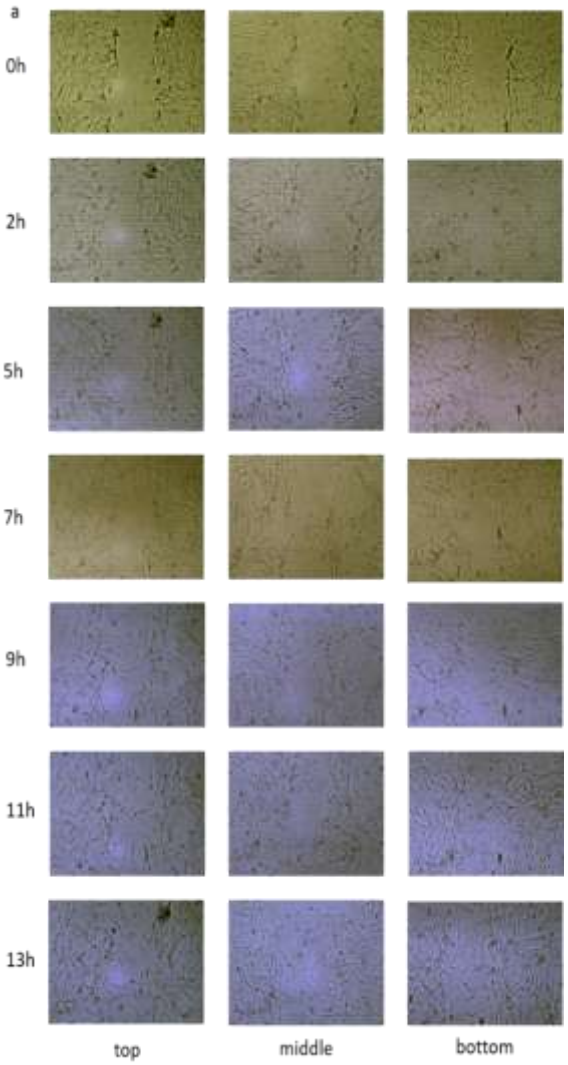

b

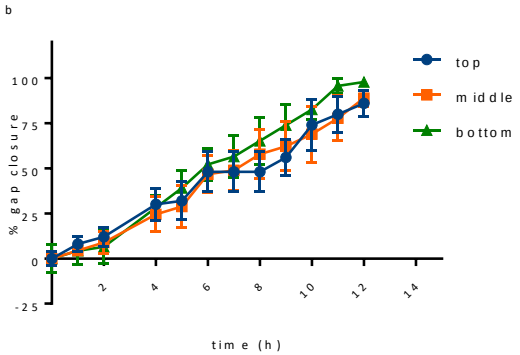

c

Tukey's multiple comparison test	
Conditions	p values
Top vs middle	0.9995
Top vs bottom	0.8335
Middle vs bottom	0.8178

Figure 3.5: Wound closure of WSI cells at different locations in the well. WSI cells were cultured at a seeding density of 5 x 10^4 viable cells/ml and allowed to adhere for 48h. The cells were then subjected to a scratch assay. Width measurements and pictures were taken at hourly intervals (a). The data were normalized and presented as means ± SEM, n=3 (b). The data was analysed by two way ANOVA with Tukey's multiple comparison as post hoc test and the p values for the comparisons are shown in table (c).

3.4.4 Testing commercial inserts on WSI scratch assay: physical removal vs cell exclusion

WSI scratch widths were found to be variable from experiment to experiment. In order to reduce variability commercial inserts form Ibdi were used. The cells were cultured in the wells of the insert and once they had adhered and grown to confluence the scratch assay could be started by simply removing the insert. The inserts would produce a scratch with a defined width of 500µm and so were tested to see how they compared to a previous experiment with heat inactivated media (Figure 3.6). It was found that gap closure took a similar amount of time to when cells were scratched using a pipette tip and was not significantly different when control and HI media were compared ($p = 0.153$) (Figure 3.6).

a

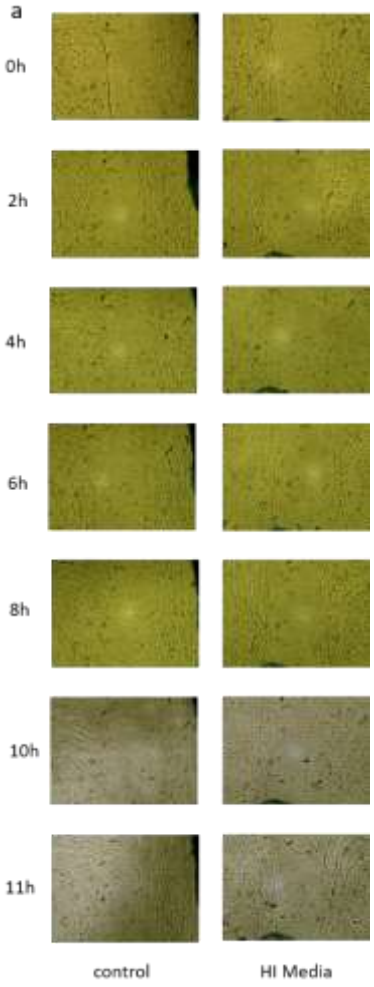

b

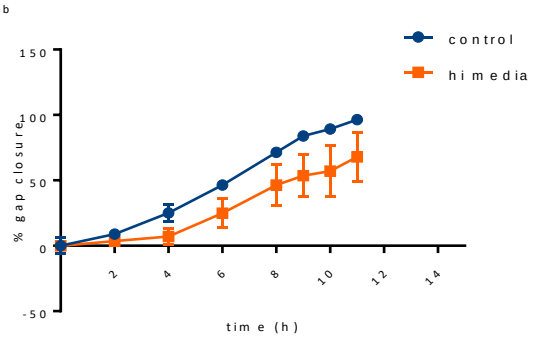

c

Sidak's multiple comparison test	
Time (h)	p values (control vs HI media)
0	>0.9999
2	>0.9999
4	0.8397
6	0.6718
8	0.4833
9	0.2481
10	0.1914
11	0.3162

Figure 3.6: The effect of HI media on wound closure of WSI cells cultured using commercial inserts. WSI cells were seeded at 5 x 10^4 viable cells/ml, allowed to adhere for 48h. The assay was begun by removing the inserts. Control well were washed and incubated in complete culture medium while cells in the HI were washed in HI media and cultured in HI media. The widths of the scratch were measured and pictures were taken at 2h intervals and after 8h they were taken at hourly intervals (a). The data were normalized and presented as means ± SEM, n=3 in graph (b). Mean percentage gap closure between treatments was compared at each time point using a two way ANOVA with Sidak's multiple comparison as post hoc test and the p values for the comparisons are shown in table (c).

3.4.5 Optimization of mitomycin C for the scratch assay

The use of Mitomycin C as an inhibitor of cell division was also optimised for the scratch assay using MTS assay. Initial testing showed that mitomycin C significantly reduced cell viability of WSI cells after 48h. The data showed that cell viability was

significantly reduced even at the lowest concentration tested in WSI cells after 48h incubation (p<0.0001).

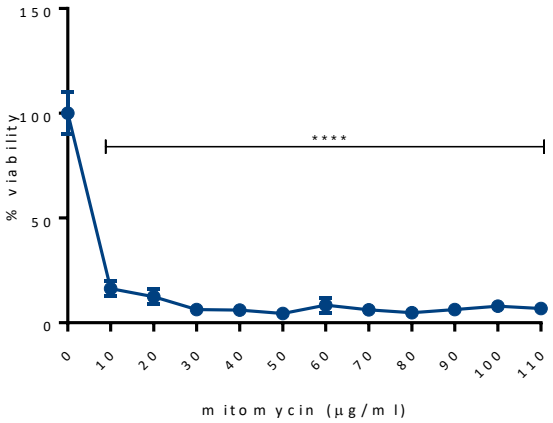

Dunnett's multiple comparisons test	
Comparisons	p values
0 vs. 10	0.0001
0 vs. 20	0.0001
0 vs. 30	0.0001
0 vs. 40	0.0001
0 vs. 50	0.0001
0 vs. 60	0.0001
0 vs. 70	0.0001
0 vs. 80	0.0001
0 vs. 90	0.0001
0 vs. 100	0.0001
0 vs. 110	0.0001

Figure 3.7: WSI cell viability after 48h following mitomycin C treatment. WSI cells were cultured in 96 well plates at a seeding density of 5 x 10^4 viable cells/ml and allowed to adhere for 48h. The cell culture medium was removed and the cells were supplemented with media containing different concentrations of Mitomycin C and incubated for another 48h following which MTS assay was performed. Data are presented as means ± SEM, n=3 and compared to untreated 0µg/ml mitomycin. Data were analysed by a one way ANOVA with Dunnett's multiple comparison as post hoc test where ****(p = 0.0001).

Mitomycin C concentration was lowered and cell viability was assayed by MTS and PI (Figure 3.8). The data showed that even at very low concentrations of 2.5g/ml mitomycin C was toxic to the cells (p<0.0001). Moreover cell death had occurred much earlier than 48h as there was no significant difference in PI (p=0.299). This meant that mitomycin C was causing cell death at much earlier time point.

a

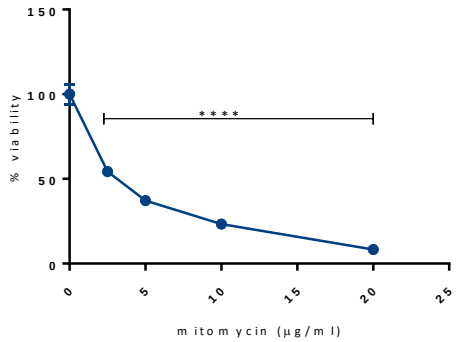

Dunnett's Multiple comparison test	
Comparisons	p values
0.0 vs. 2.5	0.0001
0.0 vs. 5.0	0.0001
0.0 vs. 10.0	0.0001
0.0 vs. 20.0	0.0001

b

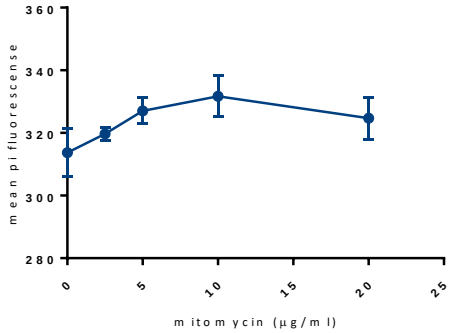

Dunnett's Multiple comparison test	
Comparisons	p values
0.0 vs. 2.5	0.8748
0.0 vs. 5.0	0.3543
0.0 vs. 10.0	0.1546
0.0 vs. 20.0	0.5073

Figure 3.8: WS1 cell viability at 48h following treatment with mitomycin C. WS1 cells were cultured in two 96 well plates at a seeding density of 5 x 10^4 viable cells/ml and allowed to adhere for 48h. The cell culture medium was removed and the cells were supplemented with complete culture media containing different concentrations of mitomycin C and incubated for another 48h following which MTS assay (a) and PI assay (b) was performed. Data are presented as means ± SEM, n=3 and data were compared to 0. Data were analysed by a one way ANOVA with Dunnett's multiple comparison as post hoc test where ****($p<0.0001$)

A mitomycin C time course was setup where cells were treated with mitomycin C and cell viability was assayed by MTS at specific time points (Figure 3.9). The data showed that cell viability decreased with time and that after 24h viability was significantly reduced even at low concentrations of mitomycin C. From the data mitomycin C did not significantly affect cell viability until 16h ($p = 0.999$). An unpaired t-test was carried out between 0h and 16h for the concentration of 10µg/ml and 20µg/ml of mitomycin C and found that both concentrations had no significant difference on cell viability ($p=0.629$ for 10µ/ml and $p=0.138$ for 20µg/ml).

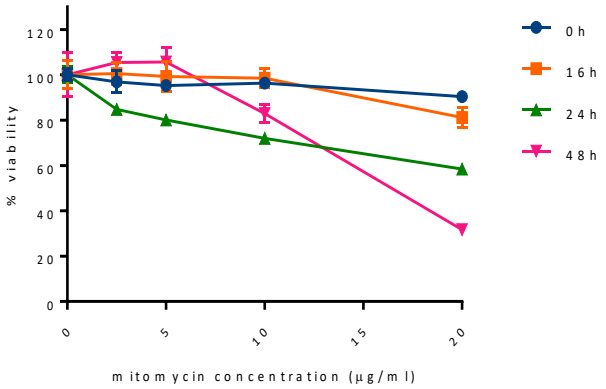

Tukey's multiple comparison test	
Conditions	p values
0h vs 16h	0.9999
0h vs 24h	0.0025
0h vs 48h	0.0302

Figure 3.9: The viability of WSI cells at different time points following treatment with mitomycin C. WSI cells were plated out in 4 plates at a density of 5 x 10^4 viable cells/ml. Cells were allowed to adhere for 48h and then treated with doubling dilutions of mitomycin C and MTS assay was performed at 0, 16, 24 and 48h after treatment. Data are represented as means ± SEM, n=3 (a).Data were analysed by two way ANOVA with and compared to 0h using Tukey's multiple comparison as post hoc test (b).

In order to confirm if 10µg/ml mitomycin C was sufficient to inhibit cell proliferation BrdU assay was performed to determine the extent by which cell proliferation was inhibited by mitomycin C (figure 3.10). The results showed that mitomycin C inhibited cell proliferation at all concentrations tested but there was no significant difference between 10µg/ml and 20µg/ml over the 12h time period. Each concentration inhibited cell proliferation by 90.48% and 95.31% respectively, thus 10µg/ml mitomycin C was chosen and used as a control to determine if gap closure occurred through cell migration alone.

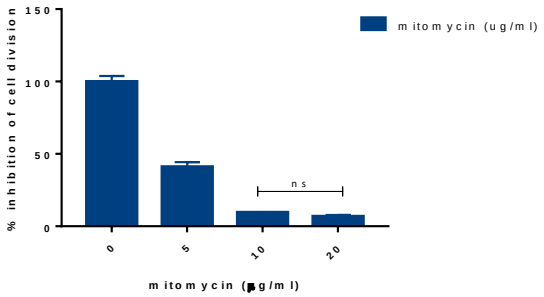

Tukey's multiple comparison test	
Comparisons	p values
0 vs. 5	<0.0001
0 vs. 10	<0.0001
0 vs. 20	<0.0001
5 vs. 10	0.0002
5 vs. 20	<0.0001
10 vs. 20	0.6248

Figure 3.10: The inhibition of WSI cell division by mitomycin C measured by BrdU assay. WSI cells were cultured on a 96 well plate at seeding density of 5 x 10^4 viable cells/ml and incubated at 37°C for 48h. Once the cells had adhered cell culture media was removed and 50µl of 2x dilutions of mitomycin C prepared in complete EMEM was added to test wells. Control wells received no mitomycin C. 20µl of BrdU was added to each well with the exception of wells in the no stain (NS) condition. 30µl of complete EMEM was then added to each well to bring mitomycin concentrations to final concentrations. Cells were then incubated for 12h under optimal culture conditions and then taken through the BrdU assay. Data were normalized presented as means ± SEM, n=3. Data were analysed by a one way ANOVA and means were compared to each other using Tukey's multiple comparison as post hoc test.

3.4.6 The effect of mitomycin C on wound closure of WSI cells.

A new microscope (EVOS Auto FL) was purchased with an on stage incubator (EVOS Auto FL onstage incubator) that could be set up to take time lapse images of the scratch at predetermined time points while simultaneously incubating the cells. Pictures of the cells were taken in phase contrast to allow for cell to be viewed in detail. The scratch assay was then carried out using this microscope. The effect of 10µg/ml of mitomycin C was tested. The scratches were analysed using a free software called TScratch. TScratch calculates the area of the scratch and shows it as a percentage of the whole image. Time lapse images can also be analysed once initial image capture has been carried out. Image analysis was used as it reduces human error and enables researchers to assess cell migration in terms of area as opposed to a single point. In order to test the image analysis software as scratch assay was setup to test the effects of mitomycin C on WSI cells (Figure 3.11). The data showed that mitomycin C did not have a significant effect on WSI gap closure (p = 0.587). This suggested that gap closure was not brought about by cell proliferation but through cell migration. The pictures shown

are of a well in each condition that was analysed by TScratch and depict wound gap as seen by the software.

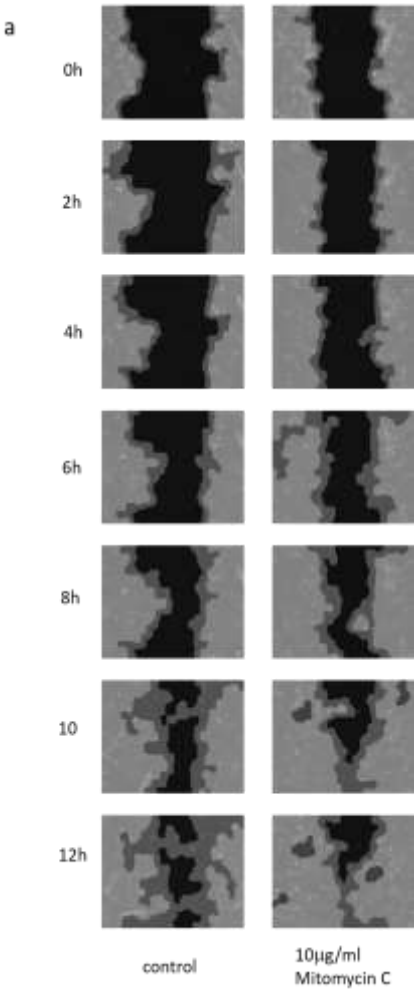

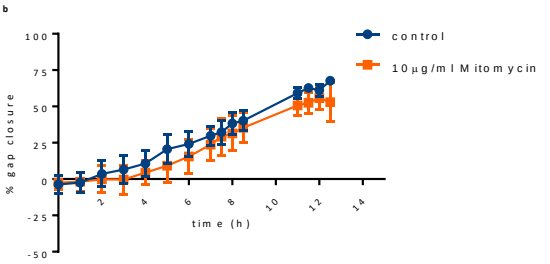

c

Sidak's multiple comparison test	
Time (h)	p values (control vs Mitomycin C)
0	>0.9999
1	>0.9999
2	>0.9999
3	>0.9999
4	>0.9999
5	0.9987
6	>0.9999
7	>0.9999
7.5	>0.9999
8	>0.9999
8.5	>0.9999
11	>0.9999
11.5	0.9997
12	>0.9999
12.5	0.9820

Figure 3.11: The effect of mitomycin C on wound closure of WS1 cells. WS1 cells were cultured on well plates at a seeding density of 5 x 10^4 viable cells/ml and allowed to adhere for 48h. Cells were then subjected to a scratch assay and pictures were taken using an automated microscope. Pictures were taken at hourly intervals for the first 7h and then at 30min intervals for the next 5h. Images were analysed using TScratch software and migration at each time point was normalized. Data are presented as means ± SEM, n=3 and mean percentage gap closure was compared to control at each time point. Data were analysed by a two way ANOVA with Sidak's multiple comparison as post hoc test.

With the automated microscope the pictures were taken at exactly the same locations and at higher resolution for the software to pick up even minute movements of the cells. The microscope could also pick up individual movements of the cells throughout the time course. Unlike epithelial cells that move as sheets fibroblasts can bud off and migrate in to the wound site independently. This blebbing effect by the production of

lamillopodia is promoted by □-catenin and allows them to migrate swiftly to a wound site (Poon, Nik, Ahn, Slade, & Alman, 2009). WSI cells showed these characteristics as they came off the monolayer they would randomly irrespective of their orientation move towards the other side of the scratch, but not always in the direction they began as shown in the figure below (Figure 3.11). The migration could also be in response chemotactic signals, but what they are exactly remains to be elucidated.

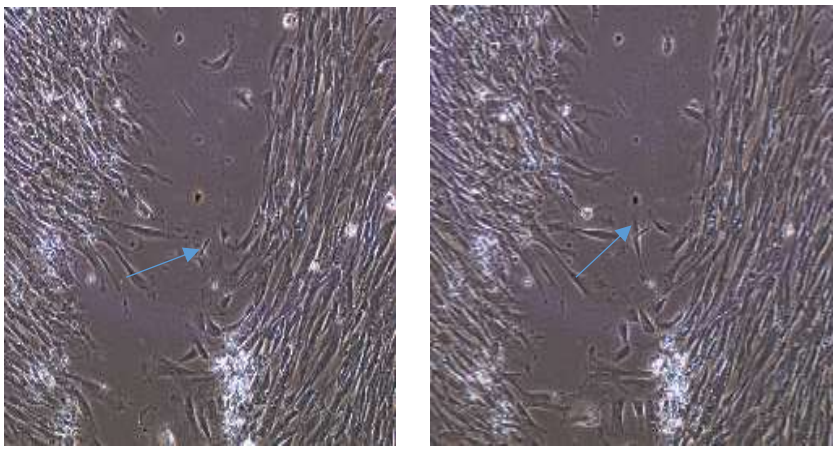

Figure 3.12: WSI cells migrate into the wound in random trajectories. The images are taken form an automated time-lase (8h-8.5h) to demonstrate that WSI cells do not migrate into the scratch following a set trajectory pattern the arrows highlight a cell that is migrating into the gap but has changed its trajectory to lie parallel to the wound edge.

A second aspect generated by the variability of the scratch has shown a correlation ($p=0.036$) in net movement of cells. If similar sized scratches were not compared, the net movement of cells in smaller scratches is lower than the net movement of cells in larger scratches over the same length of time (Figure 3.13). This would suggest that cell motility is governed by the presence of a chemotactic factor. Whether this factor is inhibitory (secreted when cells are in close proximity) or promotive (secreted when cells are further away) needs to be investigated. This effect was also observed during image capture of the cells in the scratch assay, where cells would bleb in random manner and not follow the orientation they began in (Figure 3.12).

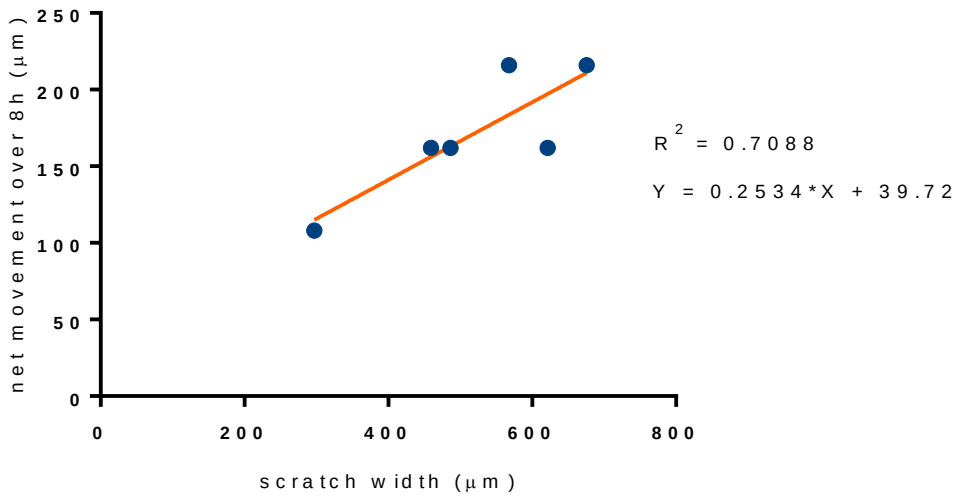

Figure 3.13: The net movement of WS1 cells with varying widths over a period of 8h. WS1 cells were cultured in 12 well plates at a cell density of 5 x 10^4 viable cells/ml. The cells were scratched using a pipette tip, washed twice and incubated in complete medium. Measurements and pictures were taken at 2h intervals. Each point represents cells in a single well and their net movement over a period of 8h.

3.5 Discussion

Previous studies have used MCF-7 (Guttilla et al., 2012), MG-63 (Ziyan, Shuhua, Xiufang, & Xiaoyun, 2011), and WS1 cells (Bizzarro et al., 2012; Zungu, Mbene, Hawkins Evans, Houreld, & Abrahamse, 2009) to investigate cell migration. Each of these cells were tested in a scratch assay evaluated for suitability to study wound healing (Figure 1). A working scratch assay has been developed and optimized using WS1 cells with the purpose of investigating wound healing in diabetes. WS1 cell were chosen as they were fibroblasts and had a finite life span similar to cells in vivo. Fibroblasts are one of the first cells that move into the wound bed following infiltration of monocytes and macrophages where they carry out the important task of synthesising ECM proteins and growth factors (Guo & Dipietro, 2010). Fibroblast at the wound edge have been shown to differentiate into morphologically distinct myofibroblasts and help in contraction of the wound (Darby et al., 2014). As the study aimed to investigate the effects of cell migration into the wound, fibroblasts were the ideal candidate to develop a scratch assay.

The advantage of a scratch assay is that it allows for the simulation of wound conditions in vitro and enables quantitative analysis on cell migration to be performed (Jonkman

et al., 2014; Liang et al., 2007). It also allows the researchers to investigate the effects of conditions such as hyperglycaemia on cell migration and to assess the efficacy of treatments or drugs that enhance wound closure by fibroblasts via promotion of cell migration. Scratch assays have been used as a high throughput screening method to screen for anticancer drugs that inhibit cancer metastasis (Hulkower & Herber, 2011). The method can easily be automated with a suitable microscope, however a scratch assay cannot simulate all the complications that can arise in a chronic diabetic wound. For instance the assay used in this study could not account for pre-existing inflammatory conditions and complications that arise as a result of insulin resistance in peripheral tissue such as neuropathy. The scratch assay also cannot account for the local wound environment found in a diabetic ulcer.

The effect of PDGF-BB was tested on WSI gap closure (Figure 3.2). The data was found to be inconsistent with the results published in other studies as PDGF-BB had no effect on WSI cell migration (W. Li et al., 2007). One reason for this could be attributed the presence of growth factors that would mask the stimulatory effects of PDGF-BB. To address this issue a scratch assay was performed on WSI cells using heat inactivated (HI) media (Figure 3.3) and no significant difference was seen. A scratch assay was then performed using 2 different concentrations of PDGF-BB in HI media (figure 3.4) and found to have no significant difference in gap closure of WSI cells. Pierce et al., (1995) have previously shown that fibroblasts in the wound bed have receptors for PDGF-BB and recommended that recombinant, rPDGF-BB be used to treat chronic wounds where the relative concentration of PDGF-BB is low. The group also identified that fibroblasts in the wound usually produce large quantities of the long isoform of PDGF called PDGF-AA_L in both chronic and acute wounds which could be another reason why PDGF-BB has no effect on WSI cells; moreover the action of PDGF-BB can only occur if the cells have receptors for PDGF-BB (Heldin, Laurent, & Heldin, 1989). PDGF-BB binds to its receptor PDGF-β which is expressed on mature granulation tissue including wound fibroblasts and perivascular cells (Pierce et al., 1995) which could mean that WSI cells possibly do not express the receptor PDGF-β; however the presence of PDGF-β was not tested in this study.

One observation was that some locations on the scratch seemed to close at a faster rate than the reference point and so a scratch assay was carried out and gap measurements were taken at the centre and extremes of the well (Figure 3.5). No significant difference

was found in gap closure between locations suggesting that the cells moved into the scratch at a steady rate across the scratch. Commercial inserts were also were also tested to see if there was a difference in migration when using mechanical or cell exclusion methods (Figure 3.6). No difference was seen in gap closure when either method was applied. The advantage of the cell exclusion method was that it required very few cells to form a monolayer, produced consistent gap width and could be used for large experiments, but their lack of reusability and cost offset their advantage. Another advantage for using commercial inserts is that they do not damage ECM components that are coated onto the plate to ensure cell adhesion (Jonkman et al., 2014), however in this study uncoated plates were used.

In order to ascertain that gap closure in this study occurred as a result of cell migration and not as a result of cell proliferation, mitomycin C was optimised using MTS assay. The doubling time for WSI was 44h and so cells were treated with mitomycin and incubated for 48h. Mitomycin C was found to be acutely toxic to the cell even at low concentrations of 10µg/ml as detected by MTS assay (Figure 3.7). Reducing the concentration to 2.5µg/ml was still found to be toxic to WSI cells (Figure 3.8). In order to circumvent this issue cell viability was assayed at various time points and showed that cellular viability did not reduce significantly after 16h when treated with 10µg/ml and 20µg/ml of mitomycin C (Figure 3.9).

A BrdU assay was performed in order to test which concentration would be most suitable to use in the scratch assay. The assay showed that there was no significant difference between either concentration as they inhibited cell proliferation by 90.48% and 95.31% respectively. 10µg/ml was therefore chosen as it inhibited cell proliferation and would be less cytotoxic to cells. Once image capture of the scratch had been automated this concentration of mitomycin C was tested on a scratch assay to see if gap closure occurred through cell proliferation or migration. No significant difference was seen between untreated control and cells treated with mitomycin C. This showed that gap closure in this study occurred through cell migration alone (Figure 3.10). The effect of an inhibitor of cell migration will be investigated in the near future.

In this study only similar sized scratch widths were measured and analysed, however a correlation was found when scratches of different sizes were compared to each other. The net movement of cells in smaller scratches was lower than the movement of cells in larger scratches over the same length of time (figure 3.13). This would suggest that

cell migration is not dependant on gap width and orientation alone and is regulated by other factors. What these factors are remains to be discovered and how can they influence wound closure both in vivo and in vitro remains to be seen. WS1 did not seem to migrate in a defined trajectory when observed through time-lapse images (figure 3.12) this could be regulated by these promotive or inhibitory factors that would cause cells to move toward them a faster or slower rate.

In this study gap width measurements at specific time points were measured for most of the experiments and in later experiments area measurements were used primarily to compare whether area measurements offered better accuracy. Image analysis on earlier experiments could not be carried out as they were of poorer quality and generated high variability. When area measurements of the scratch was attempted TScratch at times would consider areas where no cells are present as the edge of the scratch and give very high percentage cover rates. TScratch recommends using phase contrast pictures as opposed to pictures taken in bright field which were used in earlier experiments (Gebäck et al., 2009). Fibroblasts and keratinocytes are the first cells to move into the wound and initiate proliferative phase of wound healing and hence prove to be ideal candidates to investigate the effects of a treatments such as heat shock in a diabetic wounds where the migration of fibroblasts is reduced (Hehenberger, Heilborn, Brismar, & Hansson, 1998).

Chapter 4 Investigating the effect of heat shock in in vitro wound healing

4.1 Introduction

Impaired wound healing is a common problem in diabetes and is caused by underlying chronic inflammation (Magill et al., 2010). Pre-existing neuropathic conditions bring about a loss of feeling in the lower limbs, produce foot deformities and the formation of chronic wounds in the lower limbs that do not heal (Brem & Tomic-Canic, 2007). Delayed by the lack of cell migrating into the wound exposes the wound to the environment and possible infection which may eventually lead to amputation. Impaired wound healing is one of the leading causes of patient mortality in diabetes. Migration of fibroblasts into the wound is an important aspect of wound healing and thus a scratch assay was developed to investigate cell migration in the wound and the effect of hyperglycaemia and heat shock on cell migration.

The response of cells to thermal stress induces the expression of cell stress proteins or heat shock proteins (HSP). These proteins act as molecular chaperones that unfold thermally damaged proteins, direct irreparable proteins for degradation and down regulate the expression of apoptotic genes to ensure cell survival (Verghese et al., 2012). The induction of these proteins is highly conserved in all organisms and is collectively called the heat shock response. In diabetes this response is impaired (Kondo et al., 2014; Magill et al., 2010).

Induction of HSP has been shown to inhibit activation of caspases in cells and reduce reactive oxygen species (C Garrido et al., 1999). They also been shown to inhibit JNK activity and confer protection from apoptosis (Park, Lee, Huh, Seo, & Choi, 2001). Recent studies in mice and humans have shown that induction of HSP by heat shock coupled with mild electrical stimulation improves insulin sensitivity (Kondo et al., 2014). Topical application of HSP proteins have also shown to improve wound healing in mice (W. Li et al., 2007). Taken together these studies have shown that heat shock stimulates wound healing and improves insulin sensitivity. However the mechanisms by which this occurs remains poorly understood. Moreover how heat shock specifically affects cell migration is unknown. The effect of heat shock on cell migration was tested in this chapter using an in vitro scratch assay.

4.2 Aims

To investigate the effect of heat shock on WSI cell migration and to further investigate the effect of cell migration under hyperglycaemic conditions.

4.3 Methods used in this chapter

4.3.1 Scratch assay

A scratch assay was performed using WSI cells as described in detail the methods chapter 2 sections 2.3.4.2. Details for the methods for the experiments described in this chapter can be found in sections 2.3.4.8 to 2.3.4.14. All data described here have a sample number of 3.

4.4 Results

4.4.1 Is a recovery period essential for wound closure?

Following heat shock treatment a recovery period was given to cells in order to produce cell stress proteins (Figure 4.1). The results showed that heat shock of 40°C had no effect on cell migration in WSI cells ($p=0.5443$). As cells were incubated under optimal cell culture conditions following heat shock treatment (i.e. 37°C and 5% CO_2), a recovery period may not be necessary.

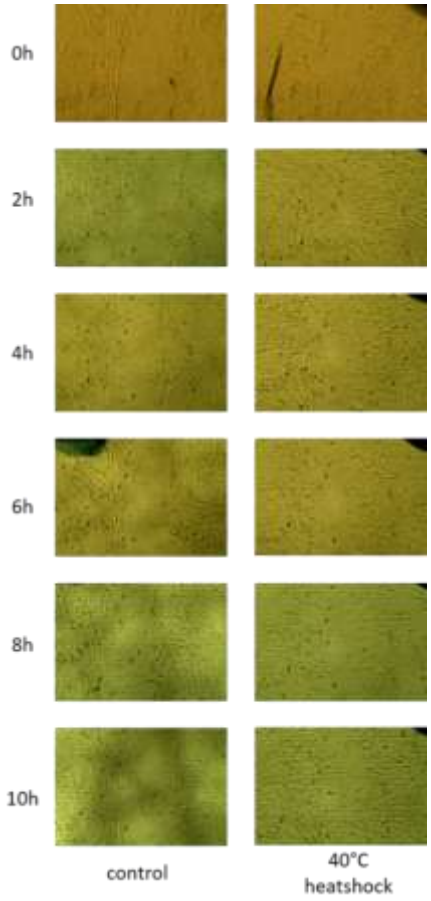

b

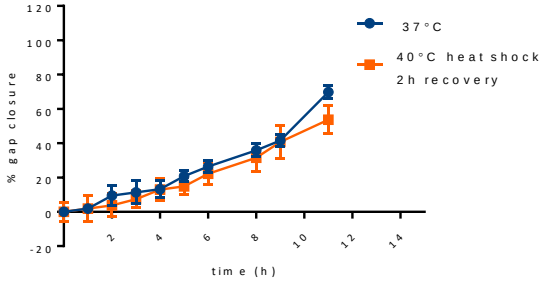

c

Sidak's multiple comparison test	
Time (h)	p values (37°C vs 40°C 2h recovery)
0	>0.9999
1	>0.9999
2	0.9987
3	>0.9999
4	>0.9999
5	0.9983
6	>0.9999
7	0.9999
8	>0.9999
9	0.4329
11	>0.9999

Figure 4.1: The effect of heat shock at 40°C for 1h followed by a 2h recovery period on wound closure of WSI cells. WSI cells were cultured at a seeding density of 5 x 10^4 viable cells/ml and allowed to adhere for 48h. They were then placed in an incubator at 40°C for 1h and then incubated for a further 2h at 37°C and put through a scratch assay. Width measurements and pictures were taken at hourly intervals (a). The data were normalized and presented as means ± SEM, n=3 (b). Mean percentage gap closure between treatments was compared at each time point using a two way ANOVA with Sidak's multiple comparison as post hoc test (c).

To ensure a recovery period was not necessary WSI cells were given a heat shock treatment at 40°C and where immediately used for a scratch assay (Figure 4.2). The data showed that heat shock treatment at 40°C had no significant effect on the migration of WSI cells (p=0.80), thus the following experiments no recovery period was used.

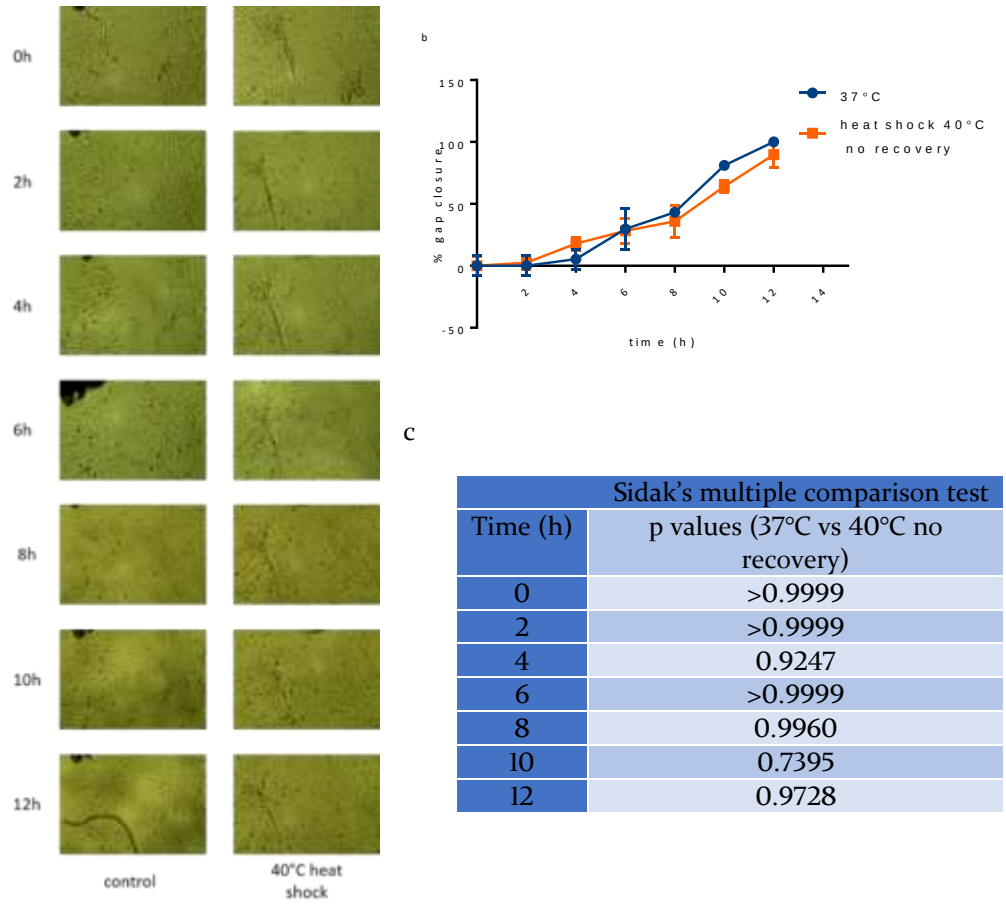

c

	Sidak's multiple comparison test
Time (h)	p values (37°C vs 40°C no recovery)
0	>0.9999
2	>0.9999
4	0.9247
6	>0.9999
8	0.9960
10	0.7395
12	0.9728

Figure 4.2: The effect of heat shock at 40°C for 1h with no recovery period on wound closure of WSI cells. WSI cells were cultured at a seeding density of 5 x 10^4 viable cells/ml and allowed to adhere for 48h. The cells in the heat shock condition were subjected to a heat shock of 40°C for 1h following which they were scratched. Width measurements and pictures were taken at 2h intervals (a). The data were normalized and presented as means ± SEM, n=3 (b). Mean percentage gap closure between treatments was compared at each time point by a two way ANOVA with Sidak's multiple comparison as post hoc test (c).

4.4.2 Heat shock treatment for 1h at various temperatures

WSI cells were given a heat shock of 1h at 39°C (Figure4.3) (p=0.205), 41°C (figure 4.4) (p=0.8905), 42°C (Figure4.5) (p=0.6541) and 45°C (figure4.6) (p=0.560). The data showed that there was no significant difference between in cell migration between controls and heat shock treatments.

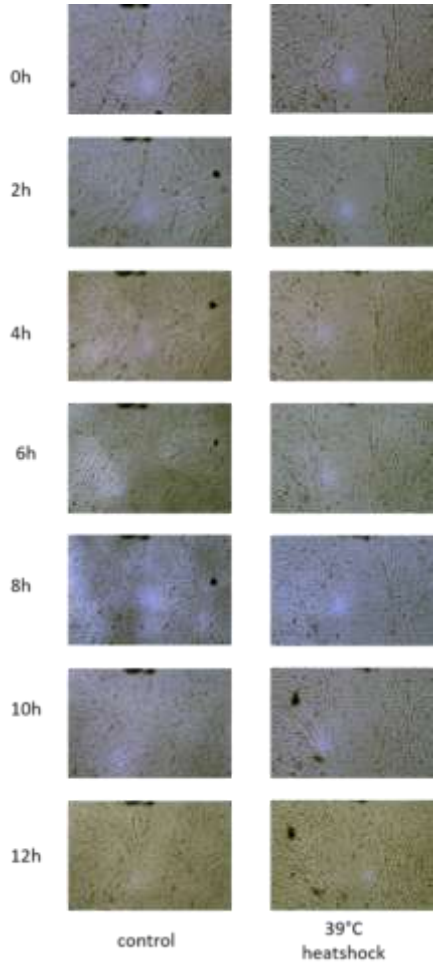

b

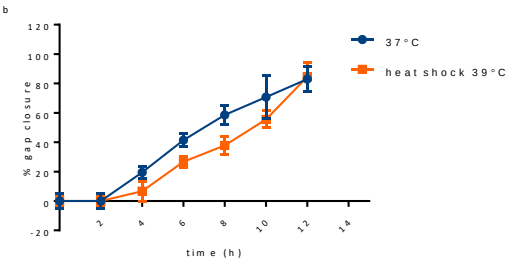

c

Sidak's multiple comparison test	
Time (h)	p values (37°C vs heat shock 39°C)
0	>0.9999
2	>0.9999
4	0.7889
6	0.6553
8	0.2626
10	0.6276
12	>0.9999

Figure 4.3: The effect of heat shock at 39°C for 1h on wound closure of WS1 cells. WS1 cells were cultured at a seeding density of 5 x 10^4 viable cells/ml and allowed to adhere for 48h. Treatment plate was placed in an incubator at 39°C for an hour while the control plate was incubated at 37°C. The cells were scratched immediately after heat shock treatment. Width measurements and pictures were taken at 2h intervals (a). The data were normalized and presented as means ± SEM, n=3 (b) Mean percentage gap closure between treatments was compared at each time point by a two way ANOVA with Sidak's multiple comparison as post hoc test (c).

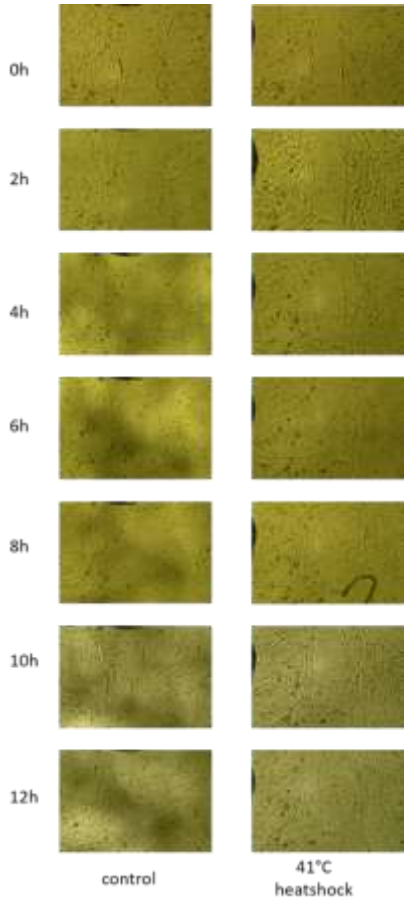

b

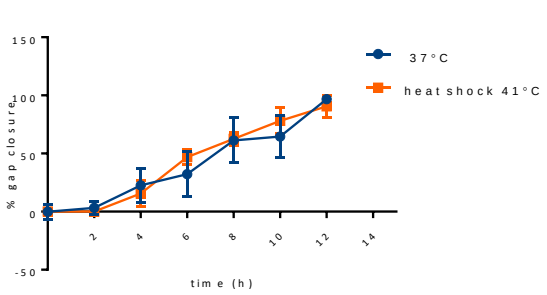

c

Sidak's multiple comparison test	
Time (h)	p values (37°C vs heat shock 41°C)
0	>0.9999
2	>0.9999
4	0.9995
6	0.9601
8	>0.9999
10	0.9728
12	0.9998

Figure 4.4: The effect of heat shock at 41°C for 1h on wound closure of WSI cells. WSI cells were cultured at a seeding density of 5 x 10^4 viable cells/ml and allowed to adhere for 48h. The treatment cell culture plate was then placed in an incubator at 41°C for an hour and put through a scratch assay whilst the control was incubated at 37°C. Width measurements and pictures were taken at 2h intervals (a). The data were normalized and presented as means ± SEM, n=3 (b). Mean percentage gap closure between treatments was compared at each time point by a two way ANOVA with Sidak's multiple comparison as post hoc test (c).

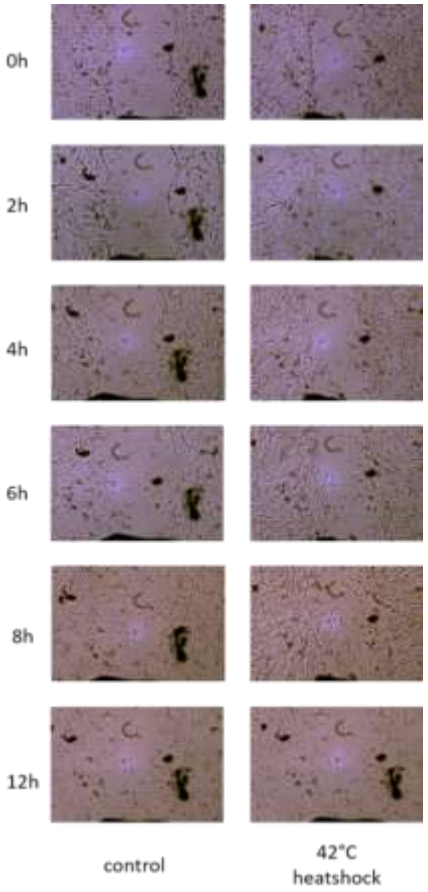

b

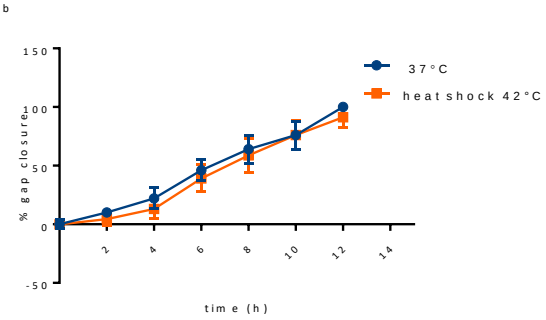

c

Sidak's multiple comparison test	
Time (h)	p values (37°C vs heat shock 42°C)
0	>0.9999
2	0.9995
4	0.9909
6	0.9982
8	0.9997
10	>0.9999
12	0.9923

Figure 4.5: The effect of heat shock at 42°C for 1h on wound closure of WSI cells. WSI cells were cultured at a seeding density of 5 x 10^4 viable cells/ml and allowed to adhere for 48h. The cells in the heat shock condition were subjected to a heat shock of 42°C for 1h while the controls were incubated at 37°C. The cells were then subjected to a scratch assay. Width measurements and pictures were taken at 2h intervals (a). The data were normalized and presented as means ± SEM, n=3 (b). Mean percentage gap closure between treatments was compared at each time point by a two way ANOVA with Sidak's multiple comparison as post hoc test (c).

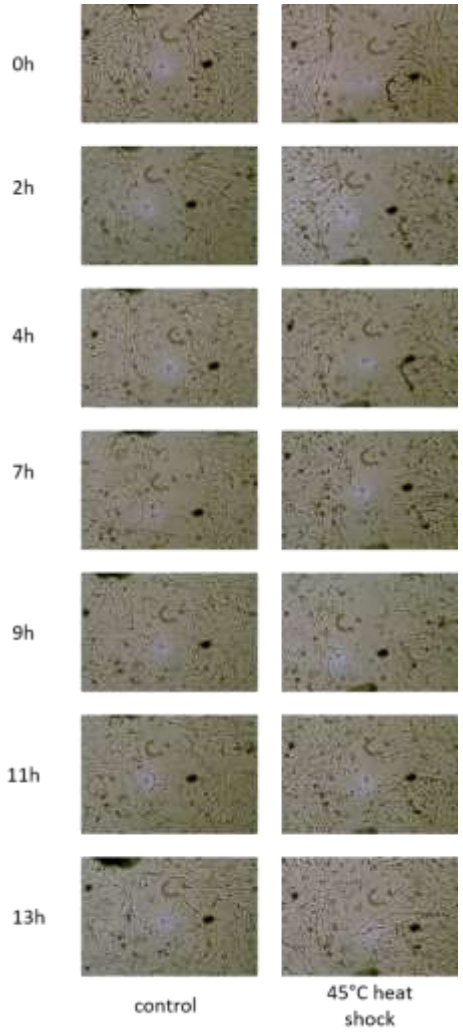

b

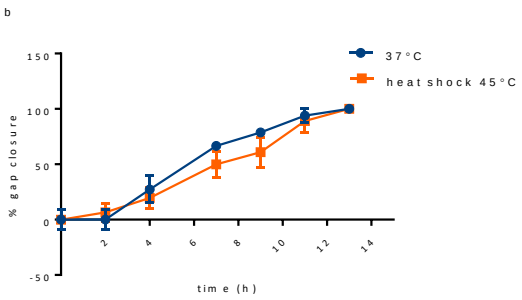

c

Sidak's multiple comparison test	
Time (h)	p values (37°C vs heat shock 45°C)
0	>0.9999
2	0.9990
4	0.9970
6	0.8231
8	0.7668
10	0.9999
12	>0.9999

Figure 4.6: The effect of heat shock at 45°C for 1h on wound closure of WSI cells. WSI cells were cultured at a seeding density of 5 x 10^4 viable cells/ml and allowed to adhere for 48h. The cells in the heat shock condition were subjected to a heat shock of 45°C for 1h while the controls were incubated at 37°C. The cells were then subjected to a scratch assay. Width measurements and pictures were taken at 2h intervals (a). The data were normalized and presented as means ± SEM, n=3 (b) Mean percentage gap closure between treatments was compared at each time point by a two way ANOVA with Sidak's multiple comparison as post hoc test (c).

As heat shock treatments at the temperatures tested seemed to have no significant effect on gap closure the effect of incubation at high temperatures was tested. A scratch assay was performed where control scratches were incubated at 37°C and the test scratches were incubated at 45°C (Figure 4.7). The data showed that incubation at 45°C had a significant effect on WSI cells (p=0.0047) and inhibited their migration. After 5h there is a significant difference (p<0.0001) in gap closure between control cells and cells incubated at 45°C. The cells begin to appear morphologically different after

3h and the change in morphology is very clear at 6h. This is because incubation at such a high temperature would cause cell death.

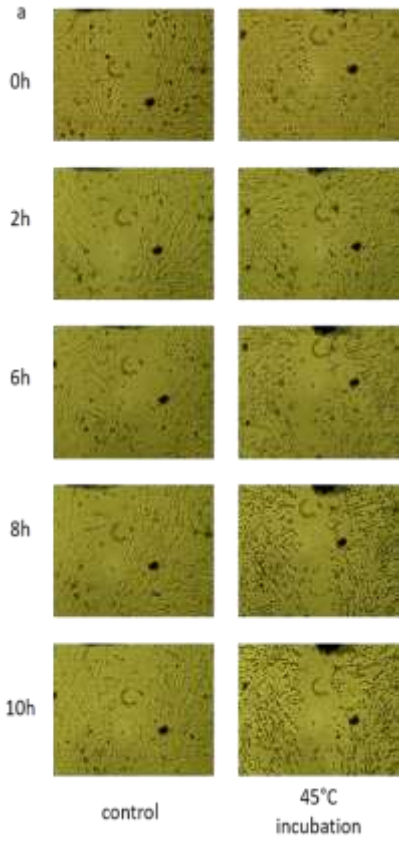

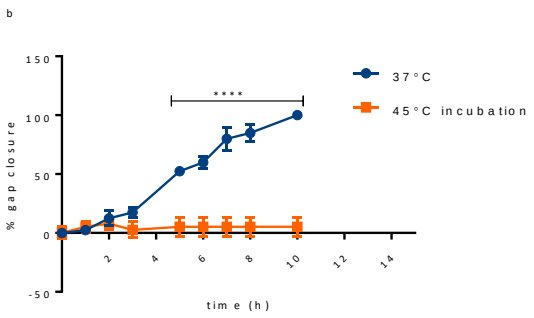

c

Sidak's multiple comparison test	
Time (h)	p values (37°C vs heat shock 42°C)
0	>0.9999
1	>0.9999
2	0.9998
3	0.6078
5	<0.0001
6	<0.0001
7	<0.0001
8	<0.0001
10	<0.0001

Figure 4.7: The effect of 45°C incubation for 10h on wound closure of WS1 cells. WS1 cells were cultured at a seeding density of 5 x 10^4 viable cells/ml and allowed to adhere for 48h. The cells were then subjected to a scratch assay. Cells in the control wells were incubated at 37°C while cells in the incubation condition were incubated at 45°C. The widths of the scratch were measured and pictures were taken at hourly intervals (a). The data were normalized and presented as means ± SEM, n=3 and significance is indicated where '****' indicates p<0.0001 (b). Mean percentage gap closure between treatments was compared at each time point by a two way ANOVA with Sidak's multiple comparison as post hoc test (c).

4.4.3 Testing commercial inserts on WS1 scratch assay: physical removal vs cell exclusion

The effect of heat shock at 39°C for 1h was tested using commercial inserts to see if there was any difference in cell migration of WS1 cells and determine whether cell exclusion or cell removal were better modes by which the scratch assay should be performed (Figure 4.8). The data and pictures showed that there is no significant

difference between gap closure between control and heat shock treatment at 39°C for an hour (p=0.171).

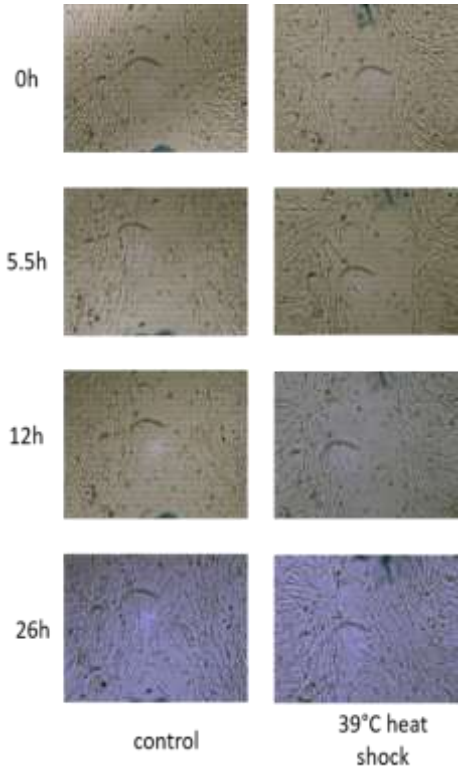

b

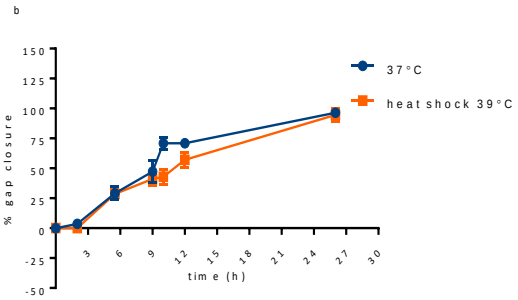

c

Sidak's multiple comparison test	
Time (h)	p values (37°C vs heat shock 39°C)
0	>0.9999
2	0.9985
5.5	>0.9999
9	0.9637
10	0.0025
12	0.3332
26	>0.9999

Figure 4.8: The effect of heat shock at 39°C for 1h on wound closure of WS1 cells using commercial inserts. WS1 cells were cultured in inserts at a seeding density of 5 x 10^4 viable cells/ml and allowed to adhere for 48h. Test well plate was incubated at 39°C for 1h and the scratch assay was started by removing the inserts. The widths of the scratch were measured and pictures were taken at 3, 6, 9, 12 and 26h intervals (a). The data were normalized and presented as means ± SEM, n=3 (b). Mean percentage gap closure between treatments was compared at each time point by two way-ANOVA with Sidak's multiple comparison as post hoc test (c).

The effect of compounding stresses heat shock and HI media were tested on WS1 gap closure (Figure 4.9). No significant difference was seen (p=0.471).

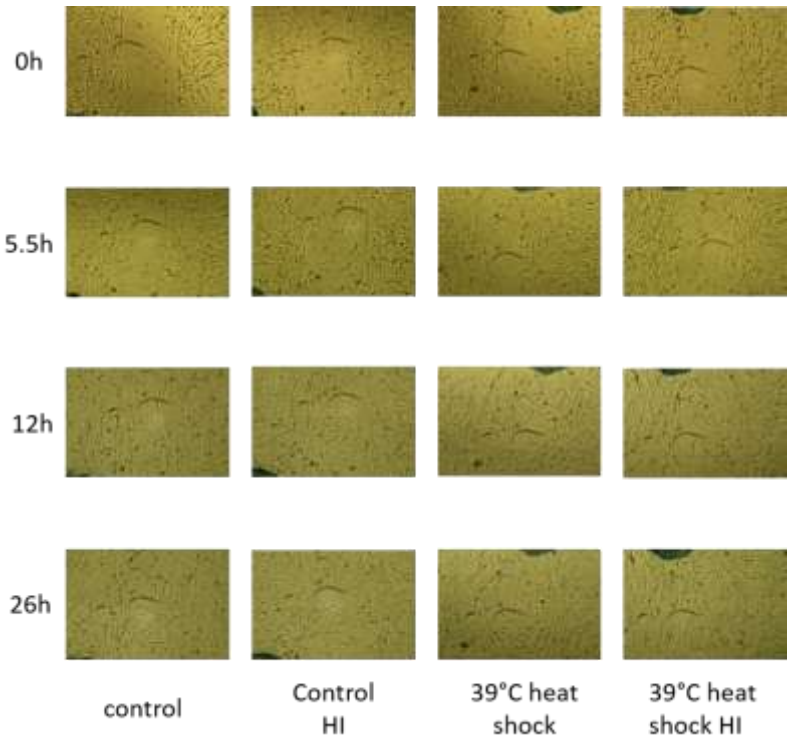

b

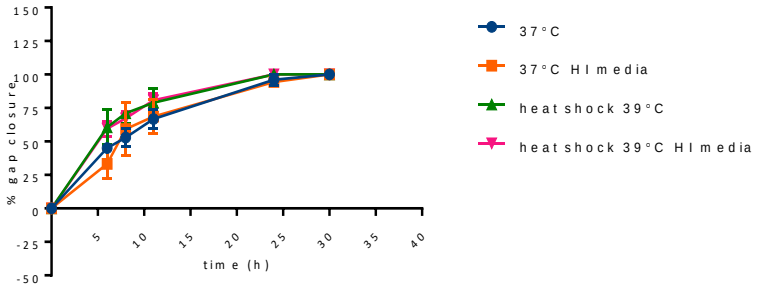

c

Dunnett's multiple comparison test	
Test conditions	p values
37°C vs 37°C HI media	0.9983
37°C vs Heat shock 39°C	0.5917
37°C vs Heat shock 39°C Hi media	0.5563

Figure 4.9: The effect of heat shock at 39°C for 1h and HI media on wound closure of WSI cells. WSI cells were cultured in inserts at a seeding density of 5 x 10^4 viable cells/ml in two well plates and allowed to adhere for 48h. The test plate was incubated at 39°C for 1h. The inserts were then removed to start the scratch assay. Cells in control conditions were washed with complete culture medium and incubated in complete culture medium. Cells in the heat inactivated condition were washed and incubated with heat inactivated media. Data are represented as means ± SEM, n=3 (b). Mean percentage gap closure between treatments was compared to control by two way ANOVA with Dunnett's multiple comparison as the post hoc test (c).

4.4.4 The effect of hyperglycaemia on WSI cells

Following on from the automation of image capture of the scratch assay in chapter 3 a control experiment was setup to assess the effect of high glucose on the scratch assay. (Figure 4.10). The data showed that 30mM glucose had no effect on wound closure (p=0.516).

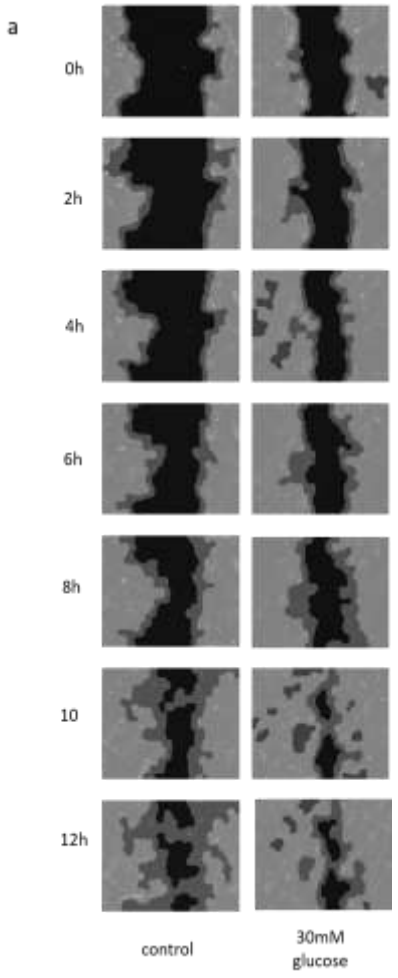

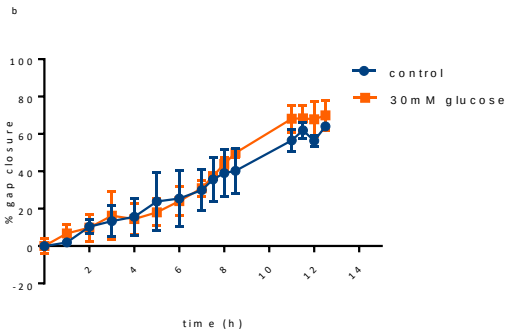

c

Sidak's multiple comparison test	
Time (h)	p values (control vs 30mM glucose)
0	>0.9999
1	>0.9999
2	>0.9999
3	>0.9999
4	>0.9999
5	>0.9999
6	>0.9999
7	>0.9999
8	>0.9999
8.5	>0.9999
11	0.9996
11.5	0.9974
12	>0.9999
12.5	0.9975

Figure 4.10: The effect of hyperglycaemia on wound closure of WSI cells. WSI cells were cultured on well plates at a seeding density of 5 x 10^4 viable cells/ml and allowed to adhere for 48h. Cells were then put through a scratch assay. Control wells received complete culture medium while hyperglycaemic wells received complete culture medium supplemented with 30mM glucose. Time lapse pictures were taken at hourly intervals for the first 7h and then at 30 min intervals for the remaining 5h (a). Cell migration was analysed using TScratch software and migration at each time point was normalized. Data are represented as means ± SEM, n=2 (b). Mean percentage gap closure between treatments was compared at each time point using a two-way ANOVA with Sidak's multiple comparison as a post hoc test.

In the following experiment the effect of heat shock and hyperglycaemia were tested (figure 4.11). The data showed that there was no significant difference in cell migration of WS1 cells when under heat shock and hyperglycaemic conditions ($p=0.188$).

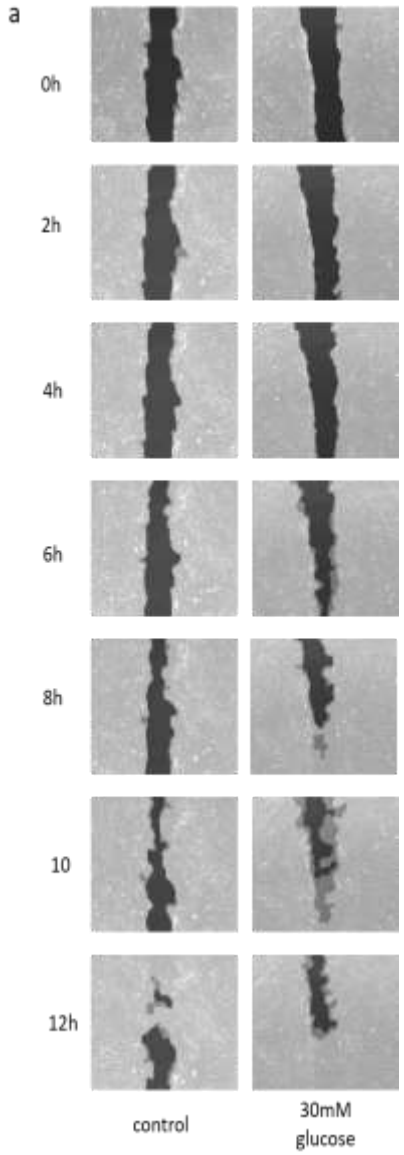

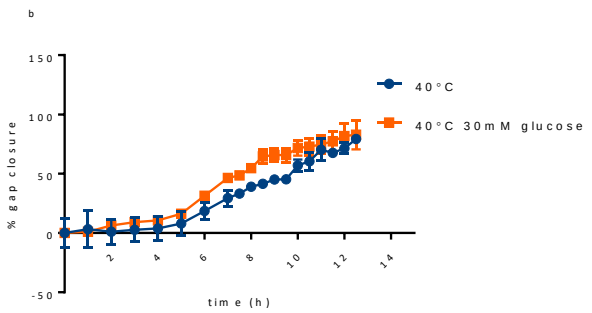

c

Sidak's multiple comparison test	
Time (h)	p values (40°C heat shock vs 40°C 30mM glucose)
0	>0.9999
1	>0.9999
2	>0.9999
3	>0.9999
4	>0.9999
5	>0.9999
6	0.9833
7	0.8300
7.5	0.9185
8	0.9116
8.5	0.3593
9	0.5549
9.5	0.5658
10	0.9484
10.5	0.9892
11	>0.9999
11.5	0.9995
12.	0.9988
12.5	>0.9999

Figure 4.11: The effect of heat shock at 40°C for 1h and hyperglycaemia on wound closure of WSI cells. WSI cells were cultured in inserts at a seeding density of 5 x 10^4 viable cells/ml and allowed to adhere for 48h. The cells were incubated at 40°C for 1h and then put through the scratch assay. Control wells received complete culture medium while hyperglycaemic wells received complete culture medium supplemented with 30mM glucose. Time lapse pictures were taken at hourly intervals for the first 7h and then at 30 min intervals for the remaining 5h (a). Cell migration was analysed using TScratch software and migration at each time point was normalized and data are represented as means ± SEM, n=2. Mean percentage gap closure between treatments was compared at each time point using a two-way ANOVA with Sidak's multiple comparison as a post hoc test.

As all other heat shock treatments did not show a significant difference on wound closure it was thought that the length of heat shock was too small to show any significant difference in cell migration. A scratch assay was then setup where the cells

were incubated at 42°C for 3h and then put through the scratch assay (Figure 4.20). The effect of high glucose and mitomycin C were also tested so data could be compared between experiments. The data showed that there was no significant difference between control, hyperglycaemia and mitomycin C on wound closure (p=0825). The experiment also showed that movement of cells into the gap was a result of cell migration alone.

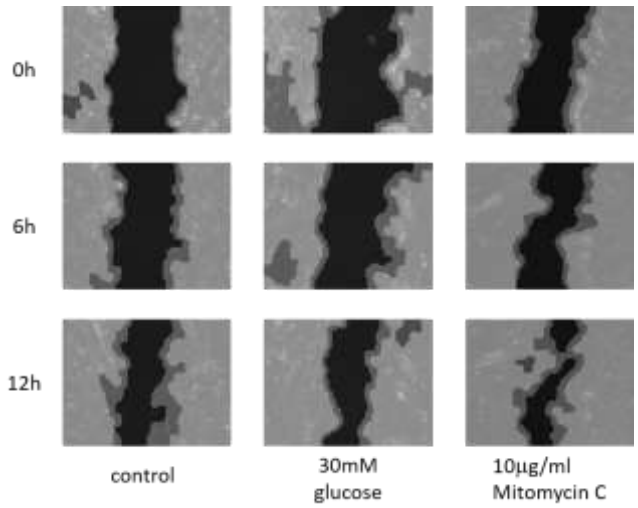

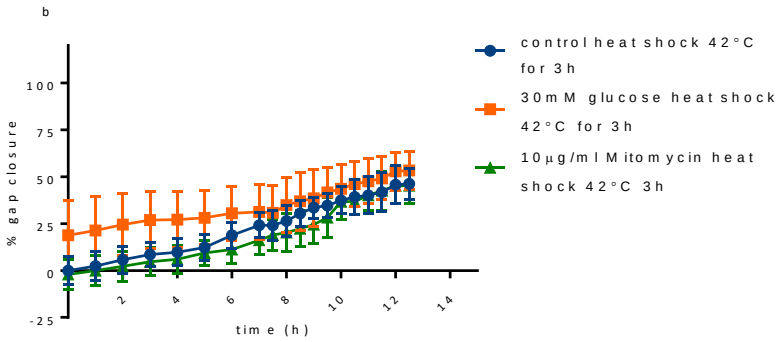

c

Tukey's multiple comparison test	
Comparisons	p values
Control heat shock 42 3h vs. 30mM glucose heat shock 42 3h	0.7629
Control heat shock 42 3h vs. 10mg/ml Mitomycin heat shock 42 3h	0.9640
30mM glucose heat shock 42 3h vs. 10mg/ml Mitomycin heat shock 42 3h	0.6170

Figure 4.12: The effect of heat shock at 42°C for 3h, hyperglycaemia and Mitomycin C on wound closure of WSI cells. WSI cells were cultured on well plates at a seeding density of 5 x 10^4 viable cells/ml and allowed to adhere for 48h. Cells were then incubated at 42°C for 3h and then put through a scratch assay. Control wells received complete culture medium while hyperglycaemic wells received complete culture medium supplemented with 30mM glucose and cells in the mitomycin condition received complete culture medium supplemented with 10µg/ml mitomycin C. Time lapse pictures were taken at hourly intervals for the first 7h and then at 30 min intervals for the remaining 5h (a). Cell migration was analysed using TScratch software and migration at each time point was normalized and data are represented as means ± SEM, n=3 (b). Mean percentage gap closure between treatments was compared using a two-way ANOVA with Tukey's multiple comparison as post hoc test.

Although gap closure had only progressed to 50% at the end of 12h when data is compared to control conditions the relationship is not significant. Comparing all the conditions to 37°C showed no significant difference between them (Figure 4.13). The p values for the two way ANOVA are depicted in the table 18.

Table 18: The effect of hyperglycaemia and heat shock on WS1 cell migration.

Two way ANOVA	
Comparisons	P values
37°C vs Heat shock 40°C 1h	0.971
37°C vs Heat shock 42°C 3h	0.590
37°C vs Heat shock 40°C 1h 30mM glucose	0.412
37°C vs Heat shock 42°C 3h 30mM glucose	0.259
37°C vs Heat shock 42°C 3h Mitomycin C	0.345

a

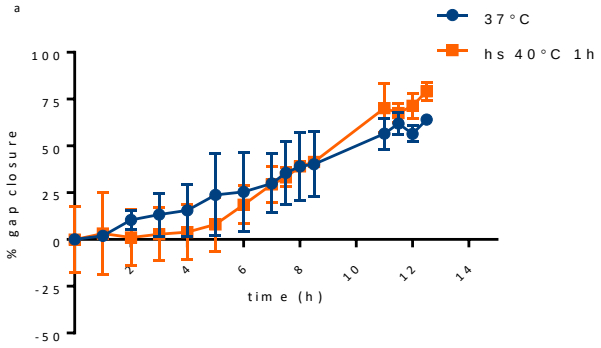

Sidak's multiple comparison test	
Time (h)	37°C vs Heat shock 40°C 1h
0.0	>0.9999
1.0	>0.9999
2.0	>0.9999
3.0	0.9996
4.0	0.9987
5.0	0.9753
6.0	>0.9999
7.0	>0.9999
7.5	>0.9999
8.0	>0.9999
8.5	>0.9999
11.0	0.9937
11.5	>0.9999
12.0	0.9840
12.5	0.9821

b

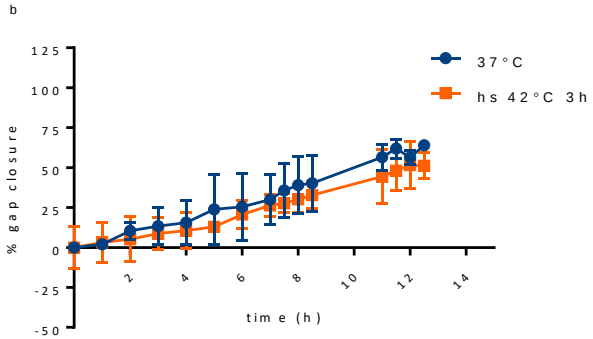

Sidak's multiple comparison test	
Time (h)	37°C vs Heat shock 42°C 3h
0.0	>0.9999
1.0	>0.9999
2.0	>0.9999
3.0	>0.9999
4.0	>0.9999
5.0	0.9992
6.0	>0.9999
7.0	>0.9999
7.5	>0.9999
8.0	>0.9999
8.5	>0.9999
11.0	0.9975
11.5	0.9897
12.0	>0.9999
12.5	0.9950

c

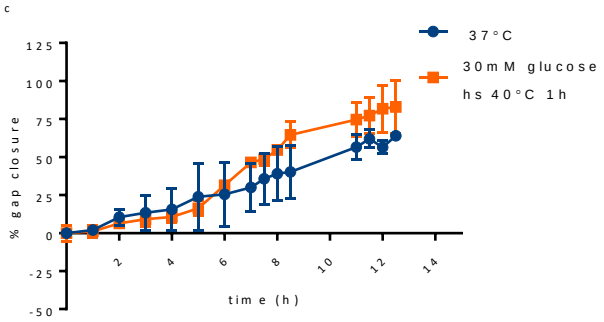

Sidak's multiple comparison test	
Time (h)	37°C vs 30mM glucose heat shock 40°C 1h
0.0	>0.9999
1.0	>0.9999
2.0	>0.9999
3.0	>0.9999
4.0	>0.9999
5.0	>0.9999
6.0	>0.9999
7.0	0.8964
7.5	0.9844
8.0	0.9294
8.5	0.3956
11.0	0.8210
11.5	0.9417
12.0	0.3393
12.5	0.7718

d

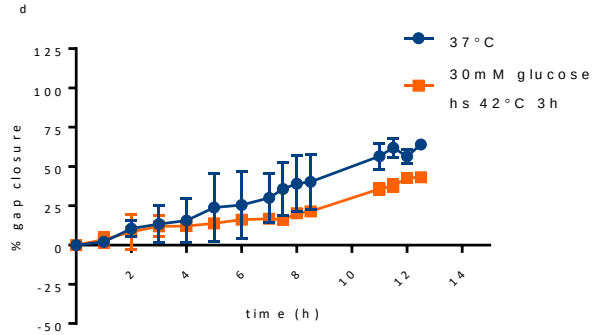

Sidak's multiple comparison test	
Time (h)	37°C vs 30mM glucose heat shock 42°C 3h
0.0	>0.9999
1.0	>0.9999
2.0	>0.9999
3.0	>0.9999
4.0	>0.9999
5.0	0.9958
6.0	0.9982
7.0	0.9519
7.5	0.5474
8.0	0.6198
8.5	0.6140
11.0	0.4489
11.5	0.2387
12.0	0.9377
12.5	0.4467

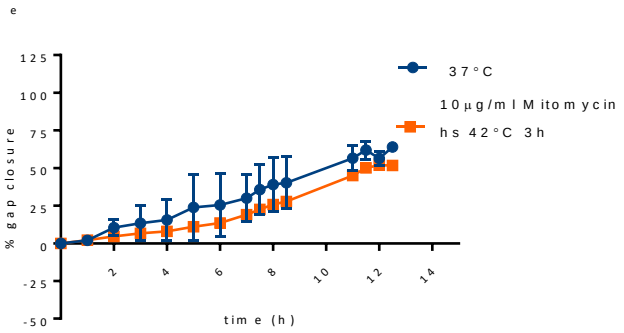

Sidak's multiple comparison test	
Time (h)	37°C vs 10µg/ml mitomycin hs42°C 3h
0.0	>0.9999
1.0	>0.9999
2.0	>0.9999
3.0	>0.9999
4.0	0.9997
5.0	0.9477
6.0	0.9722
7.0	0.9868
7.5	0.9380
8.0	0.9347
8.5	0.9603
11.0	0.9768
11.5	0.9731
12.0	>0.9999
12.5	0.9623

Figure 4.13: Comparing individual conditions to 37°C. 37°C vs heat shock 40°C for 1h (a) 37°C vs heat shock at 42°C for 3h (c) 37°C vs 30mM glucose heat shock 40°C 1h (d) 37°C vs heat shock 42°C 3h (e) 37°C vs mitomycin C heat shock 42°C for 3h. Data are represented as means ± SEM, n=3 and mean percentage gap closure between treatments was compared at each time point. Data were analysed by two way ANOVA with Sidak's multiple comparison as post hoc test.

4.5 Discussion

The study aimed to investigate the role of heat shock on wound closure in vitro. WSI cells were initially given a 2h recovery to induce HSP prior to being scratched as it was considered that they were being subjected to compounding stresses (Figure 4.1). To test if this was indeed the case, WSI cells were put through the scratch assay without a recovery period (Figure 4.2). No difference in wound closure was seen and so a recovery period was deemed unnecessary. WSI cells were treated with heat shock at range of temperatures for 1h and then scratched (39°C to 45°C). It was shown that migration of fibroblasts remains unaffected under heat shock treatments (Figures 4.2 to 4.6). WSI cells were then incubated at 45°C for the duration of the scratch assay. High temperature incubation significantly reduce cell migration (Figure 4.7) as it invariably caused cell death.

The commercial inserts from Ibidi were also tested on heat shock at 39°C treatments and found to have no effect on wound closure (Figure4.8). No difference was found in wound closure rates. Moreover the size of gap the inserts generated and size of scratch that was generated using a pipette tip were similar. Following heat shock treatment,

WSI cells were incubated in complete culture medium. The growth factors from FBS could have assisted in cell migration. A lack of growth factors would inhibit cell migration into the gap. Heat shock coupled with heat inactivated medium was then tested (Figure 4.9) and no significant difference was seen in cell migration.

Once image capture had been automated the effect of hyperglycaemia was tested on wound closure of WSI (Figure 4.10). Hyperglycaemia had no effect on the wound closure of WSI cells. WSI cells were then subjected to heat shock and hyperglycaemia and here too no difference was seen (Figure 4.11).

It was thought that heat shock treatment for 1h was too short and so longer heat shock treatment period of 3h was tested. The effect of mitomycin C was also tested in the same experiment (Figure 4.12) no significant difference was seen. The effect of a 2h heat shock has not been tested and would be looked into in the near future. All the heat shock experiments coupled with hyperglycaemia and mitomycin C were then compared to 37°C and found to have no significant differences between them (figure 4.13). This implied that over a period of 12h cell migration seen in this study was an effect of cell movement alone.

These results shown in this study indicate that hyperglycaemia (30mM) has no effect on cell migration. These results are in disagreement with (Xuan et al., 2014) who used human foreskin fibroblasts and showed that 30mM glucose inhibits fibroblast migration. One reason why they have seen this effect could be because they cultured their fibroblast in 0.35% FBS for their assay which would not be representative of in vivo as serum starvation has been shown to induce morphological changes and the Warburg effect in human foreskin fibroblast cells (Golpour et al., 2014). The Warburg effect shows that cells prefer anaerobic respiration and produce lactate even under favourable aerobic conditions and therefore would cause fibroblasts to produce lactate. High lactate levels in diabetic wounds have been shown to inhibit fibroblast migration in vitro (Hehenberger et al., 1998). Commercially available human foreskin fibroblasts from ATCC recommend 15% FBS for complete culture medium.

Lamers et al., (2011) show that cell migration rates of CHO, NIH-3T3 and mouse embryonic fibroblast are reduced in presence high glucose conditions (25mM), but does not describe how the wound healing assay was carried out or show pictures of the scratch assay. (Lamers, Almeida, Vicente-Manzanares, Horwitz, & Santos, 2011). The

data also shows that cells took 3 days for closure including mouse embryonic fibroblasts, while the data here indicates that complete closure of fibroblasts occurs in less than 24h. This could possibly be because the fibroblasts were primary cells from mice and are likely to behave differently compared to the embryonic fibroblasts used in this study.

In the last few years whole body hyperthermia treatments have been shown to improve insulin sensitivity animal models (Chung et al., 2008; Gupte, Bomhoff, Swerdlow, & Geiger, 2009; Morera, Basirico, Hosoda, & Bernabucci, 2012; Sanz Fernandez et al., 2015). Some studies have used heat shock coupled with mild electrical stimulation to show improvements in insulin sensitivity (Kondo et al., 2012; Matsuyama et al., 2014; Morino et al., 2008). These studies all have concluded that induction of HSP72 improves insulin sensitivity through inhibition of JNK and NF□B in liver, muscle and adipose tissues and improving overall glucose homeostasis even when given a high fat or high glucose diet. Data presented in this chapter used heat shock treatment and hyperglycaemia to see if heat shock improved wound closure in a model of a diabetic wounds. Heat shock treatment was found to have no effect on cell migration in the WS1 wound healing model with the exception of incubation at high temperatures where it caused cell death. Thus impaired wound healing in diabetes may not be caused by poor cell migration into the wound but could possibly be a result of other factors that would inhibit cell migration such as poor wound debridement by resident macrophages and neutrophils, a lack of growth factors, high levels of NO, chronic hypoxia and inflammatory cytokines in the wound site (Blakytny & Jude, 2006).

Chapter 5 Assays for glucose uptake and GLUT4 in U937 cells

5.1 Introduction

Diabetes is usually diagnosed by a measuring for circulating levels blood glucose. The oral glucose tolerance test (OGTT) is currently the gold standard to diagnose diabetes, however the test requires the patient to fast overnight and is labour intensive and so not used routinely. The reproducibility of the test in repeat tests is poor as well. Other alternative tests require either prompt process sample processing and can be influenced by short term lifestyle changes as in random blood glucose testing and capillary blood glucose but do not indicate long term glycaemic control (Echouffo-Tcheugui, Ali, Griffin, & Narayan, 2011). Recently testing for raised levels glycated haemoglobin (HbA1c) has been shown to identify glycaemic control over a long period and indicate possibility of diabetic complications in patients. The test however, is expensive and needs to be standardized for ethnicity and age as they produce varying levels of other interfering haemoglobin molecules (Weykamp, 2013). These test are also indirect measures to assess glycaemic control in diabetes and rely on insulin resistance and other factors to diagnose type 2 diabetes.

One aspect of diabetes in the development of chronic low grade inflammation which occurs much before any glucose intolerance or insulin resistance occurs. This can easily be seen in monocytes and macrophages that infiltrate adipose tissue at the onset of obesity (Hasty, 2008). Monitoring monocyte and macrophage activity in blood could provide insights in to the level of glycaemic control within the body much before insulin resistance occurs. Monocytes and macrophages play a central role in insulin resistance and inflammation and could provide a more effective way to see if treatment is effective (Koh & DiPietro, 2013; Samaan, 2011).

In the preceding chapter the effects of heat shock and hyperglycaemia on cell migration were investigated; and here the same stresses were used to see the effects on monocyte glucose transport and cytokine profiles. In order to test the effect of heat shock on glucose uptake and expression in monocytes, a glucose uptake assay using a fluorescent glucose analogue (2-n(7-nitrobenz-2-oxa-1,3diazol-4-yl)amino)-2-deoxyglucose (2NBDG) was developed in U937 cells. The assay was previously described to measure

glucose uptake in human CD14 monocytes (Dimitriadis et al., 2005). A monoclonal antibody for GLUT4 was purchased and optimised with an aim to be used to assess GLUT4 expression in U937 cells

5.1.1 Aims

- To optimize a glucose uptake assay in U937 monocytes using the fluorescent glucose analogue 2NBDG.
- To test the assay under cell stress conditions such as changes in pH and membrane fluidization.
- To optimize an assay to study GLUT4 expression in U937 cells under conditions of membrane fluidization and hyperglycaemia

5.2 Methods

5.2.1 2NBDG glucose uptake assay

Glucose uptake assay was carried out as described in chapter 2, section 2.3.8.1 to 2.3.8.5.

5.2.2 GLUT 4 flow cytometry

The presence of GLUT4 is described in chapter 2, section 2.3.8.6.

5.3 Results

5.3.1 Determining the number of washes to remove excess 2NBDG

The first step was to determine the number of washes required to remove excess 2NBDG from cells and ascertain that the fluorescence that would be recorded would just come from 2NBDG that was internalized by the cells. This was done by adding 2NBDG to the cells and incubating them for 1h and performing washes in DPBS. The supernatant was collected and its fluorescence was determined using a plate reader (figure 5.1). Supernatant taken immediately after incubation had the highest fluorescence which was significantly higher than the untreated cells ($p<0.001$). After one wash fluorescence was reduced by 89.4% ($p<0.01$) and after two washes fluorescence was not significantly different from untreated supernatant, therefore two washes were sufficient to remove excess 2NBDG from cells (Figure 5.1).

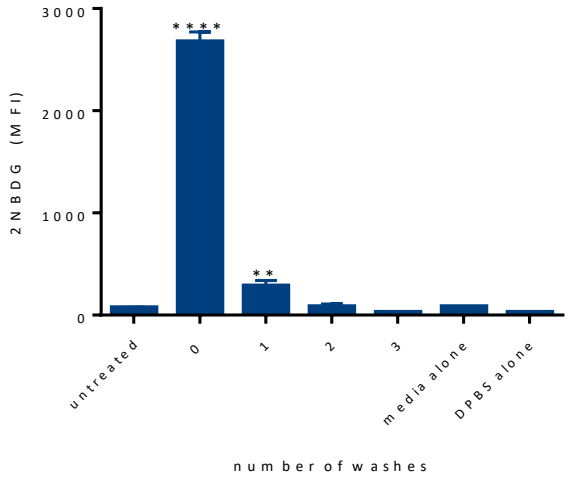

Dunnett's multiple comparison test	
Comparisons	p values
untreated vs. 0	0.0001
untreated vs. 1	0.0072
untreated vs. 2	0.9997
untreated vs. 3	0.9250
untreated vs. media	0.9998
untreated vs. DPBS	0.9362

Figure 5.1: Number of washes required to remove excess 2NBDG from medium post treatment. U937 cells were cultured at seeding density of 1 x 10^6 viable cells/ml and treated with 10µl of 2NBDG and incubated at 37°C for 1 h following which they were centrifuged at 500g for 5 min, the supernatant was stored and cells were re-suspended in DPBS. The process was repeated 3 times to produce 3 supernatant samples whose fluorescence was detected using a plate reader. Data are presented as means ± SEM, n=3 and were compared to untreated cells. Data were analysed by a one way ANOVA with Dunnett's as post hoc test where, * ($p<0.05$) and **** ($p<0.0001$).

5.3.2 Determining the optimal incubation time of 2NBDG

The optimal incubation time for 2NBDG uptake was then determined by a time course (Figure 5.2). 2NBDG was added to U937 cells every hour for 3h following which they were wash twice and analysed by flow cytometry (Figure 5.2 a & b). Fluorescence significantly increased every hour and after 2h there was no significant difference in fluorescence therefore, a 2h incubation was chosen.

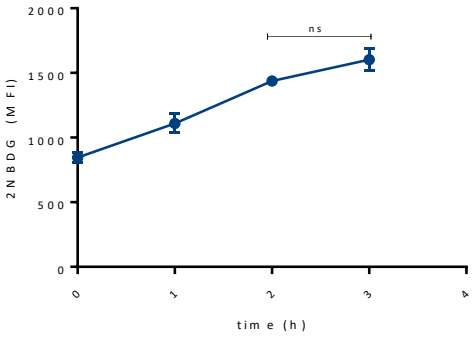

Tukeys's multiple comparison test	
Comparisons	p values
0. vs. 1.	0.0061
0. vs. 2.	<0.0001
0. vs. 3.	<0.0001
1. vs. 2.	0.0014
1. vs. 3.	<0.0001
2. vs. 3.	0.0779

b

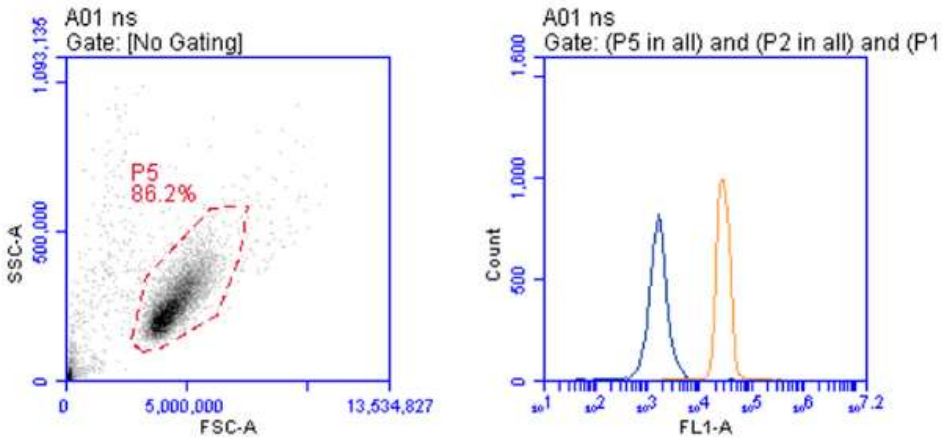

Figure 5.2: Optimal incubation time for 2NBDG. U937 cells were cultured at a seeding density of 1 x 10^6 viable cells/ml in 96 well plate. 10µl of 2NBDG was added to three wells every hour over a period of 3h. The cells were then washed twice in DPBS and analysed using flow cytometry. Data are presented as means ± SEM, n=3. Data was analysed by a one way ANOVA with Tukey's multiple comparison as post hoc test (a). A representative scatter plot of the viable cells and the mean fluorescence of unstained cells (blue) and cells that have been treated with 2NBDG (yellow) is shown (b).

5.3.3 Competitive inhibition of 2NBDG by glucose

The effect of increasing glucose concentrations was tested to see if fluorescence could be competitively inhibited (Figure 5.3). The data showed that fluorescence was highest when glucose was not present. The fluorescence of 5mM glucose was significantly lower than the fluorescence of glucose free media ($p<0.01$) while the remaining

dilutions were even more significantly lower ($p<0.001$) in comparison, indicating glucose inhibited 2NBDG fluorescence in a competitive manner.

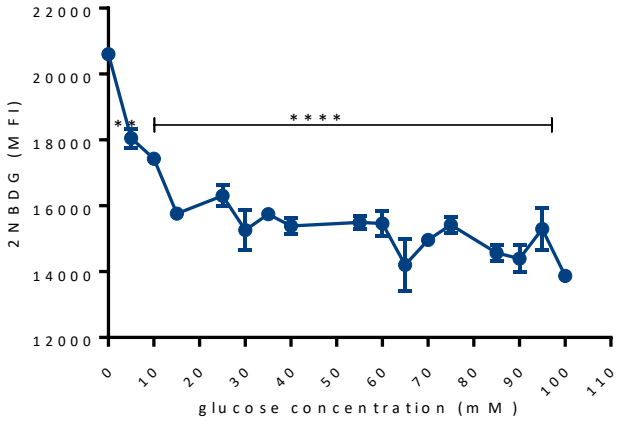

Dunnett's Multiple comparison test	
Comparisons	p values
0. vs. 5.	0.0017
0. vs. 10.	0.0001
0. vs. 15.	0.0001
0. vs. 25.	0.0001
0. vs. 30.	0.0001
0. vs. 35.	0.0001
0. vs. 40.	0.0001
0. vs. 55.	0.0001
0. vs. 60.	0.0001
0. vs. 65.	0.0001
0. vs. 70.	0.0001
0. vs. 75.	0.0001
0. vs. 85.	0.0001
0. vs. 90.	0.0001
0. vs. 95.	0.0001

Figure 5.3: The effect of glucose concentrations on 2NBDG uptake. U937 cells were seeded at cell density of 1 x 10^6 viable cells /ml. The cells were subsequently washed and re-suspended in media containing varying concentrations of glucose made in glucose free media. Control wells received glucose free media without any supplementation. Each well received 10µl of 2NBDG and the plate was incubated for 2h. The cells were then washed and analysed by flow cytometry. Data are presented as mean ± SEM, n=3 and compared to 0mM glucose. Data were analysed by one way ANOVA with Dunnett's as post hoc test where significance ** ($p<0.01$) and **** ($p=0.0001$).

5.3.4 Determining the effect of insulin on glucose uptake

The effect of insulin was then tested on 2NBDG fluorescence (Figure 5.4). The data showed that insulin had no effect on glucose uptake ($p=0.192$).

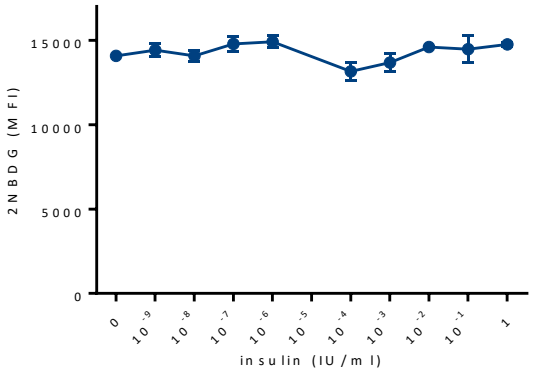

Dunnett's Multiple comparison test	
Comparisons	p values
0 vs. 10^{-9}	0.9968
0 vs. 10^{-8}	0.9999
0 vs. 10^{-7}	0.8375
0 vs. 10^{-6}	0.7004
0 vs. 10^{-4}	0.5943
0 vs. 10^{-3}	0.9918
0 vs. 10^{-2}	0.9575
0 vs. 10^{-1}	0.9919
0 vs. 1	0.8619

Figure 5.4: The effect of insulin on 2NBDG uptake. U937 cells were plated out at cell density of 1 x 10^6 cells/ml, centrifuged at 500g to remove media and re-suspended in media containing insulin ranging from 1 x 10^{-9} IU/ml to 1IU/ml and 30.8µM of 2NBDG. Following a 2h incubation cells were washed twice in DPBS and analysed by flow cytometry. Data are presented as mean ± SEM, n=3. The data were analysed by a one way ANOVA and compared 0 using Dunnett's multiple comparison as the post hoc test.

5.3.5 The effect of pH on glucose uptake

The effect of pH was investigated on glucose uptake in U937 cells (Figure 5.5). Mean fluorescence of 2NBDG was not significant until pH 4.5 ($p<0.05$). However extremes of pH had significant effect on cell viability pH 4.5 ($p<0.0001$), pH5.5 ($p<0.0001$), pH 8($p<0.0001$), pH 9 ($p<0.0001$) and pH 9.5 ($p<0.0001$) when compared to pH 7.

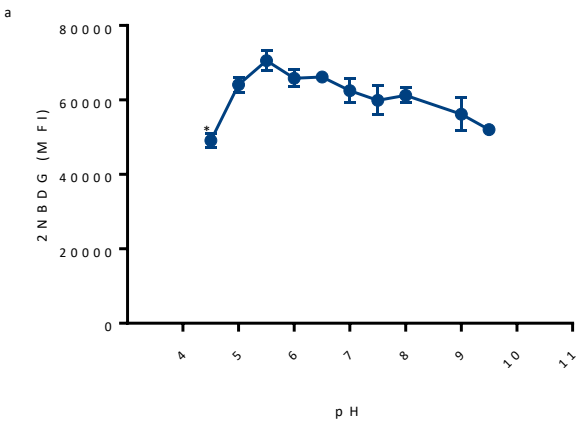

Dunnett's multiple comparison test	
Comparisons	p values
7.0 vs. 4.5	0.0356
7.0 vs. 5.0	0.9994
7.0 vs. 5.5	0.2519
7.0 vs. 6.0	0.9539
7.0 vs. 6.5	0.9243
7.0 vs. 7.5	0.9868
7.0 vs. 8.0	0.9995
7.0 vs. 9.0	0.4836
7.0 vs. 9.5	0.0804

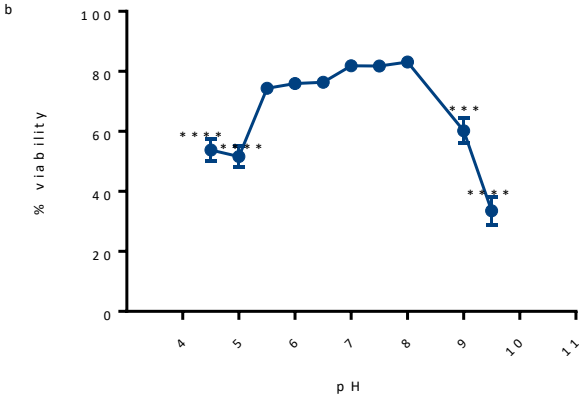

Dunnett's multiple comparison test	
Comparisons	p values
7.0 vs. 4.5	0.0001
7.0 vs. 5.0	0.0001
7.0 vs. 5.5	0.3267
7.0 vs. 6.0	0.5727
7.0 vs. 6.5	0.6445
7.0 vs. 7.5	0.9999
7.0 vs. 8.0	0.9996
7.0 vs. 9.0	0.0002
7.0 vs. 9.5	0.0001

Figure 5.5: The effect of pH on glucose uptake in U937 cells. U937 cells were cultured in 96 well plates at a cell density of 1 x 10^6 cells/ml. they were centrifuged at 500g for 5 min to remove media. The cell pellets were then re-suspended in media with pH ranging from 4.5 to 9.5 and 2NBDG was added. Following a 2h incubation the cell were washed twice and analysed by flow cytometry. The graphs show mean 2NBDG fluorescence (a) and percentage viability (b). Data are represented as means ± SEM, n=3 and were compared to pH7. Data were analysed by a one way ANOVA with Dunnett's multiple comparison as post hoc test *(p<0.05), ***(p<0.001 and ****(p<0.0001).

5.3.6 The effect of membrane fluidizers on glucose uptake

The effect of dimethyl sulfoxide (DMSO) on 2NBDG uptake was tested as DMSO changes membrane polarity and can affect cellular transport in cells (Figure 5.6). DMSO also causes cells to differentiate. Overall 2NBDG fluorescence remained insignificant until 0.781% where it became significant. At this concentration cell viability showed high variability. 2NBDG fluorescence significantly decreased

corresponding to a decrease in cell viability from 3.125% ($p<0.0001$). This could be because DMSO inhibited 2NBDG uptake at low dilutions. As concentrations of DMSO increased and membrane integrity of cells was compromised and 2NBDG began to leak corresponding to an increase in fluorescence. Higher concentrations of DMSO significantly reduced cell viability with a corresponding decrease in 2NBDG fluorescence (Figure 5.8).

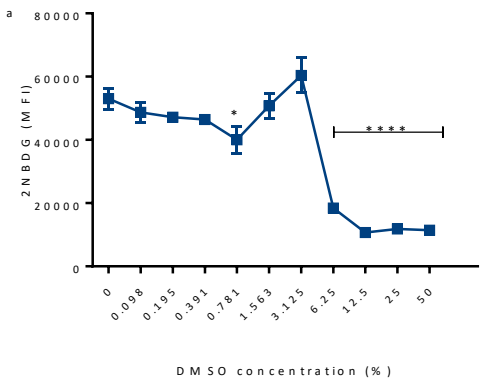

Dunnett's multiple comparison test	
Comparisons	p values
0 vs. 0.098	0.8881
0 vs. 0.195	0.6489
0 vs. 0.391	0.5225
0 vs. 0.781	0.0291
0 vs. 1.563	0.9967
0 vs. 3.125	0.4075
0 vs. 6.25	0.0001
0 vs. 12.5	0.0001
0 vs. 25	0.0001
0 vs. 50	0.0001

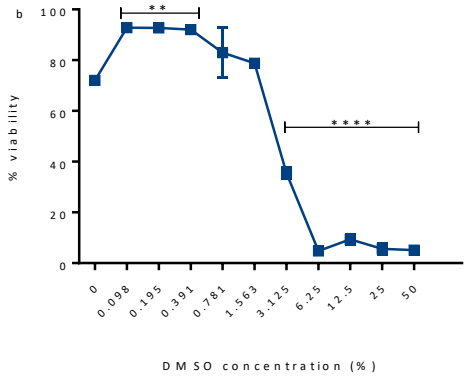

Dunnett's multiple comparison test	
Comparisons	p values
0 vs. 0.098	0.0014
0 vs. 0.195	0.0014
0 vs. 0.391	0.0021
0 vs. 0.781	0.1553
0 vs. 1.563	0.6284
0 vs. 3.125	0.0001
0 vs. 6.25	0.0001
0 vs. 12.5	0.0001
0 vs. 25	0.0001
0 vs. 50	0.0001

Figure 5.6: The effect of DMSO on glucose uptake in U937 cells. U937 cells were cultured in 96 well plates at a cell density of 1 x 10^6 cells/ml. They were centrifuged at 500g for 5 min to remove media. The cell pellets were then re-suspended in media with supplemented with DMSO concentrations ranging from 0.098% to 50%. The cells were then assayed for glucose uptake using 2NBDG and incubated for 2h. The cells were washed and re-suspended in DPBS and analysed by flow cytometry showing mean fluorescence (a) and percentage viability (b) Data are presented as means ± SEM, n=3 and were compared to 0% DMSO. Data were analysed by a one-way ANOVA with Dunnett's multiple comparison as post hoc test where *($p<0.05$), ** (0.01) and ***** ($p<0.0001$).

The effect of membrane fluidizer benzyl alcohol and phenethyl alcohol was tested on glucose uptake was tested (Figure 5.9). Membrane fluidizers denature cell membranes

and therefore affect transport of substances across cell membranes. The data show that 2NBDG fluorescence did not change significantly over the times tested (0h p=0.361; 2h p=0.431).

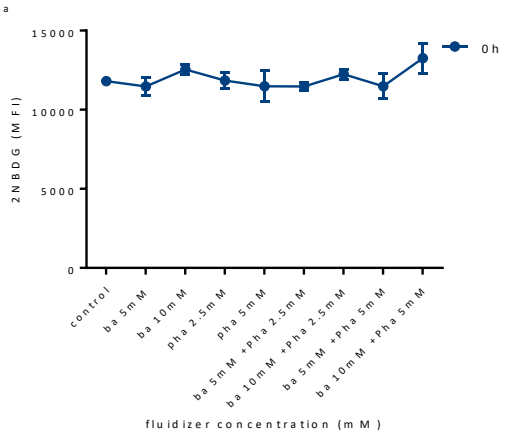

Dunnett's multiple comparisons test	
Comparisons	p values
Control vs. ba 5mM	0.9977
Control vs. ba 10mM	0.9108
Control vs. pha 2.5mM	0.9999
Control vs. pha 5mM	0.9994
Control vs. ba 5mM +Pha 2.5Mm	0.9977
Control vs. ba 10mM +Pha 2.5mM	0.9939
Control vs. ba 5mM +Pha 5mM	0.9979
Control vs. ba 10mM +Pha 5mM	0.3670

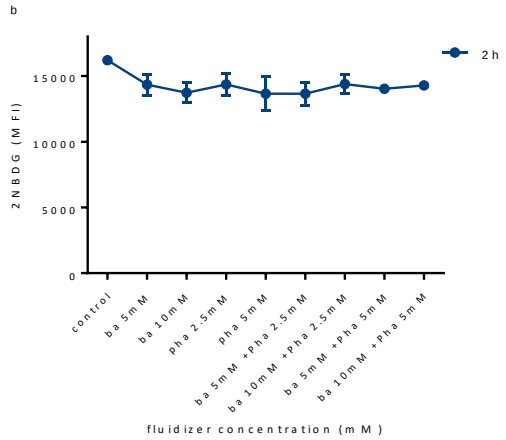

Dunnett's multiple comparisons test	
Comparisons	p values
Control vs. ba 5mM	0.9977
Control vs. ba 10mM	0.9108
Control vs. pha 2.5mM	0.9999
Control vs. pha 5mM	0.9994
Control vs. ba 5mM +Pha 2.5mM	0.9977
Control vs. ba 10mM +Pha 2.5mM	0.9939
Control vs. ba 5mM +Pha 5mM	0.9979
Control vs. ba 10mM +Pha 5mM	0.3670

Figure 5.7: The effect of membrane fluidizer benzyl alcohol (ba) and phenethyl alcohol (pha) on glucose uptake. U937 cells were plated out at cell density of 1 x 10^6 cells/ml in 2 96well plates, centrifuged at 500g and re-suspended in media containing membrane fluidizers. At each time point a plate was assayed for glucose uptake by adding 30.8µM of 2NBDG and incubated for 2h. The cells were washed and re-suspended in DPBS and analysed by flow cytometry. The graphs show mean fluorescence at 0h (a) and 2h (b) and were compared to control. Data are presented as means ± SEM where n=3. Data were analysed by a one way ANOVA with Dunnett's multiple comparison as post hoc test.

5.3.7 Determining the presence of GLUT 4 on U937 membranes

Monocytes have been shown to be sensitive to insulin as they express the insulin sensitive glucose transporter GLUT4 (Dimitriadis et al., 2005; Maratou et al., 2007).

Therefore the presence of GLUT4 was tested by Western blotting using a monoclonal antibody where GLUT4, a 50-63KDa protein was found to be retained in the hydrophilic regions and detected in whole cell extract (Figure 5.8). No signal was found in the hydrophobic region because the antibody (IF8) used in this study only recognises the hydrophilic C terminus of GLUT4. Moreover the hydrophobic region had a lot of detergent contamination and did not run properly on the gel forming a smear.

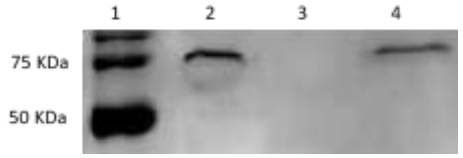

Figure 5.8: Western blot showing the presence of GLUT4 50-63KDa protein on U937 cell extracts and membrane extracts. 10% gels were cast and loaded with the following: Lane 1 ladder, Lane 2 whole cell extract, Lane 3 hydrophobic membrane fraction, Lane 4 hydrophilic membrane fraction. 15.23µg of protein was loaded into each well and the membrane was exposed for 120s

The antibody was also tested using flow cytometry to test the presence of GLUT4 on both the membrane using fixed cells and inside the cell using fixed and permeabilised cells (Figure 5.9). Fixed cells did not show a high presence of GLUT4 while fixed and permeabilised cells showed high presence of GLUT4. This suggested that GLUT4 was retained in intracellular vesicles as cells were not treated with insulin. The secondary antibody in the absence of primary antibody at both dilutions was not significantly different when compared to no stain suggesting that the washing steps were sufficient and non-specific binding was negligible. Higher dilutions of primary antibody produced a better signal with a lower dilution of secondary overall across both conditions and thus primary antibody dilution of 1:200 and secondary antibody dilution of 1:1000 was chosen (Figure 5.9).

a

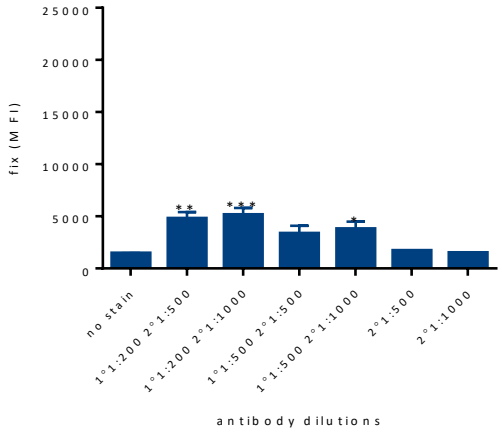

Dunnett's multiple comparison test	
Comparisons	p values
No stain vs. 1°1:200 2°1:500	0.0022
No stain vs. 1°1:200 2°1:1000	0.0009
No stain vs. 1°1:500 2°1:500	0.0888
No stain vs. 1°1:500 2°1:1000	0.0294
No stain vs. 2°1:500	0.9981
No stain vs. 2°1:1000	0.9999

b

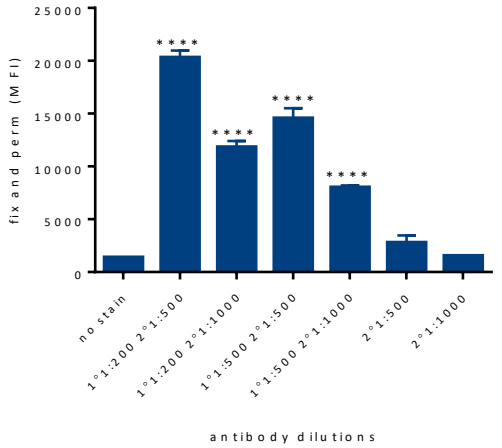

Dunnett's multiple comparison test	
Comparisons	p values
No stain vs. 1°1:200 2°1:500	0.0001
No stain vs. 1°1:200 2°1:1000	0.0001
No stain vs. 1°1:500 2°1:500	0.0001
No stain vs. 1°1:500 2°1:1000	0.0001
No stain vs. 2°1:500	0.4967
No stain vs. 2°1:1000	0.9998

Figure 5.9: Detection of GLUT4 on membrane and intracellular fractiIons of U937 cells. Membrane and cellularU937 cells were plated out at a cell density of 1 x 10^6 cells/ml. They were then either fixed (a) or fixed and permeabiliszed (b) and probed for GLUT4 using a mouse anti-glut4 monoclonal antibody. A FITC tagged anti-mouse secondary antibody was used to detect the primary antibody using flow cytometry. The mean fluorescence of viable cells is shown and was compared to no stain. Data are represented as means ± SEM, n=3 and were compared to no stain. Data was analysed by a one way ANOVA with Dunnett's multiple comparison as post hoc test where * ($p<0.05$), ** ($p<0.01$) and **** ($p<0.0001$).

5.4 Discussion

A glucose uptake assay has been optimised in this study to test the effects of hyperglycaemia and heat shock on monocytes. The protocol has been developed to measure GLUT4 in the cells and on the cell membrane. The number of washes required to remove excess 2NBDG was determined (Figure5.1). Two washes reduced fluorescence in the supernatant and so was used throughout the study. The optimal incubation for 2NBDG was determined and found to be 2h as further incubation was found to not significantly enhance the fluorescence signal as 2NBDG fluorescence (Figure 5.2) declined over time. These results were similar to a study of 2NBDG HepG2 human hepatocarcinoma cells and L6 rat skeletal muscle cells where the fluorescence of 2NBDG began to plateau after 1h incubation (Zou et al., 2005). This is because, once 2NBDG is taken up by cells is immediately phosphorylated and broken down to a non-fluorescent metabolite (Yoshioka et al., 1996). 2NBDG fluorescence was also shown to be competitively inhibited by glucose confirming that it is taken up into cells through their glucose transporters (Figure 5.3).

The glucose uptake assay used in this study found no effect of insulin on 2NBDG fluorescence (Figure 5.4). The reason for this could be attributed to the short half-life of insulin which is estimated to be between 4 to 6min as it is degraded by insulin degrading enzyme (IDE) that is ubiquitously expressed in all cells (Qiu & Folstein, 2006); however this half-life is measured in blood. The half-life of insulin in culture may be different and was not tested. IDE is a Zn metalloprotease present in the cytoplasm and is inhibited by 10-phenanthroline (Hulse, Ralat, & Wei-Jen, 2009). This could be why such a short time course of 650ms was used to in their study. Even so Dimitriadis et al., (2005) and Maratou et al., (2007) did not wash their cells prior to measurement and therefore as demonstrated in this thesis, they may have been recording residual fluorescence rather than glucose uptake in response to insulin and could possibly have compromised their data. The use of a metalloprotease inhibitor would be used in the future to determine whether U937 cells express GLUT4 in response to insulin. Another difference from Dimitriadis et al., (2005) and Maratou et al., (2007) study was that they carried out their experiments at 22°C which not representative of the condition of monocytes in vivo.

In this study glucose uptake was also tested in conditions that compromise membrane integrity and cell viability such as pH and membrane fluidizers (DMSO, benzyl alcohol

and phenethyl alcohol). Extremes of pH would create large ionic gradients across membranes which would affect proton dependent membrane transporters and uniporters such as GLUT transporters. Low pH would bring about conformational changes in proteins that denature them (Nishimura et al., 1993). Glucose uptake at pH4.5 was found to be significantly lower than at other pH values whereas extremes of pH were shown to significantly reduce cell viability (Figure 5.5).

Membrane fluidizers were used in this study as they are potent inducers of heat shock proteins. Studies using the membrane fluidizer Bimoclomol, have shown that membrane fluidizer activates the transcription factor, heat shock factor 1 (HSF-1) and brings about the induction of heat shock proteins (Hargitai et al., 2003). Another study in diabetic mouse models has shown that gavage feeding of membrane fluidizer, BGP-15 for 15 days significantly, reduced levels of phosphorylated JNK, and improved insulin sensitivity through the induction of HSP72 (Chung et al., 2008). The effect of DMSO on glucose uptake was not significant until 0.78% of DMSO where it was decreased significantly. Fluorescence then became non-significant before declining rapidly with increasing concentrations of DMSO. This decline in fluorescence was attributed to the substantial decline in cell viability with increasing concentrations of DMSO (Figure 5.6). This could be because as the viable cell population began to die and release 2NBDG into the solution which was seen as an increase in fluorescence. Benzyl alcohol and phenethyl alcohol were 2 other fluidizers used in this study and were shown to have no significant effect on glucose uptake. It is possible that the concentrations tested in this study were too low to show an effect on glucose uptake and needs to be investigated. Dempsey et al. (2010) have previously shown that treatment of Jurkat cells with 5mM benzyl alcohol and 2.5mM phenethyl alcohol translocated HSP72 and HSP60 to the membrane and induce HSP synthesis as intracellular HSP levels declined. This reduction in intracellular HSP levels sensitized the tumour cells to sub-lethal levels of cytotoxic drugs and showed that combinatorial treatment cancer cells with membrane fluidizers is a plausible approach for the treatment of drug resistant tumours. In diabetes where there is lack of HSP expression (Bitar, Farook, John, & Francis, n.d.); treatment with membrane fluidizers could be used to induce HSP expression and thus bring about resolution to inflammation brought about by immune cells in insulin sensitive tissue.

The presence of insulin sensitive glucose transporter 4 (GLUT4) has been shown in U937 cells through flow cytometry and western blot analysis in this study (Figure 5.7 and 5.8). These data are in agreement with previous studies that have showed the presence of GLUT4 in monocytes (Dimitriadis et al., 2005; Maratou et al., 2007; Simar et al., 2012). The assay could be used to monitor GLUT4 expression in monocytes when treated with heat shock and/or hyperglycaemia to obtain an insight into the glucose metabolism in these cells when subjected to such stresses. Recently Simar et al., (2012) have shown that monocytes isolated from obese individuals showed insulin resistance with no change in glucose transporter GLUT4 levels. Heat shock treatment at 42°C for 2h improved insulin sensitivity measured by a reduction in phosphorylated IRS-1, JNK and IKKβ (Simar et al., 2012).

Monocytes and macrophages are key regulators of inflammation in wound healing and diabetes. Their dysfunction in diabetic wound healing is brought about by several mechanisms acting together such as oxidative stress, excess inflammatory cytokines, hypoxia and impaired glucose homeostasis (Samaan, 2011). Heat shock has been shown to improve and alleviate inflammatory responses in these cells and bring about resolution (Simar et al., 2012). They are an ideal target for therapeutic intervention in order to reduce inflammation in diabetes. The assays optimized here could be used to test the effects of hypoxia, heat shock and drug treatments and assess whether insulin sensitization occurs by the upregulation of GLUT 4. Moreover further development could be done to monitor insulin sensitivity or resistance from monocytes isolated from insulin resistant patients and gage glucose tolerance in real time.

Chapter 6 Discussion and future work

The study described here aimed to develop an in vitro scratch assay to investigate the effects of various factors on cell migration in isolation such as, heat shock and hyperglycaemia and use the data to gain an insight into diabetic wound healing. WSI cells were chosen as they were a fibroblast cell line with a finite life. They were found to migrate quickly to 'close the wound' when subject to an artificial scratch, in a very reproducible manner. Their migration was shown to be an effect of cell movement alone as the rate of scratch closure was not significantly different over time when in the presence of DNA synthesis inhibitor, mitomycin C. Mitomycin C was used as an inhibitor of cell proliferation to see if wound closure occurred through cell migration or through migration and cell proliferation. Mitomycin C was found to be acutely toxic to WSI cells as even 2.5µg/ml. A BrdU assay was used to determine that 10µg/ml mitomycin C was sufficient to inhibit WSI cell division by 90.48% over a period of 12h. Doubling the concentration only increased inhibition to 95.31%.

The effect PDGF-BB was also tested to determine if it would promote cell migration; however PDGF-BB had no significant effect on cell migration. Cell migration was also shown to occur in the presence of heat inactivated media showing that WSI cell migration was not being promoted by growth factors present in FBS used in the culture medium. The use of commercial inserts (Ibidi) was also tested to ascertain if the varying gaps being produced through physical removal were significantly different from the uniform gaps created by the inserts. No significant difference was seen as the gap created by inserts were similar to the average sizes of the gaps measured in this study, and migration was not significantly different over time between the two methods.

The effect of heat shock at a range of temperatures (39°C to 45°C) for 1h also showed no significant difference on cell migration. Cell migration, however was shown to be significantly reduced when WSI cells were incubated at 45°C showing that prolonged heat treatment was detrimental to cell migration as it caused cell death. Combinatorial stresses of heat shock and heat inactivated media using commercial inserts were also carried out and shown to have no effect on cell migration. The image capture of the scratch assay was automated using a microscope with an onstage incubator, and image analysis software TScratch was used to measure area wide cell migration of the scratch. The effect of hyperglycaemia (30mM glucose) was tested using this system. No significant difference between control and hyperglycaemic conditions was seen. Heat

shock coupled with hyperglycaemia also had no significant difference on cell migration. It was thought that a 1h heat shock treatment was short and so a heat shock treatment time of 3h was used and found that hyperglycaemia and mitomycin C had no significant effect on cell migration. In this study serum starvation was not used as serum starvation has been shown to induce morphological changes within cells and promote the Warburg effect (Golpour et al., 2014). The data described in this thesis with regards to cell migration under hyperglycaemic conditions is in contrast with other studies as they used serum starvation which would not be similar to cells in vivo (Xuan et al., 2014). Another reason they observed an inhibitory effect could be that high lactate levels are produced by cells under serum starvation and has been shown to inhibit wound healing (Hehenberger et al., 1998). Heat shock was used to induce the production of HSP and see if HSP would improve cell migration of WS1 cells but no stimulatory effect was seen. From the data it can be concluded that heat shock has no effect on migration of fibroblast.

The effects of hypoxia on WS1 could be tested in the near future. Acute hypoxia has been shown to be a potent inducer of cell division of fibroblasts (Alaluf, Simon, Muir-Howie, Heng-Long, Evana, & Green, 1998; Hong et al., 2014; W. Li et al., 2007) while chronic hypoxic conditions have been shown to inhibit TGF-β secretion (Hong et al., 2014). Under hypoxic conditions, the transcription factor, hypoxia inducible factor-1 (HIF-1) is stabilized and carries out transcription of its target genes for VEGF that promotes angiogenesis (Hong et al., 2014). Myeloid knockouts of HIF-1 regulatory subunit HIF-1α have shown to reduce macrophage, motility, aggregation and bactericidal activity (Cramer et al., 2003). Our group has recently acquired a hypoxia chamber and the effects of hypoxia on WS1 migration could easily be carried out.

The scratch assay can also be used to test the effects of inflammatory cytokines on cell migration. Cell lines established for gingival fibroblasts (H-CL and F-CL) have been shown to produce IL-6 when treated with various inflammatory cytokines. TNF-α and IL-1α caused the greatest increase in IL-6 production was found to be 100 times more potent than LPS in inducing IL-6 (Kent, Rahemtulla, Hockett, Gilleland, & Michalek, 1998). It would be beneficial to investigate the effect of anti-inflammatory cytokine treatment on cell migration as fibroblasts in diabetic wounds are often reduced in number, found to be apoptotic, and subjected to pro-inflammatory conditions (Desta, Li, Chino, & Graves, 2010). IL-6 has been shown induce apoptosis in neutrophils and

promote the expression of M-CSF receptor on monocytes and therefore has been thought to contribute to the resolution of inflammation (Scheller, Chalaris, Schmidt-Arras, & Rose-John, 2011). Media transfer from activated monocytes treated with LPS could be carried out to investigate the effects of pro-inflammatory cytokine production on cell migration.

Co-culture experiments with macrophages could be carried out and their responses to the scratch assay could be investigated. Recently a novel compartmental model was developed for the co-culture of macrophages with fibroblasts in vitro and could be used to investigate the response of fibroblast and macrophage migration into the wound gap under various stress conditions (Zhou, Loppnow, & Groth, 2015).

The study described in this thesis only assayed the effects of acute hyperglycaemia on cell migration while fibroblasts isolated from diabetic wounds have been exposed to chronic hyperglycaemia. Ex vivo culture studies have shown that fibroblasts isolated form ob/ob mice had reduced migration rates, on fibronectin and collagen coated plates, increased matrix metalloproteinase 9 levels and reduced production of VEDGF under hypoxic conditions when compared to wild type mice. Moreover fibroblasts isolated from new-born mice were similar to wild type mice suggesting that the onset of diabetes altered fibroblast behaviour. (Lerman et al., 2003). Culturing WSI cells under hyperglycaemic conditions for a longer period and then assessing cell migration using the scratch assay coupled with heat shock treatment could provide information for the impaired fibroblast dysfunction described.

The study described in this thesis also optimized a glucose uptake assay in U937 cells using the fluorescent glucose analogue (2NBDG). The effects of glucose competition, pH and membrane fluidizers was also tested to gain an understanding of glucose transport in U937 cells. A working protocol has also been developed for the insulin stimulated glucose transporter GLUT4. Ethical approval from the Faculty of Research Ethics Committee (FREC) was obtained to test these assays on PBMC isolated form healthy subjects. 2NBDG uptake was used to assay the glucose uptake of PBMCs isolated form healthy subjects at fasting and 30min post prandial consumption of a sugary meal. The assay revealed that there was no difference in glucose uptake of PBMC under either conditions (data not shown). The glucose uptake assay has been used in other studies to show the presence of GLUT4 on monocytes. However when they tested to see if insulin produced promote glucose uptake they did not wash their cells and so

could have measured fluorescence in the buffer (Dimitriadis et al., 2005; Maratou et al., 2007).

The GLUT4 protocol has since been used to optimize the concentration of insulin required to translocate GLUT4 to membrane in U937 cells (data not shown). The presence of GLUT4 and its translocation upon treatment with insulin has been tested on PBMCs and found that only monocytes (CD14+) had GLUT4 present on their membranes (data not shown). Monocytes were then purified from healthy and overweight subjects at fasting and 30min post prandial using a monocyte purification kit. Purified monocytes were then treated with 1nM insulin to see if they translocated GLUT4 to the membrane. Monocytes isolated from subjects with high BMI showed lower levels of GLUT4 on their membrane when compared to monocytes isolated form healthy controls (data not shown). This would suggest that expression of GLUT4 within these cells was altered. Moreover membrane bound GLUT4 remained unchanged in monocytes isolated from both healthy and overweight subjects when treated with insulin. This indicated that concentration of insulin used needed to be optimized for monocytes was not comparable to the concentration of insulin optimized using U937 cells. Simar et al. (2012), have recently shown that GLUT4 expression is unaffected in obese individuals following an oral glucose tolerance test when compared to healthy controls. They further demonstrated that monocytes from obese individual showed increased levels of phosphorylated IRS-1, phosphorylated JNK and phosphorylated IKKβ and that heat shock treatment of the monocytes by incubating them at 42°C for 2h reduced the levels of phosphorylated kinases and IRS-1 thereby improving insulin sensitivity. They demonstrated that heat shock induced HSP72 and HSP27 reduced JNK phosphorylation and IKKβ (Simar et al., 2012). Our initial data are in agreement with Simar et al. (2012). Future work could be carried out to see if macrophages express GLUT4 on their membranes and if induction of HSPs could alter their phenotype in diabetes as macrophages isolated from adipose tissues show M2 phenotype but are still capable of producing large amounts of inflammatory cytokines (Zeyda et al., 2007).

In the last few years peroxisome proliferator-activators have garnered a large interest as PAPR has been shown to induce sensitivity in adipose tissue and bring about adipogenesis. PAPR (Evans, 2004). Recently the role of PAPR in diabetic wounds has been demonstrated and shows that a lack of PAPR delays wound healing and allows inflammation to progress (Mirza et al., 2015). Moreover PAPR has been shown

to promote M2 phenotype in tissues improve insulin sensitivity (Odegaard & Chawla, 2013). This makes PAPR a target of therapeutic interest not just for diabetes but other inflammatory conditions such as atherosclerosis (Neve, Fruchart, & Staels, 2000) and arthritis .

The role of HSP in improving cell survival and reducing inflammation in diabetes has been demonstrated by several groups in both human and animal models (Bitar et al., n.d.; Chung et al., 2008; W. Li et al., 2007; Morera et al., 2012; Park et al., 2001). Several studies have also demonstrated the reduced induction of HSP in diabetes and leads to the paradigm that a lack of cell stress response prolongs inflammation which in turn prolongs insulin resistance (Hooper & Hooper, 2009). Atalay et al. (2004), have shown that endurance training in streptozotocin induced diabetic mice improved HSP72 expression but the expression was much lower than that of control and HSF-1 induction was also reduced (Atalay et al., 2004). Another study has shown that a lack of HSP72 expression was correlated to heme-oxygenase, and was inversely correlated to intramuscular triglyceride suggesting that diabetic patients are more susceptible to oxidative stresses (Bruce et al., 2003). Heat shock transcription factor has been shown to be inactivated by sequential serine phosphorylation at Ser^{307} by MAP Kinase, serine 303 by glycogen synthase kinase (GSK3) and at Ser^{363} by PKC at 37°C (Chu, Zhong, Soncin, Stevenson, & Calderwood, 1998). These kinases are upregulated in insulin resistance thus impairing heat shock protein induction. Investigating ways to reduce inflammatory signalling cascades (JNK, IKK-NFB) through the induction of HSP within immune cells would bring about long term insulin sensitivity. This approach could then be extended to other inflammatory diseases such arthrosclerosis and rheumatoid arthritis.

Chapter 7 References

Abd-El-Aleem, S. a, Ferguson, M. W., Appleton, I., Kairsingh, S., Jude, E. B., Jones, K., … Ireland, G. W. (2000). Expression of nitric oxide synthase isoforms and arginase in normal human skin and chronic venous leg ulcers. The Journal of Pathology, 191(4), 434–442. http://doi.org/10.1002/1096-9896(2000)9999:9999<::AID-PATH654>3.0.CO;2-S

Aguirre, V., Uchida, T., Yenush, L., Davis, R., & White, M. F. (2000). The c-Jun NH2-terminal kinase promotes insulin resistance during association with insulin receptor substrate-1 and phosphorylation of Ser307. Journal of Biological Chemistry, 275(12), 9047–9054. http://doi.org/10.1074/jbc.275.12.9047

Aguirre, V., Werner, E. D., Giraud, J., Lee, Y. H., Shoelson, S. E., & White, M. F. (2002). Phosphorylation of Ser307 in Insulin Receptor Substrate-1 Blocks Interactions with the Insulin Receptor and Inhibits Insulin Action. Journal of Biological Chemistry, 277(2), 1531–1537. http://doi.org/10.1074/jbc.M101521200

Alaluf, Simon, Muir-Howie, H., Heng-Long, H., Evana, A. and, & Green, M. (1998). Atmospheric oxygen accelerates differentiation of human dermal fibroblasts: the key protective role of glutathione. Differentiation, CW 98 0562(66), 147–155. Retrieved from https://wor.unilever.com/cgi-bin/wor2bina/wor.pl?Action=searchbyref&inp1=CW 98 0562

Ammendrup, A., Maillard, A., Nielsen, K., Andersen, A. N., Serup, P., Madsen, O. D., … Bonny, C. (2000). The c-Jun amino-terminal kinase pathway is preferentially activated by interleukin-1 and controls apoptosis in differentiating pancreatic β-cells. Diabetes, 49(9), 1468–1476. http://doi.org/10.2337/diabetes.49.9.1468

Anzai, N., Ichida, K., Jutabha, P., Kimura, T., Babu, E., Chun, J. J., … Sakurai, H. (2008). Plasma urate level is directly regulated by a voltage-driven urate efflux transporter URATv1 (SLC2A9) in humans. Journal of Biological Chemistry, 283(40), 26834–26838. http://doi.org/10.1074/jbc.C800156200

Arana, V., Paz, Y., González, A., Méndez, V., & Méndez, J. D. (2004). Healing of diabetic foot ulcers in L-arginine-treated patients. Biomedicine & Pharmacotherapy = Biomédecine & Pharmacothérapie, 58(10), 588–97. http://doi.org/10.1016/j.biopha.2004.09.009

Arkan, M. C., Hevener, A. L., Greten, F. R., Maeda, S., Li, Z.-W., Long, J. M., … Karin, M. (2005). IKK-beta links inflammation to obesity-induced insulin resistance. Nature Medicine, 11(2), 191–198. http://doi.org/10.1038/nm1185

Aronoff, S. L., Berkowitz, K., Shreiner, B., & Want, L. (2004). Glucose Metabolism and Regulation: Beyond Insulin and Glucagon. Diabetes Spectrum, 17(3), 183–190. http://doi.org/10.2337/diaspect.17.3.183

Ashby, W. J., & Zijlstra, A. (2012). Established and novel methods of interrogating two-dimensional cell migration. Integrative Biology, 4(11), 1338–1350. http://doi.org/10.1039/c2ib20154b

Atalay, M., Oksala, N. K. J., Laaksonen, D. E., Khanna, S., Nakao, C., Lappalainen, J., …

Sen, C. K. (2004). Exercise training modulates heat shock protein response in diabetic rats. Journal of Applied Physiology (Bethesda, Md. : 1985), 97(2), 605–611. http://doi.org/10.1152/japplphysiol.01183.2003

Back, S., & Kaufman, R. (2012). Endoplasmic reticulum stress and type 2 diabetes. Annual Review of Biochemistry, (4), 767–793. http://doi.org/10.1146/annurev-biochem-072909-095555.Endoplasmic

Bermudez, V., Finol, F., Parra, N., Parra, M., Perez, A., Penaranda, L., … Velasco, M. (2010). PPAR-gamma agonists and their role in type 2 diabetes mellitus management. Am J Ther, 17(3), 274–283. http://doi.org/10.1097/MJT.0b013e3181c08081

Bianchi, L., & Dez-Sampedro, A. (2010). A single amino acid change converts the sugar sensor SGLT3 into a sugar transporter. PLoS ONE, 5(4). http://doi.org/10.1371/journal.pone.0010241

Bielefeld, K. A., Amini-Nik, S., & Alman, B. A. (2013). Cutaneous wound healing: Recruiting developmental pathways for regeneration. Cellular and Molecular Life Sciences, 70(12), 2059–2081. http://doi.org/10.1007/s00018-012-1152-9

Birbach, A., Gold, P., Binder, B. R., Hofer, E., De Martin, R., & Schmid, J. A. (2002). Signaling molecules of the NF-κB pathway shuttle constitutively between cytoplasm and nucleus. Journal of Biological Chemistry, 277(13), 10842–10851. http://doi.org/10.1074/jbc.M112475200

Bitar, M. S., Farook, T., John, B., & Francis, I. M. (n.d.). wound healing in diabetic and hypercortisolemic states, 594–601.

Bizzarro, V., Fontanella, B., Carrat??, A., Belvedere, R., Marfella, R., Parente, L., & Petrella, A. (2012). Annexin A1 N-Terminal Derived Peptide Ac2-26 Stimulates Fibroblast Migration in High Glucose Conditions. PLoS ONE, 7(9), 1–10. http://doi.org/10.1371/journal.pone.0045639

Björnholm, M., & Zierath, J. R. (2005). Insulin signal transduction in human skeletal muscle: identifying the defects in Type II diabetes. Biochemical Society Transactions, 33(Pt 2), 354–7. http://doi.org/10.1042/BST0330354

Blakytny, R., & Jude, E. (2006). The molecular biology of chronic wounds and delayed healing in diabetes. Diabetic Medicine, 23(6), 594–608. http://doi.org/10.1111/j.1464-5491.2006.01773.x

Blatti, S. P., Foster, D. N., Ranganathan, G., Moses, H. L., & Getz, M. J. (1988). Induction of fibronectin gene transcription and mRNA is a primary response to growth-factor stimulation of AKR-2B cells. Proceedings of the National Academy of Sciences of the United States of America, 85(4), 1119–23. http://doi.org/10.1073/pnas.85.4.1119

Blobe, G. C., Khan, W. A., & Hannun, Y. A. (1995). Protein kinase C: Cellular target of the second messenger arachidonic acid? Prostaglandins, Leukotrienes and Essential Fatty Acids, 52(2–3), 129–135. http://doi.org/10.1016/0952-3278(95)90011-X

Bollheimer, L. C., Skelly, R. H., Chester, M. W., McGarry, J. D., & Rhodes, C. J. (1998). Chronic exposure to free fatty acid reduces pancreatic ?? cell insulin content by

increasing basal insulin secretion that is not compensated for by a corresponding increase in proinsulin biosynthesis translation. Journal of Clinical Investigation, 101(5), 1094–1101. http://doi.org/10.1172/JCI420

Bonny, C., Oberson, A., Negri, S., Sauser, C., & Schorderet, D. F. (2001). Cell-permeable peptide inhibitors of JNK. Diabetes, 50(1), 77–82. http://doi.org/10.2337/diabetes.50.1.77

Boura-Halfon, S., & Zick, Y. (2009). Phosphorylation of IRS proteins, insulin action, and insulin resistance. American Journal of Physiology. Endocrinology and Metabolism, 296(4), E581–E591. http://doi.org/10.1152/ajpendo.90437.2008

Boyer, F., Vidot, J. B., Dubourg, A. G., Rondeau, P., Essop, M. F., & Bourdon, E. (2015). Oxidative stress and adipocyte biology: Focus on the role of AGEs. Oxidative Medicine and Cellular Longevity, 2015. http://doi.org/10.1155/2015/534873

Brem, H., & Tomic-Canic, M. (2007). Cellular and molecular basis of wound healing in diabetes. J Clin Invest, 117(5), 1219–1222. http://doi.org/10.1172/JCI32169.Despite

Brownlee, M. (2005). The pathobiology of diabetic complications: A unifying mechanism. In Diabetes (Vol. 54, pp. 1615–1625). http://doi.org/10.2337/diabetes.54.6.1615

Bruce, C. R., Carey, a. L., Hawley, J. a., & Febbraio, M. a. (2003). Intramuscular heat shock protein 72 and heme oxygenase-1 mRNA are reduced in patients with type 2 diabetes. Diabetes, 52(9), 2338. Retrieved from http://diabetes.diabetesjournals.org/content/52/9/2338.short

Bruch-Gerharz, D., Ruzicka, T., & Kolb-Bachofen, V. (1998). Nitric oxide in human skin: Current status and future prospects. Journal of Investigative Dermatology, 110(1), 1–7. http://doi.org/10.1046/j.1523-1747.1998.00084.x

Calderwood, S. K., Mambula, S. S., Gray, P. J., & Theriault, J. R. (2007). Extracellular heat shock proteins in cell signaling. FEBS Letters, 581(19), 3689–3694. http://doi.org/10.1016/j.febslet.2007.04.044

Caricilli, A. M., Picardi, P. K., de Abreu, L. L., Ueno, M., Prada, P. O., Ropelle, E. R., … Saad, M. J. A. (2011). Gut Microbiota Is a Key Modulator of Insulin Resistance in TLR 2 Knockout Mice. PLoS Biology, 9(12), e1001212. http://doi.org/10.1371/journal.pbio.1001212

Castronuovo, J. J., Ghobrial, I., Giusti, A. M., Rudolph, S., & Smiell, J. M. (1998). Effects of chronic wound fluid on the structure and biological activity of becaplermin (rhPDGF-BB) and becaplermin gel. American Journal of Surgery, 176(2 A). http://doi.org/10.1016/S0002-9610(98)00175-5

Cayatte, A. J., Kumbla, L., & Subbiah, M. T. R. (1990). Marked acceleration of exogenous fatty acid incorporation into cellular triglycerides by fetuin. Journal of Biological Chemistry, 265(10), 5883–5888.

Ceriello, a, Colagiuri, S., Gerich, J., & Tuomilehto, J. (2008). Guideline for management of postmeal glucose. Nutr Metab Cardiovasc Dis (Vol. 18). http://doi.org/10.1016/j.numecd.2008.01.012

Chang, L., Chiang, S.-H. and, & Alan, S. (2006). Insulin signaling and the Regulation of Glucose Transport. Molecular Medicine, 12(7–12), 1. http://doi.org/10.2119/2005-00029.Saltiel

Chu, B., Zhong, R., Soncin, F., Stevenson, M. A., & Calderwood, S. K. (1998). Transcriptional activity of heat shock factor 1 at 37 degrees C is repressed through phosphorylation on two distinct serine residues by glycogen synthase kinase 3 and protein kinases Calpha and Czeta. The Journal of Biological Chemistry, 273(29), 18640–18646. http://doi.org/10.1074/jbc.273.29.18640

Chung, J., Nguyen, A.-K., Henstridge, D. C., Holmes, A. G., Chan, M. H. S., Mesa, J. L., … Febbraio, M. A. (2008). HSP72 protects against obesity-induced insulin resistance. Proceedings of the National Academy of Sciences of the United States of America, 105(5), 1739–44. http://doi.org/10.1073/pnas.0705799105

Cramer, T., Yamanishi, Y., Clausen, B. E., Forster, I., Pawlinski, R., Mackman, N., … Johnson, R. S. (2003). HIF-1alpha is essential for myeloid cell-mediated inflammation. Cell, 112(5), 645–657. http://doi.org/10.1016/S0092-8674(03)00154-5

Crowe, M. J., Doetschman, T., & Greenhalgh, D. G. (2000). Delayed wound healing in immunodeficient TGF-beta 1 knockout mice. The Journal of Investigative Dermatology, 115(1), 3–11. http://doi.org/10.1046/j.1523-1747.2000.00010.x

Darby, I. A., Laverdet, B., Bonte, F., & Desmouliere, A. (2014). Fibroblasts and myofibroblasts in wound healing. Clinical, Cosmetic and Investigational Dermatology, 7, 301–311. http://doi.org/10.2147/CCID.S50046

de Luca, C., & Olefsky, J. M. (2008). Inflammation and insulin resistance. FEBS Letters, 582(1), 97–105. http://doi.org/10.1016/j.febslet.2007.11.057

De Maio, A., Gabriella Santoro, M., Tanguay, R. M., & Hightower, L. E. (2012). Ferruccio Ritossa's scientific legacy 50 years after his discovery of the heat shock response: A new view of biology, a new society, and a new journal. Cell Stress and Chaperones, 17(2), 139–143. http://doi.org/10.1007/s12192-012-0320-z

Dempsey, N. C., Ireland, H. E., Smith, C. M., Hoyle, C. F., & Williams, J. H. H. (2010). Heat Shock Protein translocation induced by membrane fluidization increases tumor-cell sensitivity to chemotherapeutic drugs. Cancer Letters, 296(2), 257–267. http://doi.org/10.1016/j.canlet.2010.04.016

Desta, T., Li, J., Chino, T., & Graves, D. T. (2010). Altered fibroblast proliferation and apoptosis in diabetic gingival wounds. Journal of Dental Research, 89(6), 609–14. http://doi.org/10.1177/0022034510362960

Detanico, T., Rodrigues, L., Sabritto, A. C., Keisermann, M., Bauer, M. E., Zwickey, H., & Bonorino, C. (2004). Mycobacterial heat shock protein 70 induces interleukin-10 production: Immunomodulation of synovial cell cytokine profile and dendritic cell maturation. Clinical and Experimental Immunology, 135(2), 336–342. http://doi.org/10.1111/j.1365-2249.2004.02351.x

Dimitriadis, G., Maratou, E., Boutati, E., Psarra, K., Papasteriades, C., & Raptis, S. A. (2005). Evaluation of glucose transport and its regulation by insulin in human monocytes using flow cytometry. Cytometry Part A, 64(1), 27–33.

http://doi.org/10.1002/cyto.a.20108

Dimitriadis, G., Mitrou, P., Lambadiari, V., Maratou, E., & Raptis, S. A. (2011). Insulin effects in muscle and adipose tissue. Diabetes Research and Clinical Practice, 93, S52–S59. http://doi.org/10.1016/S0168-8227(11)70014-6

Douard, V., & Ferraris, R. P. (2008). Regulation of the fructose transporter GLUT5 in health and disease. American Journal of Physiology. Endocrinology and Metabolism, 295(2), E227-37. http://doi.org/10.1152/ajpendo.90245.2008

Drucker, D. J. (2001). Minireview: the glucagon-like peptides. Endocrinology, 142(2), 521–527. http://doi.org/10.1210/endo.142.2.7983

Drucker, D. J. (2007). Review series The role of gut hormones in glucose homeostasis. Pancreas, 117(1), 24–32. http://doi.org/10.1172/JCI30076.24

Echouffo-Tcheugui, J. B., Ali, M. K., Griffin, S. J., & Narayan, K. M. V. (2011). Screening for type 2 diabetes and dysglycemia. Epidemiologic Reviews, 33(1), 63–87. http://doi.org/10.1093/epirev/mxq020

Ehses, J. A., Meier, D. T., Wueest, S., Rytka, J., Boller, S., Wielinga, P. Y., … Donath, M. Y. (2010). Toll-like receptor 2-deficient mice are protected from insulin resistance and beta cell dysfunction induced by a high-fat diet. Diabetologia, 53(8), 1795–1806. http://doi.org/10.1007/s00125-010-1747-3

Eming, S. A., Martin, P., & Tomic-Canic, M. (2014). Wound repair and regeneration: mechanisms, signaling, and translation. Science Translational Medicine, 6(265), 265sr6. http://doi.org/10.1126/scitranslmed.3009337

Evans, R. M. (2004). PPARs and the complex journey to obesity. Keio Journal of Medicine, 53(2), 53–58. http://doi.org/10.2302/kjm.53.53

Frank, S., Madlener, M., & Werner, S. (1996). Transforming Growth Factors β1, β2, and β3 and Their Receptors Are Differentially Regulated during Normal and Impaired Wound Healing *, 271(17), 10188–10193.

Fried, S. K., Bunkin, D. A., & Greenberg, A. S. (1998). Omental and subcutaneous adipose tissues of obese subjects release interleukin-6: Depot difference and regulation by glucocorticoid. Journal of Clinical Endocrinology and Metabolism, 83(3), 847–850. http://doi.org/10.1210/jc.83.3.847

Fröjdö, S., Vidal, H., & Pirola, L. (2009). Alterations of insulin signaling in type 2 diabetes: a review of the current evidence from humans. Biochimica et Biophysica Acta, 1792(2), 83–92. http://doi.org/10.1016/j.bbadis.2008.10.019

Fu, M. X., Requena, J. R., Jenkins, A. J., Lyons, T. J., Baynes, J. W., & Thorpe, S. R. (1996). The advanced glycation end product, Ne-(carboxymethyl)lysine, is a product of both lipid peroxidation and glycoxidation reactions. Journal of Biological Chemistry, 271(17), 9982–9986. http://doi.org/10.1074/jbc.271.17.9982

Galbo, T., Perry, R. J., Jurczak, M. J., Camporez, J.-P. G., Alves, T. C., Kahn, M., … Shulman, G. I. (2013). Saturated and unsaturated fat induce hepatic insulin resistance independently of TLR-4 signaling and ceramide synthesis in vivo. Proceedings of the National Academy of Sciences of the United States of

America, 110(31), 12780–5. http://doi.org/10.1073/pnas.1311176110

Gao, Z., Wang, Z., Zhang, X., Butler, A. a, Zuberi, A., Gawronska-kozak, B., … Inactivation, Y. J. (2007). Inactivation of PKC theta leads to increased susceptibility to obesity and dietary insulin resistance in mice. American Journal of Physiology. Endocrinology and Metabolism, 70808, 84–91. http://doi.org/10.1152/ajpendo.00178.2006.

Garrido, C., Bruey, J. M., Fromentin, a, Hammann, a, Arrigo, a P., & Solary, E. (1999). HSP27 inhibits cytochrome c-dependent activation of procaspase-9. The FASEB Journal : Official Publication of the Federation of American Societies for Experimental Biology, 13(14), 2061–2070.

Garrido, C., Gurbuxani, S., Ravagnan, L., & Kroemer, G. (2001). Heat Shock Proteins: Endogenous Modulators of Apoptotic Cell Death. Biochemical and Biophysical Research Communications, 286(3), 433–442. http://doi.org/10.1006/bbrc.2001.5427

Garvey, W. T., Maianu, L., Zhu, J., Brechtel-hook, G., Wallace, P., & Baron, A. D. (1998). Evidence for Defects in the Trafficking and Translocation of GLUT4 Glucose Transporters in Skeletal Muscle as a Cause of Human Insulin Resistance, 101(11), 2377–2386.

Gebäck, T., Schulz, M. M. P., Koumoutsakos, P., & Detmar, M. (2009). TScratch: A novel and simple software tool for automated analysis of monolayer wound healing assays. BioTechniques, 46(4), 265–274. http://doi.org/10.2144/000113083

Gedulin, B. R., & Young, A. A. (1998). Hypoglycemia overrides amylin-mediated regulation of gastric emptying in rats. Diabetes, 47(1), 93–97. http://doi.org/10.2337/diab.47.1.93

Golpour, M., Akhavan Niaki, H., Khorasani, H. R., Hajian, A., Mehrasa, R., & Mostafazadeh, A. (2014). Human fibroblast switches to anaerobic metabolic pathway in response to serum starvation: a mimic of warburg effect. International Journal of Molecular and Cellular Medicine, 3(2), 74–80. Retrieved from http://www.pubmedcentral.nih.gov/articlerender.fcgi?artid=4082808&tool=pmcentrez&rendertype=abstract

Gorboulev, V., Schürmann, A., Vallon, V., Kipp, H., Jaschke, A., Klessen, D., … Koepsell, H. (2012). Na +-D-glucose cotransporter SGLT1 is pivotal for intestinal glucose absorption and glucose-dependent incretin secretion. Diabetes, 61(1), 187–196. http://doi.org/10.2337/db11-1029

Gordon, S., & Martinez, F. O. (2010). Alternative activation of macrophages: Mechanism and functions. Immunity, 32(5), 593–604. http://doi.org/10.1016/j.immuni.2010.05.007

Greene, M. W., Morrice, N., Garofalo, R. S., & Roth, R. A. (2004). Modulation of human insulin receptor substrate-1 tyrosine phosphorylation by protein kinase Cdelta. The Biochemical Journal, 378(Pt 1), 105–16. http://doi.org/10.1042/BJ20031493

Griffin, M. E., Marcucci, M. J., Cline, G. W., Bell, K., Barucci, N., Lee, D., … Shulman, G. I. (1999). Free fatty acid-induced insulin resistance is associated with activation of protein kinase C theta and alterations in the insulin signaling cascade. Diabetes, 48(6), 1270–1274. http://doi.org/10.2337/diabetes.48.6.1270

Guerre-Millo, M. (2002). Adipose tissue hormones. Journal of Endocrinological Investigation, 25(10), 855–861. http://doi.org/10.1007/BF03344048

Guo, S., & Dipietro, L. a. (2010). Factors affecting wound healing. Journal of Dental Research, 89(3), 219–29. http://doi.org/10.1177/0022034509359125

Gupte, A. a, Bomhoff, G. L., Swerdlow, R. H., & Geiger, P. C. (2009). Heat Treatment Improves Glucose Tolerance and a High-Fat Diet. Diabetes, 58(March), 567–578. http://doi.org/10.2337/db08-1070.

Guttilla, I. K., Phoenix, K. N., Hong, X., Tirnauer, J. S., Claffey, K. P., & White, B. A. (2012). Prolonged mammosphere culture of MCF-7 cells induces an EMT and repression of the estrogen receptor by microRNAs. Breast Cancer Research and Treatment, 132(1), 75–85. http://doi.org/10.1007/s10549-011-1534-y

Harada, N., & Inagaki, N. (2012). Role of sodium-glucose transporters in glucose uptake of the intestine and kidney. Journal of Diabetes Investigation, 3(4), 352–353. http://doi.org/10.1111/j.2040-1124.2012.00227.x

Hargitai, J., Lewis, H., Boros, I., Racz, T., Fiser, A., Kurucz, I., … Latchman, D. S. (2003). Bimoclomol, a heat shock protein co-inducer, acts by the prolonged activation of heat shock factor-1. Biochemical and Biophysical Research Communications, 307(3), 689–695. http://doi.org/10.1016/S0006-291X(03)01254-3

Harper, D., Young, A., & McNaught, C. E. (2014). The physiology of wound healing. Surgery (United Kingdom), 32(9), 445–450. http://doi.org/10.1016/j.mpsur.2014.06.010

Hasty, A. H. (2008). NIH Public Access, 3(5), 545–556. http://doi.org/10.2217/17460875.3.5.545.Macrophage

Havel, P. J. (2014). Update on Adipocyte Hormones. Diabetes, 53(February 2004), 143–151. http://doi.org/10.2337/diabetes.53.2007.S143

Hehenberger, K., Heilborn, J. D., Brismar, K., & Hansson, a. (1998). Inhibited proliferation of fibroblasts derived from chronic diabetic wounds and normal dermal fibroblasts treated with high glucose is associated with increased formation of l-lactate. Wound Repair and Regeneration : Official Publication of the Wound Healing Society [and] the European Tissue Repair Society, 6(2), 135–141. http://doi.org/10.1046/j.1524-475X.1998.60207.x

Heldin, C. H., & Westermark, B. (1999). Mechanism of action and in vivo role of platelet-derived growth factor. Physiological Reviews, 79(4), 1283–1316.

Heldin, P., Laurent, T. C., & Heldin, C. H. (1989). Effect of growth factors on hyaluronan synthesis in cultured human fibroblasts. Biochem J, 258, 919–22. Retrieved from http://www.pubmedcentral.nih.gov/articlerender.fcgi?artid=1138453&tool=pmcentrez&rendertype=abstract

Hirosumi, J., Tuncman, G., Chang, L., Görgün, C. Z., Uysal, K. T., Maeda, K., … Hotamisligil, G. S. (2002). A central role for JNK in obesity and insulin resistance. Nature, 420(6913), 333–336. http://doi.org/10.1038/nature01137

Hong, W. X., Hu, M. S., Esquivel, M., Liang, G. Y., Rennert, R. C., McArdle, A., … Longaker, M. T. (2014). The Role of Hypoxia-Inducible Factor in Wound Healing. Advances in Wound Care, 3(5), 390–399. http://doi.org/10.1089/wound.2013.0520

Hooper, P. L., & Hooper, P. L. (2009). Inflammation, heat shock proteins, and type 2 diabetes. Cell Stress and Chaperones, 14(2), 113–115. http://doi.org/10.1007/s12192-008-0073-x

Hotamisligil, G. S., Arner, P., Caro, J. F., Atkinson, R. L., & Spiegelman, B. M. (1995). Increased adipose tissue expression of tumor necrosis factor-alpha in human obesity and insulin resistance. The Journal of Clinical Investigation. http://doi.org/10.1172/JCI117936

Hulkower, K. I., & Herber, R. L. (2011). Cell migration and invasion assays as tools for drug discovery. Pharmaceutics, 3(1), 107–124. http://doi.org/10.3390/pharmaceutics3010107

Hulse, R. E., Ralat, L. a, & Wei-Jen, T. (2009). Structure, function, and regulation of insulin-degrading enzyme. Vitamins and Hormones, 80(8), 635–648. http://doi.org/10.1016/S0083-6729(08)00622-5

Itani, S. I., Ruderman, N. B., Schmieder, F., & Boden, G. (2002). Lipid-induced insulin resistance in human muscle is associated with changes in diacylglycerol, protein kinase C, and IkappaB-alpha. Diabetes, 51(7), 2005–2011. http://doi.org/10.2337/diabetes.51.7.2005

Jetton, T. L., Lausier, J., Larock, K., Trotman, W. E., Larmie, B., Habibovic, A., … Leahy, J. L. (2005). Mechanisms of Compensatory b-Cell Growth in Insulin-Resistant Rats Roles of Akt Kinase, 54(August).

Jonkman, J. E. N., Cathcart, J. A., Xu, F., Bartolini, M. E., Amon, J. E., Stevens, K. M., & Colarusso, P. (2014). An introduction to the wound healing assay using live-cell microscopy. Cell Adhesion and Migration, 8(5), 440–451. http://doi.org/10.4161/cam.36224

Jude, E. B., Blakytny, R., Bulmer, J., Boulton, A. J. M., & Ferguson, M. W. J. (2002). Transforming growth factor-beta 1, 2, 3 and receptor type I and II in diabetic foot ulcers. Diabetic Medicine, 19(6), 440–447. http://doi.org/10.1046/j.1464-5491.2002.00692.x

Jude, E. B., Boulton, a J., Ferguson, M. W., & Appleton, I. (1999). The role of nitric oxide synthase isoforms and arginase in the pathogenesis of diabetic foot ulcers: possible modulatory effects by transforming growth factor beta 1. Diabetologia, 42(6), 748–757. http://doi.org/10.1007/s001250051224

Kam, Y., Guess, C., Estrada, L., Weidow, B., & Quaranta, V. (2008). A novel circular invasion assay mimics in vivo invasive behavior of cancer cell lines and distinguishes single-cell motility in vitro. BMC Cancer, 8, 198. http://doi.org/10.1186/1471-2407-8-198

Kamei, N., Tobe, K., Suzuki, R., Ohsugi, M., Watanabe, T., Kubota, N., … Kadowaki, T. (2006). Overexpression of monocyte chemoattractant protein-1 in adipose tissues causes macrophage recruitment and insulin resistance. Journal of Biological Chemistry, 281(36), 26602–26614. http://doi.org/10.1074/jbc.M601284200

Kaneto, H., Matsuoka, T., Nakatani, Y., Kawamori, D., Matsuhisa, M., & Yamasaki, Y. (2005). Oxidative stress and the JNK pathway in diabetes. Current Diabetes Reviews, 1(1), 65–72. http://doi.org/10.2174/1573399052952613

Kaneto, H., Nakatani, Y., Miyatsuka, T., Kawamori, D., Matsuoka, T., Matsuhisa, M., … Hori, M. (2004). Possible novel therapy for diabetes with cell-permeable JNK-inhibitory peptide. Nature Medicine, 10(10), 1128–1132. http://doi.org/10.1038/nm1111

Karpe, P. A., & Tikoo, K. (2014). Heat shock prevents insulin resistance-induced vascular complications by augmenting angiotensin-(1-7) signaling. Diabetes, 63(3), 1124–1139. http://doi.org/10.2337/db13-1267

Keese, C. R., Wegener, J., Walker, S. R., & Giaever, I. (2004). Electrical wound-healing assay for cells in vitro. Proceedings of the National Academy of Sciences, 101(6), 1554–1559. http://doi.org/10.1073/pnas.0307588100

Kent, L. W., Rahemtulla, F., Hockett, R. D., Gilleland, R. C., & Michalek, S. M. (1998). Effect of lipopolysaccharide and inflammatory cytokines on interleukin-6 production by healthy human gingival fibroblasts. Infection and Immunity, 66(2), 608–614.

Kersten, S., Seydoux, J., Peters, J. M., Gonzalez, F. J., Desvergne, B., & Wrahli, W. (1999). Peroxisome proliferator-activated receptor alpha mediates the adaptive response to fasting. Journal of Clinical Investigation, 103(11), 1489–1498. http://doi.org/10.1172/JCI6223

Kharroubi, I., Ladrière, L., Cardozo, A. K., Dogusan, Z., Cnop, M., & Eizirik, D. L. (2004). Free fatty acids and cytokines induce pancreatic β-cell apoptosis by different mechanisms: Role of nuclear factor-κB and endoplasmic reticulum stress. Endocrinology, 145(11), 5087–5096. http://doi.org/10.1210/en.2004-0478

Kim, J. J., & Sears, D. D. (2010). TLR4 and Insulin Resistance. Gastroenterology Research and Practice, 2010, 1–12. http://doi.org/10.1155/2010/212563

Kim, J. K., Fillmore, J. J., Sunshine, M. J., Albrecht, B., Higashimori, T., Kim, D. W., … Shulman, G. I. (2004). PKC-?? knockout mice are protected from fat-induced insulin resistance. Journal of Clinical Investigation, 114(6), 823–827. http://doi.org/10.1172/JCI200422230

Kirchhof, M., Popat, N., & Malowany, J. (2009). Diagnostic Review A Historical Perspective of the Diagnosis of Diabetes. Uwomj 78(1)2008, 78(1), 7–11.

Klok, M. D., Jakobsdottir, S., & Drent, M. L. (2007). The role of leptin and ghrelin in the regulation of food intake and body weight in humans: A review. Obesity Reviews, 8(1), 21–34. http://doi.org/10.1111/j.1467-789X.2006.00270.x

Koh, T. J. and, & DiPietro, L. A. (2013). Inflammation and wound healing : The role of the macrophage, 16(2008), 19–25.

http://doi.org/10.1017/S1462399411001943.Inflammation

Kolluru, G. K., Bir, S. C., & Kevil, C. G. (2012). Endothelial dysfunction and diabetes: Effects on angiogenesis, vascular remodeling, and wound healing. International Journal of Vascular Medicine, 2012(Figure 1). http://doi.org/10.1155/2012/918267

Kondo, T., Motoshima, H., Igata, M., Kawashima, J., Matsumura, T., Kai, H., & Araki, E. (2014). The role of heat shock response in insulin resistance and diabetes. Diabetes & Metabolism Journal, 38, 100–6. http://doi.org/10.4093/dmj.2014.38.2.100

Kondo, T., Sasaki, K., Matsuyama, R., Morino-Koga, S., Adachi, H., Suico, M. A., … Araki, E. (2012). Hyperthermia with mild electrical stimulation protects pancreatic ??-cells from cell stresses and apoptosis. Diabetes, 61(4), 838–847. http://doi.org/10.2337/db11-1098

Kotas, M. E., & Medzhitov, R. (2015). Homeostasis, Inflammation, and Disease Susceptibility. Cell, 160(5), 816–827. http://doi.org/10.1016/j.cell.2015.02.010

Kumar Sharma, A., Bharti, S., Ojha, S., Bhatia, J., Kumar, N., Ray, R., … Singh Arya, D. (2011). Up-regulation of PPARγ, heat shock protein-27 and -72 by naringin attenuates insulin resistance, β-cell dysfunction, hepatic steatosis and kidney damage in a rat model of type 2 diabetes. British Journal of Nutrition, 106(11), 1713–1723. http://doi.org/10.1017/S000711451100225X

Kurucz, I., Morva, a, Vaag, a, Eriksson, K. F., Huang, X., Groop, L., & Koranyi, L. (2002). Decreased expression of heat shock protein 72 in skeletal muscle of patients with type 2 diabetes correlates with insulin resistance. Diabetes, 51(4), 1102–1109. http://doi.org/10.2337/diabetes.51.4.1102

Lamers, M. L., Almeida, M. E. S., Vicente-Manzanares, M., Horwitz, A. F., & Santos, M. F. (2011). High Glucose-Mediated Oxidative Stress Impairs Cell Migration. PLoS ONE, 6(8), e22865. http://doi.org/10.1371/journal.pone.0022865

Leibovich, S. J., & Ross, R. (1975). The role of the macrophage in wound repair. A study with hydrocortisone and antimacrophage serum. The American Journal of Pathology, 78(1), 71–100. Retrieved from http://www.pubmedcentral.nih.gov/articlerender.fcgi?artid=1915032&tool=pmcentrez&rendertype=abstract

Lerman, O. Z., Galiano, R. D., Armour, M., Levine, J. P., & Gurtner, G. C. (2003). Cellular dysfunction in the diabetic fibroblast: impairment in migration, vascular endothelial growth factor production, and response to hypoxia. The American Journal of Pathology, 162(1), 303–12. http://doi.org/10.1016/S0002-9440(10)63821-7

Li, J., Chen, J., & Kirsner, R. (2007). Pathophysiology of acute wound healing. Clinics in Dermatology, 25(1), 9–18. http://doi.org/10.1016/j.clindermatol.2006.09.007

Li, W., Li, Y., Guan, S., Fan, J., Cheng, C.-F., Bright, A. M., … Woodley, D. T. (2007). Extracellular heat shock protein-90alpha: linking hypoxia to skin cell motility and wound healing. The EMBO Journal, 26(5), 1221–1233. http://doi.org/10.1038/sj.emboj.7601727

Liang, C.-C., Park, A. Y., & Guan, J.-L. (2007). In vitro scratch assay: a convenient and

inexpensive method for analysis of cell migration in vitro. Nature Protocols, 2(2), 329–333. http://doi.org/10.1038/nprot.2007.30

Lianos, G. D., Alexiou, G. A., Mangano, A., Mangano, A., Rausei, S., Boni, L., … Roukos, D. H. (2015). The role of heat shock proteins in cancer. Cancer Letters, 360(2), 114–118. http://doi.org/10.1016/j.canlet.2015.02.026

Lim, G. E., Huang, G. J., Flora, N., Leroith, D., Rhodes, C. J., & Brubaker, P. L. (2009). Insulin regulates glucagon-like peptide-1 secretion from the enteroendocrine L cell. Endocrinology, 150(2), 580–591. http://doi.org/10.1210/en.2008-0726

Lobmann, R., Ambrosch, A., Schultz, G., Waldmann, K., Schiweck, S., & Lehnert, H. (2002). Expression of matrix-metalloproteinases and their inhibitors in the wounds of diabetic and non-diabetic patients. Diabetologia, 45(7), 1011–1016. http://doi.org/10.1007/s00125-002-0868-8

Magill, J. C., Byl, M. F., Goldwaser, B., Instructor, M. P., Yates, B., Morency, J. R., … Associate, M. J. T. (2010). Heat Shock Proteins in Diabetes and Wound Healing, 3(1), 1–19. http://doi.org/10.1115/1.3071969.Automating

Malhotra, J. D., Miao, H., Zhang, K., Wolfson, A., Pennathur, S., Pipe, S. W., & Kaufman, R. J. (2008). Antioxidants reduce endoplasmic reticulum stress and improve protein secretion. Proceedings of the National Academy of Sciences of the United States of America, 105(47), 18525–18530. http://doi.org/10.1073/pnas.0809677105

Maratou, E., Dimitriadis, G., Kollias, a., Boutati, E., Lambadiari, V., Mitrou, P., & Raptis, S. a. (2007). Glucose transporter expression on the plasma membrane of resting and activated white blood cells. European Journal of Clinical Investigation, 37(4), 282–290. http://doi.org/10.1111/j.1365-2362.2007.01786.x

Martinez-Ferrer, M., Afshar-Sherif, A.-R., Uwamariya, C., de Crombrugghe, B., Davidson, J. M., & Bhowmick, N. a. (2010). Dermal transforming growth factor-beta responsiveness mediates wound contraction and epithelial closure. The American Journal of Pathology, 176(1), 98–107. http://doi.org/10.2353/ajpath.2010.090283

Martins, A. R., Nachbar, R. T., Gorjao, R., Vinolo, M. A., Festuccia, W. T., Lambertucci, R. H., … Hirabara, S. M. (2012). Mechanisms underlying skeletal muscle insulin resistance induced by fatty acids: importance of the mitochondrial function. Lipids in Health and Disease, 11, 30. http://doi.org/10.1186/1476-511X-11-30

Matsuyama, S., Moriuchi, M., Suico, M. A., Yano, S., Morino-Koga, S., Shuto, T., … Kai, H. (2014). Mild electrical stimulation increases stress resistance and suppresses fat accumulation via activation of LKB1-AMPK signaling pathway in C. elegans. PLoS ONE, 9(12), 1–23. http://doi.org/10.1371/journal.pone.0114690

McCance, D. R., Dyer, D. G., Dunn, J. a, Bailie, K. E., Thorpe, S. R., Baynes, J. W., & Lyons, T. J. (1993). Maillard reaction products and their relation to complications in insulin-dependent diabetes mellitus. The Journal of Clinical Investigation, 91(6), 2470–2478. http://doi.org/10.1172/JCI116482

McGarry, J. D. (2002). Banting Lecture 2001:Dysregulation of Fatty Acid Metabolism

in the Etiology of Type 2 Diabetes. Diabetes, 51, 7–18. http://doi.org/10.2337/diabetes.51.1.7

Mirza, R. E., Fang, M. M., Novak, M. L., Urao, N., Sui, A., Ennis, W. J., & Koh, T. J. (2015). Macrophage PPAR?? and impaired wound healing in type 2 diabetes. Journal of Pathology, 236(4), 433–444. http://doi.org/10.1002/path.4548

Morera, P., Basirico, L., Hosoda, K., & Bernabucci, U. (2012). Chronic heat stress up-regulates leptin and adiponectin secretion and expression and improves leptin, adiponectin and insulin sensitivity in mice. Journal of Molecular Endocrinology, 48(2), 129–138. http://doi.org/10.1530/JME-11-0054

Morimoto, RI, Christen, Y., Shen, K., & Frydman, J. (2013). Protein Quality Control in Neurodegenerative Diseases. Springer, 121–132. http://doi.org/10.1007/978-3-642-27928-7

Morino, S., Kondo, T., Sasaki, K., Adachi, H., Suico, M. A., Sekimoto, E., … Kai, H. (2008). Mild electrical stimulation with heat shock ameliorates insulin resistance via enhanced insulin signaling. PLoS ONE, 3(12). http://doi.org/10.1371/journal.pone.0004068

Neve, B. P., Fruchart, J. C., & Staels, B. (2000). Role of the peroxisome proliferator-activated receptors (PPAR) in atherosclerosis. Biochemical Pharmacology, 60(8), 1245–1250. http://doi.org/10.1016/S0006-2952(00)00430-5

Nishimura, H., Pallardo, F. V., Seidner, G. A., Vannucci, S., Simpson, I. A., & Birnbaum, M. J. (1993). Kinetics of GLUT1 and GLUT4 glucose transporters expressed in Xenopus oocytes. Journal of Biological Chemistry, 268(12), 8514–8520.

Nystrom, F. H., & Quon, M. (1999). Insulin signalling: Metabolic pathways and mechanisms for specificity. Cellular Signalling, 11(8), 563–574. http://doi.org/10.1016/S0898-6568(99)00025-X

Odegaard, J. I., & Chawla, A. (2013). Pleiotropic actions of insulin resistance and inflammation in metabolic homeostasis. Science (New York, N.Y.), 339(6116). http://doi.org/10.1126/science.1230721

Odegaard, J. I., Ricardo-Gonzalez, R. R., Goforth, M. H., Morel, C. R., Subramanian, V., Mukundan, L., … Chawla, A. (2007). Macrophage-specific PPARgamma controls alternative activation and improves insulin resistance. Nature, 447(7148), 1116–20. http://doi.org/10.1038/nature05894

Olczyk, P., Mencner, A., & Komosinska-vassev, K. (2014). The Role of the Extracellular Matrix Components in Cutaneous Wound Healing, 2014, 12–14.

Ott, C., Jacobs, K., Haucke, E., Navarrete Santos, A., Grune, T., & Simm, A. (2014). Role of advanced glycation end products in cellular signaling. Redox Biology, 2(1), 411–429. http://doi.org/10.1016/j.redox.2013.12.016

Ouchi, N., Parker, J. L., Lugus, J. J., & Walsh, K. (2011). Adipokines in inflammation and metabolic disease. Nature Reviews. Immunology, 11(2), 85–97. http://doi.org/10.1038/nri2921

Pal, D., Dasgupta, S., Kundu, R., Maitra, S., Das, G., Mukhopadhyay, S., …

Bhattacharya, S. (2012). Fetuin-A acts as an endogenous ligand of TLR4 to promote lipid-induced insulin resistance. Nature Medicine, 18(8), 1279–1285. http://doi.org/10.1038/nm.2851

Panunti, B., & Fonseca, V. (2006). Effects of PPAR gamma agonists on cardiovascular function in obese, non-diabetic patients. Vascular Pharmacology, 45(1), 29–35. http://doi.org/10.1016/j.vph.2005.11.013

Park, H. S., Lee, J. S., Huh, S. H., Seo, J. S., & Choi, E. J. (2001). Hsp72 functions as a natural inhibitory protein of c-Jun N-terminal kinase. EMBO Journal, 20(3), 446–456. http://doi.org/10.1093/emboj/20.3.446

Patel, S., & Santani, D. (2009). Role of NF-??B in the pathogenesis of diabetes and its associated complications. Pharmacological Reports, 61(4), 595–603. http://doi.org/http://dx.doi.org/10.1016/S1734-1140(09)70111-2

Paul, R. G., & Bailey, A. J. (1999). The effect of advanced glycation end-product formation upon cell-matrix interactions. International Journal of Biochemistry and Cell Biology, 31(6), 653–660. http://doi.org/10.1016/S1357-2725(99)00023-0

Peng, H. B., Spiecker, M., & Liao, J. K. (1998). Inducible nitric oxide: an autoregulatory feedback inhibitor of vascular inflammation. Journal of Immunology (Baltimore, Md. : 1950), 161(4), 1970–1976.

Pierce, G. F., Tarpley, J. E., Allman, R. M., Goode, P. S., Serdar, C. M., Morris, B., … Vande Berg, J. (1994). Tissue repair processes in healing chronic pressure ulcers treated with recombinant platelet-derived growth factor BB. The American Journal of Pathology, 145(6), 1399–1410. Retrieved from http://www.ncbi.nlm.nih.gov/pmc/articles/PMC1887508/

Pierce, G. F., Tarpley, J. E., Tseng, J., Bready, J., Chang, D., Kenney, W. C., … Farrell, C. L. (1995). Detection of platelet-derived growth factor (PDGF)-AA in actively healing human wounds treated with recombinant PDGF-BB and absence of PDGF in chronic nonhealing wounds. Journal of Clinical Investigation, 96(3), 1336–1350. http://doi.org/10.1172/JCI118169

Pinto, A. B., Carayannopoulos, M. O., Hoehn, A., Dowd, L., & Moley, K. H. (2002). Glucose transporter 8 expression and translocation are critical for murine blastocyst survival. Biology of Reproduction, 66(6), 1729–1733. http://doi.org/10.1095/biolreprod66.6.1729

Polvani, S., Tarocchi, M., Tempesti, S., Bencini, L., & Galli, A. (2016). Peroxisome proliferator activated receptors at the crossroad of obesity, diabetes, and pancreatic cancer. World Journal of Gastroenterology, 22(8), 2441–2459. http://doi.org/10.3748/wjg.v22.i8.2441

Poon, R., Nik, S. A., Ahn, J., Slade, L., & Alman, B. a. (2009). Beta-catenin and transforming growth factor beta have distinct roles regulating fibroblast cell motility and the induction of collagen lattice contraction. BMC Cell Biology, 10, 38. http://doi.org/10.1186/1471-2121-10-38

Posnett, J., & Franks, P. J. (2010). The burden of chronic wounds in the UK. Nursing Times, 104(3), 44–45.

Qiu, W. Q., & Folstein, M. F. (2006). Insulin, insulin-degrading enzyme and amyloid-

?? peptide in Alzheimer's disease: Review and hypothesis. Neurobiology of Aging, 27(2), 190–198. http://doi.org/10.1016/j.neurobiolaging.2005.01.004

Ricardo-Gonzalez, R. R., Red Eagle, A., Odegaard, J. I., Jouihan, H., Morel, C. R., Heredia, J. E., … Chawla, A. (2010). IL-4/STAT6 immune axis regulates peripheral nutrient metabolism and insulin sensitivity. Proceedings of the National Academy of Sciences of the United States of America, 107(52), 22617–22622. http://doi.org/10.1073/pnas.1009152108

Richter, K., Haslbeck, M., & Buchner, J. (2010). The Heat Shock Response: Life on the Verge of Death. Molecular Cell, 40(2), 253–266. http://doi.org/10.1016/j.molcel.2010.10.006

Riss, T. L., Niles, A. L., & Minor, L. (2004). Cell Viability Assays Assay Guidance Manual. Assay Guidance Manual, 1–23. http://doi.org/10.1016/j.acthis.2012.01.006

Roden, M., Price, T. B., Perseghin, G., Petersen, K. F., Rothman, D. L., Cline, G. W., & Shulman, G. I. (1996). Mechanism of free fatty acid-induced insulin resistance in humans. Journal of Clinical Investigation, 97(12), 2859–2865. http://doi.org/10.1172/JCI118742

Roth, R., Ibberson, M., Riederer, B. M., Uldry, M., Guhl, B., Thorens, B., … Morphology, B. M. R. (2002). Immunolocalization of GLUTX1 in the Testis and to Specific Brain Areas and Vasopressin- Containing Neurons, 143(1), 276–284. http://doi.org/10.1210/endo.143.1.8587

Saltiel, A. R., & Kahn, C. R. (2001). Insulin signalling and the regulation of glucose and lipid metabolism. Nature, 414(6865), 799–806. http://doi.org/10.1038/414799a

Samaan, M. C. (2011). The macrophage at the intersection of immunity and metabolism in obesity. Diabetology & Metabolic Syndrome, 3(1), 29. http://doi.org/10.1186/1758-5996-3-29

Sanz Fernandez, M. V., Stoakes, S. K., Abuajamieh, M., Seibert, J. T., Johnson, J. S., Horst, E. a., … Baumgard, L. H. (2015). Heat stress increases insulin sensitivity in pigs. Physiological Reports, 3(8), e12478. http://doi.org/10.14814/phy2.12478

Scheller, J., Chalaris, A., Schmidt-Arras, D., & Rose-John, S. (2011). The pro- and anti-inflammatory properties of the cytokine interleukin-6. Biochimica et Biophysica Acta - Molecular Cell Research, 1813(5), 878–888. http://doi.org/10.1016/j.bbamcr.2011.01.034

Schmitz-Peiffer, C., & Biden, T. J. (2008). Protein Kinase C Function in Muscle, Liver, and -Cells and Its Therapeutic Implications for Type 2 Diabetes. Diabetes, 57(7), 1774–1783. http://doi.org/10.2337/db07-1769

Schmitz, O., Brock, B., & Rungby, J. (2004). Amylin Agonists: A Novel Approach in the Treatment of Diabetes. Diabetes, 53(suppl_3), S233–S238. http://doi.org/10.2337/diabetes.53.suppl_3.S233

Schuit, F. C., In't Veld, P. A., & Pipeleers, D. G. (1988). Glucose stimulates proinsulin biosynthesis by a dose-dependent recruitment of pancreatic beta cells. Proceedings of the National Academy of Sciences of the United States of

America, 85(11), 3865–3869. http://doi.org/10.1073/pnas.85.11.3865

Seino, Y., Fukushima, M., & Yabe, D. (2010). GIP and GLP-1, the two incretin hormones: Similarities and differences. Journal of Diabetes Investigation, 1(1–2), 8–23. http://doi.org/10.1111/j.2040-1124.2010.00022.x

Serra, C., Federici, M., Buongiorno, A., Senni, M. I., Morelli, S., Segratella, E., … Bouché, M. (2003). Transgenic mice with dominant negative PKC-theta in skeletal muscle: A new model of insulin resistance and obesity. Journal of Cellular Physiology, 196(1), 89–97. http://doi.org/10.1002/jcp.10278

Shoelson, S. E., Lee, J., & Goldfine, A. B. (2006). Inflammation and insulin resistance. The Journal of Clinical Investigation. http://doi.org/10.1172/JCI29069C1

Shoelson, S., Lee, J., & Yuan, M. (2003). PAPER Inflammation and the IKKb/IjB/NF-jB axis in obesity-and diet-induced insulin resistance. International Journal of Obesity, 27, 49–52. http://doi.org/10.1038/sj.ijo.0802501

Simar, D., Jacques, A., & Caillaud, C. (2012). Heat shock proteins induction reduces stress kinases activation, potentially improving insulin signalling in monocytes from obese subjects. Cell Stress and Chaperones, 17(5), 615–621. http://doi.org/10.1007/s12192-012-0336-4

Simpson, I. A., Dwyer, D., Malide, D., Moley, K. H., Travis, A., & Vannucci, S. J. (2008). The facilitative glucose transporter GLUT3: 20 years of distinction. AJP: Endocrinology and Metabolism, 295(2), E242–E253. http://doi.org/10.1152/ajpendo.90388.2008

Sims, T. J., Rasmussen, L. M., Oxlund, H., & Bailey, A. J. (1996). The role of glycation cross-links in diabetic vascular stiffening. Diabetologia, 39(8), 946–951. http://doi.org/10.1007/s001250050536

Singh, R., Barden, A., Mori, T., & Beilin, L. (2001). Advanced glycation end-products: A review. Diabetologia, 44(2), 129–146. http://doi.org/10.1007/s001250051591

Sonnemann, K. J., & Bement, W. M. (2011). Wound Repair: Toward Understanding and Integration of Single-Cell and Multicellular Wound Responses. Annual Review of Cell and Developmental Biology, 27(1), 237–263. http://doi.org/10.1146/annurev-cellbio-092910-154251

Tang, T., Zhang, J., Yin, J., Staszkiewicz, J., Gawronska-Kozak, B., Jung, D. Y., … Ye, J. (2010). Uncoupling of inflammation and insulin resistance by NF-??B in transgenic mice through elevated energy expenditure. Journal of Biological Chemistry, 285(7), 4637–4644. http://doi.org/10.1074/jbc.M109.068007

Thorens, B. (2014). GLUT2, glucose sensing and glucose homeostasis. Diabetologia, 58(2), 221–232. http://doi.org/10.1007/s00125-014-3451-1

Thorens, B., & Mueckler, M. (2014). The SLC2 (GLUT) Family of Membrane Transporters. Mol Aspects Med, 34(0), 121–138. http://doi.org/10.1016/j.biotechadv.2011.08.021.Secreted

Timothy Garvey, W., Maianu, L., Huecksteadt, T. P., Birnbaum, M. J., Molina, J. M., & Ciaraldi, T. P. (1991). Pretranslational suppression of a glucose transporter protein causes insulin resistance in adipocytes from patients with non-insulin-

dependent diabetes mellitus and obesity. Journal of Clinical Investigation, 87(3), 1072–1081. http://doi.org/10.1172/JCI115068

Tsukumo, D., Carvalho-Filho, M., Carvalheira, J., Prada, P., Hirabara, S., Schenka, A., … Saad, M. (2007). Loss-of-function mutation in Toll-like receptor 4 prevents diet-induced obesity and insulin resistance. Diabetes, 56(August), 1986–1998. http://doi.org/10.2337/db06-1595.CLS

Van Belle, T., Coppieters, K., & Von Herrath, M. (2011). Type 1 Diabetes: Etiology, Immunology, and Therapeutic Strategies. Physiol Rev, 91, 79–118. http://doi.org/10.1152/physrev.00003.2010.

van der Meer, A. D., Vermeul, K., Poot, A. a, Feijen, J., & Vermes, I. (2010). A microfluidic wound-healing assay for quantifying endothelial cell migration. American Journal of Physiology. Heart and Circulatory Physiology, 298(2), H719-25. http://doi.org/10.1152/ajpheart.00933.2009

Van Greevenbroek, M. M. J., Schalkwijk, C. G., & Stehouwer, C. D. A. (2013). obesity-associated low-grade inflammation in type 2 diabetes mellitus: causes and consequences. Netherlands Journal of Medicine, 71(4), 174–187.

Van Horssen, R., & Ten Hagen, T. L. (2011). Crossing barriers: The new dimension of 2D cell migration assays. Journal of Cellular Physiology, 226(1), 288–290. http://doi.org/10.1002/jcp.22330

Van Noort, J. M., Bsibsi, M., Nacken, P., Gerritsen, W. H., & Amor, S. (2012). The link between small heat shock proteins and the immune system. International Journal of Biochemistry and Cell Biology, 44(10), 1670–1679. http://doi.org/10.1016/j.biocel.2011.12.010

Velnar, T., Bailey, T., & Smrkolj, V. (2009). The wound healing process: an overview of the cellular and molecular mechanisms. The Journal of International Medical Research, 37(5), 1528–1542. http://doi.org/10.1177/147323000903700531

Verghese, J., Abrams, J., Wang, Y., & Morano, K. A. (2012). Biology of the heat shock response and protein chaperones: budding yeast (Saccharomyces cerevisiae) as a model system. Microbiology and Molecular Biology Reviews : MMBR, 76(2), 115–58. http://doi.org/10.1128/MMBR.05018-11

Verweij, J., & Pinedo, H. M. (1990). Mitomycin C: mechanism of action, usefulness and limitations. Anti-Cancer Drugs, 1(April), 5–13.

Waltenberger, J., Lange, J., & Kranz, a. (2000). Vascular endothelial growth factor-A-induced chemotaxis of monocytes is attenuated in patients with diabetes mellitus: A potential predictor for the individual capacity to develop collaterals. Circulation, 102(2), 185–190. http://doi.org/10.1161/01.CIR.102.2.185

Wang, Y., Schmeichel, A. M., Iida, H., Schmelzer, J. D., & Low, P. A. (2006). Enhanced inflammatory response via activation of NF-??B in acute experimental diabetic neuropathy subjected to ischemia-reperfusion injury. Journal of the Neurological Sciences, 247(1), 47–52. http://doi.org/10.1016/j.jns.2006.03.011

Wetzler, C., Kampfer, H., Stallmeyer, B., Pfeilschifter, J., & Frank, S. (2000). Large and sustained induction of chemokines during impaired wound healing in the genetically diabetic mouse: Prolonged persistence of neutrophils and

macrophages during the late phase of repair. Journal of Investigative Dermatology, 115(2), 245–253. http://doi.org/10.1046/j.1523-1747.2000.00029.x

Weykamp, C. (2013). HbA1c: A review of analytical and clinical aspects. Annals of Laboratory Medicine, 33(6), 393–400. http://doi.org/10.3343/alm.2013.33.6.393

Whitley, D., Goldberg, S. P., & Jordan, W. D. (1999). Heat shock proteins: A review of the molecular chaperones. Journal of Vascular Surgery, 29(4), 748–751. http://doi.org/10.1016/S0741-5214(99)70329-0

Wood, I. S., & Trayhurn, P. (2003). Glucose transporters (GLUT and SGLT): expanded families of sugar transport proteins. The British Journal of Nutrition, 89(1), 3–9. http://doi.org/10.1079/BJN2002763

Xu, H., Barnes, G. T., Yang, Q., Tan, G., Yang, D., Chou, C. J., … Others. (2003). Chronic inflammation in fat plays a crucial role in the development of obesity-related insulin resistance. Journal of Clinical Investigation, 112(12), 1821–1830. http://doi.org/10.1172/JCI200319451.Introduction

Xuan, Y. H., Huang, B. Bin, Tian, H. S., Chi, L. S., Duan, Y. M., Wang, X., … Jin, L. T. (2014). High-Glucose Inhibits Human Fibroblast Cell Migration in Wound Healing via Repression of bFGF-Regulating JNK Phosphorylation. PloS One, 9(9), e108182. http://doi.org/10.1371/journal.pone.0108182

Yagihashi, S., Mizukami, H., & Sugimoto, K. (2011). Mechanism of diabetic neuropathy: Where are we now and where to go? Journal of Diabetes Investigation. http://doi.org/10.1111/j.2040-1124.2010.00070.x

Yang, Y., Lu, H. L., Zhang, J., Yu, H. Y., Wang, H. W., Zhang, M. X., & Cianflone, K. (2006). Relationships among acylation stimulating protein, adiponectin and complement C3 in lean vs obese type 2 diabetes. International Journal of Obesity (2005), 30(3), 439–446. http://doi.org/10.1038/sj.ijo.0803173

Yarrow, J. C., Perlman, Z. E., Westwood, N. J., & Mitchison, T. J. (2004). A high-throughput cell migration assay using scratch wound healing, a comparison of image-based readout methods. BMC Biotechnology, 4, 21. http://doi.org/10.1186/1472-6750-4-21

Yin, M. J., Yamamoto, Y., & Gaynor, R. B. (1998). The anti-inflammatory agents aspirin and salicylate inhibit the activity of I(kappa)B kinase-beta. Nature, 396(6706), 77–80. http://doi.org/10.1038/23948

Yoshioka, K., Saito, M., Oh, K.-B., Nemoto, Y., Matsuoka, H., Natsume, M., & Abe, H. (1996). NII-Electronic Library Service Intracellular Fate of 2-NBDG, a Fluorescent Probe for Glucose Uptake Activity, in Escherichia coli Cells. Biosci. Biotech. Biochem, 60(11), 1899–190. http://doi.org/10.1271/bbb.60.1899

Young, C. D., Lewis, A. S., Rudolph, M. C., Ruehle, M. D., Jackman, M. R., Yun, U. J., … Anderson, S. M. (2011). Modulation of glucose transporter 1 (GLUT1) expression levels alters mouse mammary tumor cell growth in vitro and in vivo. PLoS ONE, 6(8). http://doi.org/10.1371/journal.pone.0023205

Yu, C., Chen, Y., Cline, G. W., Zhang, D., Zong, H., Wang, Y., … Shulman, G. I. (2002). Mechanism by Which Fatty Acids Inhibit Insulin Activation of Insulin Receptor Substrate-1 (IRS-1) associated Phosphatidylinositol 3 Kinase Activity in Muscle.

Journal of Biological Chemistry, 277(52), 50230–50236. http://doi.org/10.1074/jbc.M200958200

Yu, J., Shi, L., Wang, H., Bilan, P. J., Yao, Z., Samaan, M. C., … Niu, W. (2011). Conditioned medium from hypoxia-treated adipocytes renders muscle cells insulin resistant. European Journal of Cell Biology, 90(12), 1000–1015. http://doi.org/10.1016/j.ejcb.2011.06.004

Zeyda, M., Farmer, D., Todoric, J., Aszmann, O., Speiser, M., Györi, G., … Stulnig, T. (2007). Human adipose tissue macrophages are of an anti-inflammatory phenotype but capable of excessive pro-inflammatory mediator production. International Journal of Obesity, 31, 1420–1428. http://doi.org/10.1038/sj.ijo.0803632

Zhou, G., Loppnow, H., & Groth, T. (2015). A macrophage/fibroblast co-culture system using a cell migration chamber to study inflammatory effects of biomaterials. Acta Biomaterialia, 26, 54–63. http://doi.org/10.1016/j.actbio.2015.08.020

Ziyan, W., Shuhua, Y., Xiufang, W., & Xiaoyun, L. (2011). MicroRNA-21 is involved in osteosarcoma cell invasion and migration. Medical Oncology, 28(4), 1469–1474. http://doi.org/10.1007/s12032-010-9563-7

Zou, C., Wang, Y., & Shen, Z. (2005). 2-NBDG as a fluorescent indicator for direct glucose uptake measurement. Journal of Biochemical and Biophysical Methods. http://doi.org/10.1016/j.jbbm.2005.08.001

Zungu, I. L., Mbene, A. B., Hawkins Evans, D. H., Houreld, N. N., & Abrahamse, H. (2009). Phototherapy promotes cell migration in the presence of hydroxyurea. Lasers in Medical Science, 24(2), 144–150. http://doi.org/10.1007/s10103-007-0533-z